Bioavailability of organic micropollutants in cell-based bioassays

Dissertation

der Mathematisch-Naturwissenschaftlichen Fakultät

der Eberhard Karls Universität Tübingen

zur Erlangung des Grades eines

Doktors der Naturwissenschaften

(Dr. rer. nat.)

vorgelegt von

M. Sc. Fabian Christoph Fischer

aus Bielefeld

Tübingen

2018

Gedruckt mit Genehmigung der Mathematisch-Naturwissenschaftlichen Fakultät der Eberhard Karls Universität Tübingen.

Tag der mündlichen Qualifikation:	19. Oktober 2018
Dekan:	Prof. Dr. Wolfgang Rosenstiel
1. Berichterstatterin:	Prof. Dr. Beate I. Escher
2. Berichterstatter:	Prof. Dr. Kai-Uwe Goss
3. Berichterstatter:	Prof. Dr. Olaf A. Cirpka

Contents

Abstract

The application of *in vitro* cell-based bioassays is increasing in chemical risk and hazard assessment and their implementation in high-throughput screening (HTS) format can contribute significantly to meet the high demands on effect data for the increasing number and variety of anthropogenic chemicals. Their suitability to replace whole-organism tests in human health risk assessment depends on the ability to quantitatively predict effects in humans, referred to as quantitative *in vitro-in vivo* extrapolation (QIVIVE). The quantification of chemical bioavailability is an important prerequisite for the QIVIVE, but is challenging to do analytically due to the small medium volumes used in HTS. This thesis aimed to develop and experimentally parameterize exposure models that enable the prediction of the bioavailability of neutral and ionizable chemicals in various cell-based bioassays. In a first step, a steady-state mass balance model was parameterized and applied to the effect data of 100 neutral, anionic, cationic and multiprotic chemicals from the reporter gene assays of the HTS platform "Toxicology in the 21st Century" (Tox21). The influence of cellular uptake kinetics on cell exposure during the typical 24-hour bioassay was evaluated while emphasizing the role of the medium composition on the kinetics and extent of uptake. Chemical sorption to the plastic of multiwell plates (polystyrene) that are used for HTS was measured and predicted by a kinetic model for various multiwell plate formats and medium compositions. Integrating all evaluated processes demonstrated that the fetal bovine serum (FBS) that is commonly supplemented to mammalian cell-based bioassays is the major determinant for *in vitro* chemical bioavailability. Despite reducing exposure and the apparent assay sensitivity, the proteins and lipids in the FBS represent a large reservoir of reversibly bound chemicals that generally compensate for the chemical depletion of the exposure medium by cellular uptake, growth, sorption to well plate materials, and volatilization, keeping the exposure fairly constant during the bioassay duration. Area under the curve analyses showed that the kinetics of cellular uptake can generally be neglected in exposure models. The application of higher medium FBS contents maximized the ca-

pacity of the chemical reservoir and decreased the relevance of kinetic processes, leading to an increased predictive power of the mass balance model. Based on the generated knowledge, the thesis illustrates how simple equations that apply predicted parameters can improve chemical dosing, prevent experimental errors, and facilitate the interpretation of experiments. Experimentally parameterized equilibrium mass balance and kinetic models can be used for improved analysis of effect data for subsequent application to QIVIVE models and comparison to other exposure scenarios.

Zusammenfassung

Die Anwendung von zellbasierten Biotestverfahren in der Risikobewertung von Chemikalien steigt kontinuierlich und die Durchführung in Hochdurchsatz kann dazu beitragen, den hohen Bedarf an Effektdaten für die hohe Anzahl und hohe Komplexität an anthropogenen Chemikalien zu decken. Die Eignung von zellbasierten Biotestverfahren als Alternative zu Tierversuchen ist abhängig davon, Effekte robust von der Zellebene auf den gesamten Organismus extrapolieren zu können, was als quantitative *in vitro-in vivo* Extrapolation bezeichnet wird (QIVIVE). Diese Dissertation fokussierte sich auf die Herleitung und Parametrisierung von Expositionsmodellen, die die Bioverfügbarkeit von neutralen und ionisierbaren Chemikalien in verschiedenen zellbasierten Biotestverfahren vorhersagen. Ein Massenbilanzmodell wurde parametrisiert und auf die Effektdaten von 100 neutralen, anionischen, kationischen und multiprotischen organischen Chemikalien der Hochdurchsatz-Datenbank „Toxicology in the 21st Century“ (Tox21) angewandt. Der Einfluss von zellulären Aufnahmekinetiken auf die 24-stündige Chemikalienexposition von typischen zellbasierten Biotestverfahren wurde untersucht, wobei ein besonderer Fokus auf die Rolle der Mediumkomposition gelegt wurde. Die Reduzierung von Bioverfügbarkeit durch die Sorption von Chemikalien an das Plastik von Multititerplatten (Polystyrol), die für den Hochdurchsatz verwendet werden, wurde über ein kinetisches Sorptionsmodell für verschiedene experimentelle Setups vorhergesagt und bewertet. Die Integration aller untersuchten Prozesse zeigte, dass das fötale Rinderserum (FBS), welches dem Medium als Nährstoffreservoir zugesetzt wird, den wichtigsten Einflussparameter für die chemische Bioverfügbarkeit darstellt. Obwohl sie die Exposition und die Sensitivität der Biotestverfahren herabsetzen, stellen die Proteine und Lipide im FBS ein großes Reservoir an resorbierbaren Chemikalien dar, das den Verlust durch Aufnahme und Wachstum der Zellen, Sorption an Multititerplatten, und Verflüchtigung zu einem großen Teil kompensiert. Integration der gemessenen Aufnahmekurven zeigte, dass die Kinetiken der Zellaufnahme generell vernachlässigt werden können. Die Anwendung von höheren FBS Gehalten im Medium

erhöht die Kapazität des Chemikalienreservoirs im Medium, wodurch sich der Einfluss von kinetischen Prozessen minimiert und die Aussagekraft von Gleichgewichtsmodellen maximiert. Die Dissertation zeigt, wie die Anwendung einfacher Gleichungen die Dosierung von Chemikalien in zellbasierten Biotestverfahren verbessern kann. Komplexere Gleichgewichts- und Kinetikmodelle können die Datenqualität von Effektdaten so weit erhöhen, dass sie in QIVIVE Modelle einfließen und mit anderen Expositionszenarien verglichen werden können.

Acknowledgements

"Be warned" said a large proportion of my friends, family, and (former) colleagues after I told them that I plan to do my PhD. "It is going to be a rough time" and "you are not going to spend a lot of time outside" were also phrases I continued to hear. In the end, a lot of these people helped me to eventually conquer this challenge without losing myself and them. This I want to acknowledge in the following to the highest degree.

First, I would like to acknowledge and emphasize the support, encouragement, and commitment of my supervisor Beate Escher, who recognized very early that giving me the freedom to generate my own ideas is of great importance for me and my work. While she was always challenging me to become better, she remained fair in her criticism and her expectations. I want to point out that, given she is the busiest person I know, her door was always open and she reacted to questions and issues, foremost if urgent, almost instantaneously. Thank you Beate, I could not have wished for a better mentor.

Kai-Uwe Goss and Olaf Cirpka are thanked for co-supervising the PhD thesis and providing me with their enormous expertise and many useful discussions on my experiments, data, and manuscripts. I would also like to thank Sabine Schäfer for the supervision of my master thesis and publishing it together with me, which facilitated the start of my PhD thesis. Furthermore, I would like to thank her for drawing my attention towards the open PhD position at the UFZ in the first place.

The CELLTOX department, other colleagues at the UFZ, and external co-authors of my Publications are highly acknowledged for providing me an optimal working environment with interesting and controversial discussions on my project as well as associated ideas and issues.

I would like to thank all my friends and family, who always showed interest while demonstrating deep understanding for my moods and my absence throughout the last three years. I would like to point out the unconditional support of my mother and the backup of my good friends Tim Hallau, Jonas Frohwitter, and Cedric Abele.

In the end and foremost, I would like to express my deepest thanks and all my love to Jessica Hellweg, who supported me better than I could have ever imagined throughout this intensive time. She always listened knowingly and stood on my side at all times. Thank you for being who you are, Jessica.

1 Introduction

1.1 Chemicals in the environment

Humanity is facing complex challenges like overpopulation, climate change, and the rapid global technologization. A rather inconspicuous but serious risk for human and environmental health represent anthropogenic organic chemicals that had been and are continuously emitted into the environment. Nowadays, large quantities of chemicals are produced to cover the increasing demands for pharmaceuticals, personal care products, pesticides, and chemicals used in textiles, coatings, and electronics such as flame retardants, fluids, and plasticizers. In July 2018, the number of registered chemicals rose to 142 million (CAS 2018). The enormous number of anthropogenic chemicals and possible associated risks were recognized by the regulators by adopting regulations such as REACH that prescribe the Regulation, Evaluation, Authorization and Restriction of manufactured CHemicals (European Parliament and Council 2006). With regard to their relatively low environmental concentrations compared to macropollutants such as phosphor, most environmental organic chemicals can be classified as micropollutants. Large quantities of organic chemicals are produced as manufacturing by-products, such as organic solvents, heavy metals, and products of incomplete combustion (U.S. EPA 2017). Abiotic and biotic chemical transformation during waste water treatment or in the different environmental compartments increase the number of environmental chemicals of anthropogenic origin even further (Margot et al. 2015), and the quantity of their emission is often inherently uncertain. Neither the authorities nor the public was aware of risks of chemical pollution because effects were not directly tangible. Awareness has risen since the publication of Rachel Carson's "Silent Spring" in the U.S., in which she criticized the careless use of pesticides taking the example of the insecticide dichlorodiphenyltrichloroethane (DDT) and its effects on the eggshells of predatory birds (Carson 1962). Her popular slogans such as "Can you imagine a spring without the voices of birds?" questioned the usage of toxins in the environment. DDT was prohibited for agricultural use in the U.S. in 1972 followed by a

world-wide formulized ban under the Stockholm Convention on Persistent Organic Pollutants (POPs) in 2001. Even though DDT concentrations are generally declining, there are still substantial amounts stored in sinks like soils and sediments (Kiersch et al. 2010), and the transformation products dichlorodiphenyldichloroethane (DDD) and dichlorodiphenyldichloroethylene (DDE) are ubiquitously present in the environment (Pérez-Maldonado et al. 2010). Controversial use of chemicals is central topic nowadays, for instance the effects of neonicotinoid pesticides on bees (Blacquière et al. 2012) or the potential carcinogenity of the widely applied herbicide glyphosate (Williams et al. 2016, Tarazona et al. 2017). The field of human health risk assessment (HHRA) aims to evaluate if and to which level exposure to chemicals poses or is likely to pose a risk to humans, thereby considering differences in age and residence as well as consumerism, work, and other behaviors between individuals and populations. Equivalently to HHRA, the environmental risk assessment (ERA) aims to identify the potential adverse effects of chemicals on environmental organisms of different trophic level, such as bacteria, algae, amphibians, insects, plants, and mammals (U.S. EPA 2000). Both frameworks require comprehensive data on (i) the measured or predicted exposure concentrations that humans and the environment are facing and (ii) the potential effects of chemicals at relevant concentrations to determine acceptable thresholds and safety levels that assure the public and environmental health as well as the ecosystem integrity and functioning.

1.2 Chemical fate and exposure

The assessment of the chemical fate in the environment incorporates different local and global transport processes between the atmosphere, stagnant and moving water bodies, soils and sediments, as well as biological processes that influence the distribution and extent of chemical accumulation in the environment. The distribution of chemicals in the environment determines the extent of contact between chemicals and organisms, which can be summarized as total chemical exposure. Exposure to micropollutants in contaminated environmental compartments is defined by the extent of chemical bioavailability, i.e. the chemical fraction that is available for uptake by environmental organisms and humans. The environmental fate of a chemical is determined by its physicochemical properties, such as the sorption affinity to organic matter, the tendency to evaporate, and the persistence against degradation processes. A popular example of a rather unexpected chemical fate was the accumulation of polychlorinated biphenyls (PCBs) in the arctic environment and across the food-chain of arctic terrestrial mammals. The PCBs were long-distance transported along the chemical gradient to the arctic, where chemical accumulation was increased by the low temperatures, reducing the proportion of PCBs in the compartments of higher chemical mobility (water and air) (Meyer and Wania 2007). The accumulation in soils, sediments, and in the food-chain was further increased by the high persistence of PCBs against abiotic and biotic degradation (Court et al. 1997, Kelly and Gobas 2003). Even though chemical restrictions and regulations led to considerable decline in chemical concentrations of priority micropollutants such as DDT and PCBs, the number of environmental chemicals largely increased within the last decades. New emerging micropollutants like pharmaceuticals and personal care products are object to HHRA and ERA and the consideration of mixture effects has become of greater importance. The complexity of the chemical structures and physicochemical properties increased, for instance the large amount and variety of ionizable chemicals, which dissociate into a charged and a neutral species at a given pH. Ionizable chemicals often exhibit multifaceted chemical partitioning in the environment because of their complex sorptive affinity to different envi-

ronmental matrices (e.g., organic carbon), complicating the prediction of the chemical distribution between environmental compartments and the estimation of exposure levels. Different routes of exposure are addressed in HHRA, such as chemical uptake via oral ingestion, inhalation, and dermal uptake. The amount of chemical uptake determines the total dose in the body, which is quantified as the amount of chemical per kilogram bodyweight per hour of exposure (mg kg^{-1} h^{-1}). The chemical exposure and resulting total dose of a chemical can vary between individuals, groups, and populations dependent on age, origin, and behavior. For instance, high PCB concentrations were measured in the breast milk of Inuit women that resulted from the traditional consume of beluga and seal blubber, a fat tissue in which the lipophilic PCBs highly accumulated (Dewailly et al. 1993). The bioavailability of a chemical in the human body is often expressed as the unbound fraction in the blood (f_{unbound}), which is the chemical fraction that is available for chemical absorption by cells and tissue. The f_{unbound} is strongly dependent on the affinity of chemicals to sorptive biomatrices in the plasma, foremost the protein human serum albumin (HSA). The steady-state internal unbound chemical concentration in the blood (C_{unbound}, mg L^{-1}) results from the f_{unbound} and the chemical absorption, distribution, metabolism and elimination (ADME) in the body. The ADME processes vary considerably between chemicals dependent on their physicochemical properties but are also influenced by the condition and health of individuals. The mathematical prediction of chemical ADME is the main objective of the physiologically based pharmacokinetic (PBPK) framework (e.g., Brown et al. 1997), and large databases that gather measured and predicted data on the ADME of a variety of chemicals exist, such as the chemical dashboard provided by the U.S. EPA (https://comptox.epa.gov/dashboard). The C_{unbound} in blood represents a suitable parameter for *in vivo* bioavailability that can directly be linked to adverse effects measured in humans.

1.3 Chemical risk assessment

Exposure to micropollutants can have multiple adverse effects on the public health. The field of HHRA aims to evaluate if and to which level exposure to a chemical poses a risk to humans. First, the effects that single chemicals and their mixtures can exhibit on the cellular, tissue, organ, whole-organism, and population level are identified. Then, the chemical dose that is required to cause these effects is measured and compared to the chemical exposure that is expected over a certain timeframe or the entire lifespan of an individual, a group, or a population. The ratio of chemical exposure and effect concentrations ultimately determines the level of risk a chemical poses. In other words, a chemical can be extremely potent with relatively low exposure concentrations while a rather inactive chemical can be taken up in considerable extents; both scenarios can present a risk. Dependent on the level of risk, measures can be taken to decrease the chemical exposure, such as the prohibition of DDT for agricultural use. Whether or not such measures are taken not only depends on the hazard potential of a chemical, but also its social and economic benefits. Particularly in the case of pharmaceuticals, benefits and risks need to be broadly evaluated before making a decision. Harmful effects of chemicals on humans include diseases, cancer, malformation, decreased reproductive capacity, neurotoxicity, psychological stress, and others. The important first step in assessing the harm of a chemical is to identify its mode(s) of toxic action (MoA). The MoA combines the physiological and behavior alternations that are characteristic for a certain biological response (Rand 1995). The framework of adverse outcome pathways (AOPs) attempts to identify and seamlessly connect the series of biological events that cause an adverse effect in the body (Ankley et al. 2010). This pathway includes the initiating event on the molecular level (MIE) and following key events (e.g., disruption of a signaling pathway), as well as resulting observable or measurable alterations or malformations on organ and/or whole-organism level. The significance of AOPs depends on the availability and quantity of data for each individual part. Clinical studies on humans that mimic realistic exposure scenarios represent the optimal data source, however, those studies are in most cases not proportionate in ethi-

cal terms and costs. Statistical studies that evaluate whether direct contact with chemical sources or sinks correlate with incidents of diseases can be suitable data sources for HHRA. These studies are highly dependent on the accuracy of the exposure information and do not mechanistically reveal the MoA in most cases, still, they can indicate risk groups. The most common way to assess the harm of a chemical is chemical effect testing on mammals such as mice, rats, monkeys, and rabbits. Controlling the exposure under desired test conditions enables the adjustment of specific chemical doses and subsequent determination of thresholds of toxicological concern such as the acceptable daily intake (ADI), the lowest-observed-adverse-effect level (LOAEL), and the no-observed adverse effect level (NOAEL), which can be compared to predicted or measured exposure concentrations. Equivalently to HHRA, the ERA evaluates the effects of chemicals on environmental organisms of different trophic level (U.S. EPA 2000). Numerous single species bioassays have been developed that target different acute and chronic endpoints such as lethality, growth, reproduction, or mobility of well-studied organisms, such as phytotoxicity tests with algae (OECD, 2011) and immobilization tests with *Daphnia magna* (OECD, 2004). The toxicity data generated for these *in vivo* bioassays can be applied into HHRA, and models were already developed that extrapolate effects on these species to humans, such as the usage of the fish embryo toxicity assay with *Danio rerio* (FET assay) as indicator for developmental toxicity (e.g., Embry et al. 2010). The general weakness of animal testing as data source for HHRA is the extrapolation of measured effects to the human level, which is associated with considerable uncertainties. With the increasing number and heterogeneity of chemicals and the implementation of new regulations such as REACH, the demand for chemical effect assessment largely increased within the last two decades, leading to substantial costs but likewise ethical concerns considering the large number of animals used for effect testing. Initiatives such as the 3 R's program were implemented that aim to Reduce, Refine and Replace animal tests whenever possible.

1.4 *In vitro* cell-based bioassays

In vitro bioassays with mammalian cell lines have a great potential to cover the high demands on chemical effect characterization because of their cost-efficiency, their potential to be run in high-throughput, and their classification as non-animal tests. In contrast to animal tests, cell-based bioassays assess the specific effect of chemical(s) on the suborgan level, with the potential to reveal the MoA to greater detail. The application of cell-based bioassays has emerged in the last years in human toxicology and ecotoxicology, foremost recombinant cell-based bioassays that apply genetically modified cells, in which a reporter gene was transferred and coupled to the receptor of interest. The reporter gene encodes for the transcription and translation of a reporter protein such as luciferase or β-lactamase. Upon chemical interaction with the receptor, the reporter proteins are synthesized and can be visualized by adding a substrate that is transformed by the enzymes causing the substrate to exhibit fluorescence or bioluminescence (luciferase and β-lactamase). The fluorescence or bioluminescence intensity can be measured as quantitative effect endpoint because it is proportional to the receptor activity triggered by the chemical exposure. Several cell constructs that test on different MoA, such as hormone activity or adaptive stress responses have been developed (e.g., Huang et al. 2014). The application of *in vitro* cell-based bioassays in high tier multiwell plates (384- and 1536-well plates) coupled with the use of robotic pipetting systems enable their implementation in high-throughput screening (HTS), allowing the simultaneous effect fingerprinting of thousands of chemicals. One of the biggest effort hitherto is the implementation of the "Toxicology in the 21st Century" (Tox21) program, a HTS platform in which 10,000 chemicals were screened in 70 *in vitro* test systems with cells and isolated subcellular biomarkers (Tox21 10K library, U.S. EPA). The assays were carried out in 1536-well plates with small assay medium volumes of 5-6 µL, minimizing the amount of consumables and chemicals needed for effect measurements. The implementation of *in vitro* test systems in miniaturized scale complicates the analytical measurement of exposure concentrations, therefore the nominal concentration (C_{nom}), which is the theoretical added amount of chemical per volume bio-

assay, is typically used as exposure metric for *in vitro* effects in most studies and databases such as the Tox21 database (Huang et al. 2011, Shukla et al. 2012, Huang et al. 2014).

1.5 Exposure assessment in *in vitro* cell-based bioassays

A critical requirement for the application of *in vitro* cell-based bioassays in chemical risk assessment is the suitability of *in vitro* effect data to predict effects on the whole-organism level, referred to as quantitative *in vitro-in vivo* extrapolation (QIVIVE). Appropriate QIVIVE necessitates that chemical bioavailability can be robustly quantified both *in vitro* and *in vivo*, as is illustrated by Figure 1. The quantification of chemical bioavailability enables the discrimination of toxicokinetic and toxicodynamic processes (TKTD), in other words, it can be evaluated whether differences in effects between chemicals are the result of differences in bioavailability or true differences in the potency of the chemical to cause damage to biomolecules in the human body. In QIVIVE models, bioavailability is quantified as the f_{unbound} in human plasma, which is either measured by equilibrium dialysis or predicted based on mass balance modeling under the consideration of sorptive colloids in the blood (e.g., Ghafourian and Amin 2013). By extending the equation for the steady-state total concentration in blood by Wetmore (2015) by f_{unbound}, the steady-state C_{unbound} in the blood can be calculated (eq. 1).

$$C_{\text{unbound}} = \frac{k_0}{\text{GFR} \cdot f_{\text{unbound}} + \frac{(Q_1 \cdot f_{\text{unbound}} \cdot \text{CL}_{\text{int}})}{(Q_1 + f_{\text{unbound}} \cdot \text{CL}_{\text{int}})}} \cdot f_{\text{unbound}} \qquad (1)$$

k_0 is the total chemical dose in the body (in mg per kg per hour), GFR is the glomerular filtration rate (6.7 L h^{-1}, Rule et al. 2004), Q_1 is the liver blood flow (90 L h^{-1}, Davies and Morries 1993), and CL_{int} is the intrinsic metabolic clearance representative for the whole liver. The suitability of *in vitro* effect data to be used in QIVIVE models requires the control and quantification of exposure concentrations in the medium of cell-based bioassays (Figure 1). The proteins that are present in the fetal bovine serum (FBS) supplemented to mammalian cell culture media were already recognized as influencing factor for bioavailability by Gülden and Seibert in 1997. They stated that chemical partitioning can considerably reduce the freely dissolved, bioavailable concentration in the medium (C_{free}) dependent on the sorptive affinity

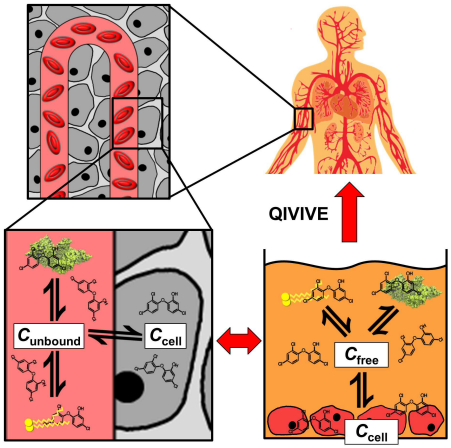

Figure 1: Framework of *in vitro* bioassay exposure modeling and link to QIVIVE: Quantifying exposure on the *in vitro* level to anchor *in vitro* effects for reliable extrapolation to expose concentrations in the human body [human body image adapted from www.medwrite.biz, accessed on 04 August 2018].

of the evaluated chemicals to the medium proteins (Gülden et al. 2002). The application of different FBS contents due to varying protocols would result in incomparable results between different laboratories (Gülden et al. 1997). The complex chemical partitioning to the medium constituents as well as further reduction of C_{free} by sorption to multiwell plates (Gellert and Stommel 1999), the cells (Gülden et al. 2001), and the headspace above the well led to the conclusion that C_{nom} is an inadequate exposure metric for *in vitro* effect data (Gülden and Seibert 2005, Kramer et al. 2012, Armitage et al. 2014, Groothuis et al. 2015). For better comparability and interpretability of *in vitro* effect data, the C_{free} was proposed as quantitative metric because it is considered the chemical concentration that is available for direct diffusion through membranes (Heringa et al. 2003, Escher and Hermens 2004, Heringa et al. 2004, Gülden and Seibert 2005). C_{free} represents the most appropriate input parameter for QIVIVE models as it can be directly related to C_{unbound} (Figure 1) (Wetmore et al. 2012, Wetmore 2015). Because C_{free} is directly proportional to the concentration at the target site (C_{target}),

it can be expected that similar C_{free} in different exposure scenarios result in equal effects. In both *in vitro* and *in vivo* exposure scenarios, C_{free} can directly be linked to the total cellular concentration (C_{cell}) by the cell-water partition constant $K_{\text{cell/w}}$. The variability in bioavailability between chemicals and cell-based bioassays can obscure whether differences between *in vitro* platforms are truly the result of intrinsic sensitivity differences between the applied cell lines, the receptor expression and/or reporter gene design, or whether they were simply caused by differences in chemical bioavailability. Because of the lack of exposure control, *in vitro* cell-based bioassays were criticized for their reduced sensitivity, low inter-assay comparability, and the low suitability to predict effects on the *in vivo* level (Gülden and Seibert 2005). These apparent disadvantages can be overcome by improved dosimetry. Passive dosing and solid-phase microextraction (SPME) with polydimethylsiloxane (PDMS) was proposed to control and measure C_{free} in cell-based bioassays (Smith et al. 2010, Kramer et al. 2010). However, the application of cell-based bioassays in HTS systems requires the usage of multiwell plates with 384- and 1536-wells and corresponding medium volumes of 40 µL and 6 µL, necessitating the cost-intensive miniaturization of the PDMS devices to perform passive dosing and sampling directly in the assay medium. Therefore, exposure measurements are not suitable for the routine application of cell-based bioassays in HTS. Mass balance models represent a suitable alternative for the quantification of exposure concentrations. These models aim to quantify equilibrium chemical partitioning between the assay compartments, yielding the calculation of C_{free} and C_{cell} (Kramer et al. 2012, Groothuis et al. 2015). The first comprehensive equilibrium mass balance model applicable to various *in vitro* cell-based bioassays was developed by Armitage et al. in 2014. The study focused on neutral organic chemicals and their partitioning between medium components and cells. A large proportion of emerging micropollutants that are nowadays emitted into the environment are ionizable organic chemicals, such as pharmaceuticals, which necessitates the inclusion of these chemicals into the *in vitro* exposure framework. In the Armitage model, relevant chemical parameters were predicted based on simple quantitative structure-activity re-

lationships (QSARs) while relevant system parameters were estimated from earlier study results. Kinetic processes such as biotransformation, sorption to well materials, as well as cellular uptake and growth were discussed as possibly influencing factors but were largely neglected.

1.6 Aim of doctoral thesis

This thesis aimed to progress the assessment of exposure in *in vitro* cell-based bioassays as basis for improved dosing of chemicals, analysis and interpretation of *in vitro* effect data, and extrapolation to *in vivo* exposure scenarios. To achieve this, a prior examination was required regarding which conditions and processes in *in vitro* cell-based bioassays are fixed, and which are adjustable for improved dosimetry, in keeping with the motto: "nature versus nurture". The first goal was to develop an equilibrium mass balance model to predict C_{free} and C_{cell} in the reporter gene assays of the Tox21 database, while extending the applicability domain of the model to ionizable chemicals. We aimed to increase the accuracy of the model compared to existing models by (i) applying more precise chemical parameters that mechanistically depict the chemical interaction between the assay compartments and by (ii) providing and using experimental data on the relevant system parameters, such as the composition of the cells and the assay medium. In *Publication* 1, the model was applied to predict the Tox21 effect data of 100 neutral, anionic, cationic, and multiprotic chemicals with heterogenous physicochemical properties in order to verify the conclusions of earlier studies on *in vitro* bioavailability, to compare the model output with existing mass balance models, and to discuss the applicability of *in vitro* mass balance models to control and quantify *in vitro* exposure. In the further progress of the thesis, we aimed to assess the relevance of kinetic processes on *in vitro* exposure. A thorough literature research revealed that knowledge gaps existed on the kinetics of cellular uptake in *in vitro* cells and the extent of chemical sorption to multiwell plates, which we wanted to address by generating experimental data and the development of mathematical models that describe the kinetics (Figure 2). The developed mass balance model in *Publication* 1 assumed instantaneous equilibrium between cells and medium. The validity of this assumption was evaluated in *Publication* 2 by applying a method based on fluorescence microscopy and automated image analysis, capable of measuring C_{cell} over time during the typical 24-hour bioassay duration. With a small set of ten neutral and ionizable fluorophores and two cell lines, we aimed to assess whether cellular uptake kinetics need to

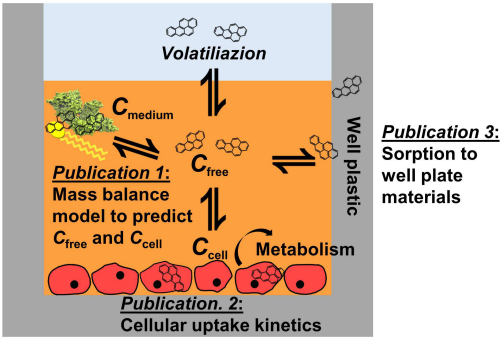

Figure 2: Typical setup of an *in vitro* cell-based bioassay with chemical concentrations in the assay compartments medium (C_{medium}, orange), cells (C_{cell}, red) and the bioavailable, freely dissolved concentration (C_{free}). The thesis aimed to develop a mass balance model to predict C_{free} and C_{cell} (*Publication* 1), to evaluate the relevance of cellular uptake kinetics (*Publication* 2), and to assess the chemical sorption to the well plate materials (*Publication* 3).

be considered in *in vitro* exposure models or whether the equilibrium assumption of the mass balance model sufficiently describes cellular exposure. Because pharmacological studies suggested an influence of HSA on the kinetics of drug uptake in human cells, a particular emphasis was set on the role of the medium FBS on the kinetics and extent of cellular uptake, not lastly to experimentally verify the model results presented in *Publication* 1. Chemical sorption to the plastic of multiwell plates was neglected in *in vitro* exposure models due to the lack of experimental data on the extent and kinetics of chemical partitioning to polystyrene, the common material used for the production of multiwell plates. As multiwell plates are widely used in HTS platforms, *Publication* 3 aimed to fill this data gap by developing a polystyrene-water partition experiment capable of simultaneously measuring diffusion coefficients in polysytrene D_{PS} and polystyrene-water partition constants $K_{\mathrm{PS/w}}$. The experimental database formed the basis for a predictive kinetic model to evaluate the relevance of multiwell plate sorption when applying different multiwell plates (96-, 384-, 1536-well plates) and media with FBS contents in the typical range of 0.5%-10%. The data on the kinet-

ics of cellular uptake and multiwell plate sorption were discussed with regard to the validity of the equilibrium assumption in existing mass balance models, while questioning the necessity of time-dependent exposure metrics such as the area under the curve (AUC). Based on the generated knowledge, the thesis demonstrates that simple exposure modeling can prospectively improve chemical dosing in *in vitro* cell-based bioassays while preventing poor data quality as a result of experimental artifacts. It is eventually evaluated whether and to what extent the progress in the framework of *in vitro* exposure modeling achieved within the thesis can increase the suitability of *in vitro* effect data to predict effects on the whole-organism level.

2 Summary

2.1 Theory of *in vitro* exposure models

This chapter provides the basic mathematical description of the mass balance model from *Publication* 1 and the kinetic models derived from the experimental data generated in *Publication* 2 and *Publication* 3, including the required system and chemical descriptors. Typical *in vitro* cell-based bioassays that apply mammalian cells consist of the compartments assay medium, the applied cell line, the well material (polystyrene), and the headspace above the medium (Figure 3).

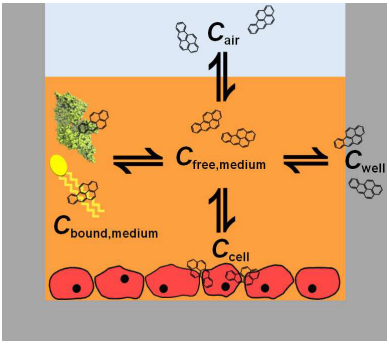

Figure 3: Typical setup of an *in vitro* cell-based bioassay with chemical concentrations in the assay compartments medium (C_{medium}, orange), cells (C_{cell}, red), well (C_{well}, grey) and air (C_{air}, light blue).

In order to quantify the chemical partitioning between these compartments, the phase volumes of these compartments have to be defined. The total volume of the assay V_{assay} can be defined as the sum of the respective compartment volumes (eq. 2).

$$V_{assay} = V_{medium} + V_{cell} + V_{well} + V_{air} \quad (2)$$

Chemical partitioning between these compartments can be quantitatively parameterized by the corresponding partition constants with the unit liter per liter (L L^{-1}), such as the cell-medium $K_{cell/medium}$, the air-medium

$K_{\mathrm{air/medium}}$, and the polystyrene-medium $K_{\mathrm{PS/medium}}$ partition constants. Partition constants to biological matrices and polymers are often reported as L kg^{-1} in the literature, which can be converted into L L^{-1} by consideration of the matrix density (1.04 kg L^{-1} for polystyrene, 1.0 kg L^{-1} for lipids, 1.36 kg L^{-1} for proteins). Please note that the application of the partition constants assumes equilibrium between cells, medium, air, and polysytrene, which can be kinetically hindered as discussed in chapters 2.2-2.4. The partition constants can be transmuted into one another with the thermodynamic cycle, as is exemplarily illustrated in eq. 3 for the cell-polystyrene partition constant $K_{\mathrm{cell/PS}}$.

$$K_{\mathrm{cell/PS}} = \frac{K_{\mathrm{cell/medium}}}{K_{\mathrm{PS/medium}}} \tag{3}$$

One of the major challenges of the thesis was the inclusion of ionizable chemicals into the *in vitro* exposure framework. Based on the pH value of the assay medium (typically physiological pH of 7.4) and acidity constant pK_a value of the chemical (corresponding $pK_b = 1 - pK_a$), the ionizable chemical dissociates into a neutral and a charged species. The neutral fraction $\alpha_{\mathrm{neutral}}$ can be derived by eq. 4.

$$\alpha_{\mathrm{neutral}} = \frac{1}{1 + 10^{(\mathrm{pH} - \mathrm{pK_a})}} \tag{4}$$

The distribution ratio of the chemical can be quantified by $\alpha_{\mathrm{neutral}}$ and the ionized fraction α_{ion} and their corresponding partition constants, as shown exemplarily for the cell-medium distribution ratio $D_{\mathrm{cell/medium}}$ (eq. 5).

$$D_{\mathrm{cell/medium}} = \alpha_{\mathrm{neutral}} \cdot K_{\mathrm{cell/medium}}(\mathrm{neutral}) + \alpha_{\mathrm{ion}} \cdot K_{\mathrm{cell/medium}}(\mathrm{ion}) \tag{5}$$

Because the distribution ratio of neutral chemicals equals the partition constant, the distribution ratio is used for both neutral and ionizable chemicals in the following. Note that chemical partitioning of the charged species to polystyrene was expected to be negligible ($K_{\mathrm{PS/medium}}$ (ion) = 0). Earlier studies have shown that the proteins and lipids in the medium represent the dominant sorptive colloids in the medium (Seibert et al. 2002, Kramer et al. 2012). In order to derive $D_{\mathrm{medium/w}}$, bovine serum albumin (BSA) and phos-

pholipid liposomes (lip) were used as surrogates for medium proteins and lipids, respectively. By combining the $D_{\mathrm{BSA/w}}$ and $D_{\mathrm{lip/w}}$ of the chemicals and the volume fractions of water $VF_{\mathrm{w/medium}}$, proteins $VF_{\mathrm{proteins/medium}}$, and lipids $VF_{\mathrm{lipids/medium}}$ in the medium, the $D_{\mathrm{medium/w}}$ can be derived (eq. 6).

$$D_{\mathrm{medium/w}} = VF_{\mathrm{w/medium}} + VF_{\mathrm{proteins/medium}} \cdot D_{\mathrm{BSA/w}} + VF_{\mathrm{lipids/medium}} \cdot D_{\mathrm{lip/w}} \tag{6}$$

Similar to the medium, the $D_{\mathrm{cell/w}}$ was determined based on experimentally measured phase volumes and corresponding partition constants, using BSA and lip as surrogates for cellular proteins and lipids (eq. 7).

$$D_{\mathrm{cell/w}} = VF_{\mathrm{w/cell}} + VF_{\mathrm{proteins/cell}} \cdot D_{\mathrm{BSA/w}} + VF_{\mathrm{lipids/cell}} \cdot D_{\mathrm{lip/w}} \tag{7}$$

By applying the compartment volumes and corresponding distribution ratios into the mass balance model, chemical fractions in equilibrium can be quantified, for instance the chemical fraction in the medium f_{medium} (eq. 8).

$$f_{\mathrm{medium}} = \left(1 + D_{\mathrm{cell/medium}} \cdot \frac{V_{\mathrm{cell}}}{V_{\mathrm{medium}}} + D_{\mathrm{air/medium}} \cdot \frac{V_{\mathrm{air}}}{V_{\mathrm{medium}}} + D_{\mathrm{PS/medium}} \cdot \frac{V_{\mathrm{PS}}}{V_{\mathrm{medium}}}\right)^{-1} \tag{8}$$

From the chemical fractions, the C_{nom} (mol L^{-1}), and the ratio of the total volume of the assay V_{assay} to volume of interest, the corresponding chemical concentration in an assay compartment can be calculated, such as the C_{medium} (mol L^{-1}) (eq. 9), the $C_{\mathrm{free,medium}}$ (mol L^{-1}) (eq. 10), and the C_{cell} (mol L^{-1}) (eq. 11).

$$C_{\mathrm{medium}} = C_{\mathrm{nom}} \cdot f_{\mathrm{medium}} \cdot \frac{V_{\mathrm{assay}}}{V_{\mathrm{medium}}} \tag{9}$$

$$C_{\mathrm{free,medium}} = C_{\mathrm{nom}} \cdot f_{\mathrm{free}} \cdot \frac{V_{\mathrm{assay}}}{V_{\mathrm{w,medium}}} \tag{10}$$

$$C_{\text{cell}} = C_{\text{nom}} \cdot f_{\text{cell}} \cdot \frac{V_{\text{assay}}}{V_{\text{cell}}} \tag{11}$$

With the equations 2-11, chemical equilibrium partitioning between the assay compartments is quantitatively described. The detailed derivation of the equations can be found in section 2 of *Publication* 1. The uptake curves of the evaluated neutral and ionizable chemicals in two cell lines evaluated in *Publication* 2 generally suggest a first order uptake kinetics equation as suitable mathematical description of cellular uptake over time in *in vitro* cell assays. $C_{\text{cell}}(t)$ is given by eq. 12.

$$C_{\text{cell}}(t) = C_{\text{cell},0} + (C_{\text{cell,eq}} - C_{\text{cell},0}) \cdot (1 - \mathrm{e}^{-k \cdot t}) \tag{12}$$

$C_{\text{cell},0}$ is the concentration that results from immediate chemical sorption to the outer cell membrane (y-intercept), $C_{\text{cell,eq}}$ is the concentration in cell-medium equilibrium (can be derived by eq. 11), k is the uptake rate constant (h^{-1}), and t is time (h). *Publication* 3 focused on the evaluation of the kinetics of multiwell plate sorption and the relevance for C_{medium}. In an aqueous medium with a defined uniform chemical concentration (C_{medium}, $\mathrm{mg\ L}^{-1}$), the concentration of the chemical in the polystyrene of the multiwell plate (C_{PS}, $\mathrm{mg\ kg}^{-1}$) meets the one-dimensional diffusion equation:

$$\frac{\partial C_{\text{PS}}}{\partial t} - D_{\text{PS}} \cdot \frac{\partial^2 C_{\text{PS}}}{\partial x^2} = 0 \tag{13}$$

subject to the following boundary and initial conditions:

$$C_{\text{PS}}(w, t) = D_{\text{PS/medium}} \cdot C_{\text{medium}}(t) \quad \forall t > 0 \tag{14}$$

$$C_{\text{PS}}(x, t = 0) = 0 \quad \forall x \tag{15}$$

x denotes the coordinate orthogonal to the surface, w is the width of the polystyrene, and t is time. Equations 13-15 were Laplace-transformed to set up an analytical model that predicts the chemical depletion in the medium

caused by sorption to polystyrene in the well (eq. 16).

$$\tilde{C}_{\text{medium}}(s) = \frac{C_{\text{medium}}(0)}{s + \sqrt{D_{\text{PS}} \cdot s} \cdot \frac{A_{\text{PS}}}{V_{\text{medium}}} \cdot D_{\text{PS/medium}} \cdot \varrho_{\text{PS}} \cdot \tanh\left(\sqrt{\frac{s}{D_{\text{PS}}}} \cdot w\right)} \quad (16)$$

$\tilde{C}_{\text{medium}}(s)$ is the Laplace-transformed medium concentration time series, A_{PS} is the surface area of the polystyrene being in contact with the medium in the well, ϱ_{PS} is the mass density of polystyrene (1.04 kg L^{-1}) and s is the complex Laplace coordinate (t^{-1}). For details of the derivation in the Laplace space, see the Supporting Information of *Publication* 3.

2.2 *Publication* 1: Modeling exposure in the Tox21 *in vitro* bioassays

The *in vitro* database Tox21 includes effect data of GeneBLAzer reporter gene bioassays that cover a broad range of cellular signaling pathways. This database was already used for different QIVIVE models, however, without considering the chemical bioavailability in the bioassays (e.g., Elmore et al. 2014, Knudsen et al. 2015). The Tox21 bioassays were performed in HTS format by robotic systems applying 1536-well plates and low medium volumes of 5-6 µL (Attene Ramos et al. 2013), which hampered the analytical quantification of C_{free} and C_{cell}. Thus, the 50% effect concentrations (EC_{50}) of the evaluated chemicals are reported based on C_{nom}, i.e. $EC_{50,\text{nom}}$. In *Publication* 1, a mass balance model was applied to the Tox21 reporter gene assays for modeling of freely dissolved and cellular effect concentrations ($EC_{50,\text{free}}$, $EC_{50,\text{cell}}$). Information on the bioassay setups was extracted from the Tox21 assay protocols. $EC_{50,\text{nom}}$ for 100 neutral, anionic, cationic, and multiprotic chemicals with heterogenous physicochemical properties and various MoA were gathered from the Tox21 effect database. These chemicals were identified as priority micropollutants due to their presence in German rivers, thus exposure of humans and environmental organisms is likely (Busch et al. 2016). The developed mass balance model should represent a step forward compared to the existing mass balance model applicable to HTS databases (Armitage et al. 2014). Earlier studies demonstrated that proteins and lipids are the dominant sorptive matrices for organic chemicals in *in vitro* media and cells (Gülden et al. 2001, Gülden et al. 2002), therefore corresponding volumes were estimated in Armitage et al. (2014). Here, proteins and lipids in cells and media were experimentally quantified by adaption and refinement of standardized photometric methods for measuring protein (Lowry assay, Lowry 1951) and lipid concentrations (sulpho-phospho-vanillin (SPV) method, Frings 1970) in various tissues. The water phase of the cells was neglected in mass balance models up to this point as they mainly focused on neutral hydrophobic chemicals that predominantly sorb to cellular proteins and lipids. The inclusion of hydrophilic neutral (e.g., caffeine) and ioniz-

able (e.g., metoprolol) chemicals necessitated the consideration of the water content in the cells to prevent the underestimation of C_{cell} for hydrophilic chemicals. Therefore, the total volume of the cells and their water content were determined in *Publication* 1 by measuring the wet weight before and the dry weight of the Tox21 cell lines after freeze-drying. The application of mass balance models to HTS platforms requires the accessibility to chemical partition constants. In Armitage et al. (2014), partition constants to proteins and lipids were derived from the log K_{ow} of the chemical, which can lead to a significant uncertainty and inaccuracy particularly for ionizable chemicals, as the charged species does not partition into octanol but can show high sorptive affinities to biomolecules. Expanding on this basis, we used BSA and lip as surrogates for proteins and lipids in medium and cells, respectively. For the 100 chemicals, experimental values were gathered from the literature. If no experimental data were available, mechanistic models were presented and applied to predict the BSA-water partition constants $K_{\mathrm{BSA/w}}$ and lip-water partition constants $K_{\mathrm{lip/w}}$, which were expressed as distribution ratios ($D_{\mathrm{BSA/w}}$, $D_{\mathrm{lip/w}}$) to account for the speciation of the ionizable chemicals at the medium pH of 7.4. Polyparameter free energy relationships (PP-LFERs) that consider various physicochemical properties of the chemicals and differences between the two sorbates, were applied for neutral chemicals and the neutral fraction of ionizable chemicals (Endo and Goss 2014). A great challenge was posed by the prediction of $D_{\mathrm{BSA/w}}$ and $D_{\mathrm{lip/w}}$ for the charged species of ionizable chemicals and permanently charged chemicals, for which COSMOmic and 3D-QSARs were used that account for three-dimensional interactions between chemicals and sorbents. By inclusion of these mechanistic models, we extended the applicability domain of *in vitro* mass balance models to complex chemicals, such as polar, permanently charged, and multiprotic chemicals, which make up a large proportion of environmental chemicals nowadays as pharmaceuticals and personal care products. The medium of the evaluated Tox21 reporter gene assays consisted of a basic medium supplemented with a FBS content between 0.5% and 10%. The basic medium contained a buffer that stabilizes the pH of the medium, commonly at the physiological pH of 7.4, as well as

different hormones, amino acids, vitamins (Dulbecco and Freeman 1959), and an antibiotic agent like streptomycin or penicillin to prevent bacterial contamination. The FBS was supplemented to the basic medium as nutrient supply to ensure optimal cell health and growth. The FBS has a high protein content of up to 10%, of which are approximately 60% albumin, but also containing important micronutrients such as vitamins, salts, and growth hormones (Gstraunthaler and Lindl 2013). The experimental determination of protein and lipid contents in the medium revealed that the media consisted of protein concentrations between 0.1 and 0.5 mL L^{-1} and lipid concentrations of 0.02 to 0.03 mL L^{-1}. Testing the medium constituents (basic medium and FBS) independently confirmed that the proteins and lipids mainly originate from the FBS supplemented to the medium, however, the basic medium also consisted of small amounts of proteins and lipids. The determined water, protein, and lipid contents of the Tox21 cells did not vary considerably between the different cell lines with standard deviations of 52%, 41% and 20%, respectively. The largest difference was observed for hepatic cell lines which consisted of considerably higher amounts of lipids compared to the other cell lines, resulting from the fatty acid synthesis expressed by the cells (Gibbons et al. 1994). The relatively small variations in the protein and lipid contents of the evaluated cell lines suggest using the average protein and lipid contents if experimental data on the phase volumes is not available. Modeling the bioavailability of 100 neutral and ionizable chemicals in the Tox21 reporter gene assays demonstrated that the medium represents the dominant sorptive sink for all evaluated chemicals. Due to their high $D_{\mathrm{BSA/w}}$ and $D_{\mathrm{lip/w}}$, most of the chemicals were predominantly bound to proteins and lipids in the medium, leading to an unsystematic and considerable reduction of C_{free} compared to C_{nom} (Figure 3 in *Publication* 1). These findings confirmed that C_{nom} is not a suitable parameter for chemical bioavailability in *in vitro* cell-based bioassays, emphasizing the necessity for *in vitro* exposure models that quantify C_{free} (Kramer et al. 2012, Armitage et al. 2014, Groothuis et al. 2015). The chemical partitioning into the cells was minor with a maximum of 16% for highly hydrophobic chemicals ($\log D_{\mathrm{lip/w}} > 6$), explaining the low sensitivity that was observed

for the Tox21 reporter gene assays (Capuzzi et al. 2016). The high degree of chemical partitioning to the medium appeared to be contradictory at first as the determined cell-water distribution ratios $D_{\mathrm{cell/w}}$ were higher compared to the corresponding medium-water distribution ratios $D_{\mathrm{medium/w}}$ by factors between 10 and 100 for most chemicals. However, comparing water, protein and lipid fractions in both the cells and the medium revealed that the medium makes up more than 99% of the total assay volume, i.e. the cumulate volume of water, proteins, and lipids. In other words, not the sorptive affinity of the chemical(s) determined the overall partitioning between the medium and cells, but the large medium volume to cell volume ratio. Comparing bioassays that applied high medium FBS contents of 10% with bioassays using 1% FBS emphasized that the FBS content is directly proportional to the sorptive capacity of the medium (Gülden et al. 1997), hence determining the C_{free} and C_{cell} in and the sensitivity of the bioassay (Figure 5 in *Publication* 1). In contrast to C_{free}, C_{cell} was proportional to C_{nom} for chemicals with a $\log D_{\mathrm{lip/w}} > 3$, as exemplarily illustrated for the androgen receptor (AR) assay in Figure 3B of *Publication* 1. This finding gains more relevance considering the application of relative effect potencies (REP) to characterize the *in vitro* toxicity of chemicals and mixtures (Villeneuve 2000, Escher et al. 2008). In REP analyses, the $EC_{50,\mathrm{nom}}$ of a chemical or mixture is related to the toxicity of a potent reference chemical. Provided that the proportional difference between C_{nom} and C_{cell} is given ($\log D_{\mathrm{lip/w}} > 3$), both $\mathrm{REP}_{\mathrm{nom}}$ and $\mathrm{REP}_{\mathrm{cell}}$ are equal, hence the toxic equivalency factor (TEF) approach remains valid for *in vitro* systems even though bioavailability can vary considerably between the assays, which enables the comparison of *in vitro* REPs to *in vivo* TEF (Van den Berg et al. 2006). The chemicals exhibited multifaceted chemical partitioning between proteins, lipid, and water in the medium and cells dependent on their $D_{\mathrm{BSA/w}}$ and $D_{\mathrm{lip/w}}$ (Figure 5 in *Publication* 1). These results deviate from the model results of Armitage et al. (2014) because here, $D_{\mathrm{BSA/w}}$ and $D_{\mathrm{lip/w}}$ were derived as experimental values from the literature or predicted by mechanistic models, illustrating the multifaceted partitioning between proteins, lipids, and water, whereas the Armitage model was inherently consistent due to the derivation of both

$D_{\mathrm{BSA/w}}$ and $D_{\mathrm{lip/w}}$ from the log K_{ow} of the chemical. Even though f_{cell} is small, the intracellular partitioning of a chemical between cellular water, proteins, and lipids is expected to be of great importance for the effects that result from chemical exposure. Due to the lower water volume fraction compared to the medium (average VF_{cell} of 88.4% compared to VF_{medium} of >99%), chemical partitioning to proteins and lipids was considerably higher compared to the corresponding distribution in the medium (Figure 5 in *Publication* 1). A large proportion of the chemicals, particularly neutral hydrophobic chemicals, were substantially sorbed to lipids in the cells, due to their higher $D_{\mathrm{lip/w}}$ compared to their sorptive affinity to proteins ($D_{\mathrm{BSA/w}}$). The minimum toxicity a chemical can cause is the disturbance of the cellular membrane structure and functioning, referred to as non-specific baseline toxicity or narcosis (Verhaar et al. 1996). The high sorptive affinity to cellular lipids could explain why the superhydrophobic neutral chemicals evaluated in *Publication* 1, particularly polycyclic aromatic hydrocarbons (PAHs) and PCBs, were reported to cause cytotoxicity at relatively low C_{free} (Judson et al. 2016). Given that measured effects were reported as $EC_{50,\mathrm{nom}}$ in the Tox21 database, chemical risk classification and prioritization based on the Tox21 effect data suffers from low comparability between the assays and a low extrapolation potential to other exposure scenarios, such as the application to QIVIVE models. The developed mass balance model can be applied by risk assessors to model $EC_{50,\mathrm{free}}$ and $EC_{50,\mathrm{cell}}$ to increase the significance and comparability of the *in vitro* effect data reported for the Tox21 reporter gene assays. Our model was already adapted by the U.S. EPA to evaluate the influence of cytotoxicity in the assays (Fay et al. 2018). The dominant role of the medium on chemical partitioning and the low degree of depletion by cellular uptake that was revealed for the evaluated *in vitro* cell-based bioassays, led to the assumption that the medium acts as chemical reservoir of reversibly bound chemicals potentially compensating for other depletive processes like sorption to the multiwell plate plastic polystyrene, which were central hypotheses tested in the *Publications* 2 and 3.

2.3 *Publication* 2: Cellular uptake kinetics of neutral and charged chemicals in *in vitro* assays measured by fluorescence microscopy

The kinetics of cellular uptake can represent an important parameter when assessing the cellular chemical exposure in *in vitro* cell-based bioassays. Because the mass balance model published in *Publication* 1 assumes instantaneous equilibrium between medium and cells, slow cellular uptake kinetics in relation to the total exposure time of typically 24 hours can lead to a considerable derivation of the cellular dose, i.e. the C_{cell} over time ($C_{\text{cell}}(t)$). In *Publication* 2, a method was developed that combined fluorescence and bright-field microscopy with automated image analysis to measure cellular uptake of ten neutral, anionic, cationic, and zwitterionic fluorophores during the 24-hour bioassay duration in 96-well plates with 200 µL medium. Two widely used human reporter gene cell lines were tested: the AREc32 cell line derived from MCF-7 human breast cancer cells (Wang et al. 2006) and the GR-UAS-bla based on the human embryonic cell line HEK293T, which was part of the Tox21 reporter gene assays (Attene Ramos 2013). Existing literature observed that the uptake of organic chemicals into *in vitro* fish and murine cells is relatively fast with equilibrium between cells and medium attained within 1-2 hours (Stadnicka-Michalak et al. 2014, Ali et al. 2015). The number of chemicals and cell lines tested was limited in these studies, requiring further data on different experimental setups, cell lines, and chemicals. We expected that only neutral chemicals or the neutral fraction of ionizable chemicals can permeate the cell membrane, whereas permeation of the charged species through the hydrophobic, nonpolar center of the membrane is slow and not likely to contribute to the cellular exposure within a 24-hour *in vitro* cell-based bioassay (Bean et al. 1968). Because pharmacological studies suggested an influence of HSA on the kinetics of drug uptake in human cells, the role of the medium FBS content on the kinetics of cellular uptake was one of the research questions addressed in *Publication* 2. Cellular uptake kinetics and extent of uptake were measured at five different medium FBS contents between 0.5% and 10%, the typi-

cal FBS range applied in the Tox21 reporter gene assays. We hypothesized two transport mechanisms driven by the FBS in the medium: First, the FBS might transport organic chemicals over the aqueous boundary layer (ABL) that builds up between the cell surface and the medium phase, because chemical diffusion through the ABL can take considerable time for unbound chemicals dependent on their diffusion coefficient in the medium. Due to the high amount of chemicals sorbed to the FBS molecules that likewise diffuse over the ABL, mass transfer would be faster compared to a medium without sorptive colloids. At the cell surface, chemicals desorb from the FBS driven by the chemical gradient built up by cellular uptake. This FBS-facilitated transport was inspired by the observation that the presence of dissolved organic matter accelerated the kinetics of chemical partitioning between different polymers and water (ter Laak et al. 2009). Second, chemicals could be co-transported by FBS molecules that are incorporated into the cells by endocytosis, which was termed HSA-mediated transport in pharmacological studies and adapted as FBS-mediated transport in *Publication* 2 (Poulin and Haddad 2015, Poulin et al. 2016). The experimental results of *Publication* 2 confirmed the high sorptive capacity of the medium that was indicated by the model results in *Publication* 1, because the chemical fluorescence intensity in the medium (FI_{medium}) was relatively constant during the 24-hour assay duration (<20% variability for all chemicals), confirming stable medium concentrations (C_{medium}) for the evaluated chemicals. The uptake curves for the chemicals generally demonstrated that cellular uptake can be delayed considerably, with time until 95% cell-medium equilibrium ($t_{95\%}$) even exceeding the 24-hour assay duration, as illustrated exemplarily for the neutral benzo(a)pyrene (B(a)P[N]), the permanently charged cation TMA-DPH[+], and the anion 1-pyrene-decanoic acid (1-PYR-DEC[-]) (Figure 4).

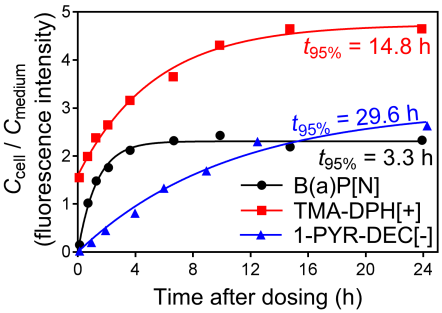

Figure 4: Ratio of C_{cell} and C_{medium} over time of B(a)P[N], TMA-DPH[+] and 1-PYR-DEC[-] in the GR assay applying medium supplemented with 0.5% FBS, as well as first-order uptake kinetics fits and corresponding $t_{95\%}$. C_{cell} and C_{medium} were measured as fluorescence intensities in the cells and medium ($\text{FI}_{\text{medium}}$, FI_{cell}) as described in *Publication* 2.

The fluorescence intensities in the cells (FI_{cell}) of six of the ten neutral and ionizable chemicals tested in *Publication* 2 reached equilibrium within 24 hours. The general observation was that neutral chemicals were taken up considerably faster by a factor of up to 12 compared to partially or permanently charged chemicals (Figure 2 in *Publication* 2), and that $t_{95\%}$ were reduced when increasing the medium FBS content from 0.5% to 10% (Figure 3 in *Publication* 2). The uptake kinetics of the two evaluated cell lines at the five different FBS contents indicated that the overall uptake of organic chemicals into *in vitro* cells and the resulting C_{cell} can be influenced by the interaction of several different transport mechanisms, as summarized in Figure 5. Transport into the cells was detectable for ionizable chemicals in *Publication* 2, even for permanently charged chemicals, questioning passive transport by diffusion through the cell membrane as only transport process involved (Bean et al. 1968). Diffusive transport over ion channels along the chemical gradient might have led to the considerable uptake of the ionized chemicals. The conformation of these ion channels enables the charged chemical to diffuse through the membrane following the chemical gradient, thus energy in form of ATP is not necessarily required (Bean 1992, Cavero and Guillon 1993). Ion channels can be part of the membrane of different cells, but were reported to be particularly frequent in cancer cell lines

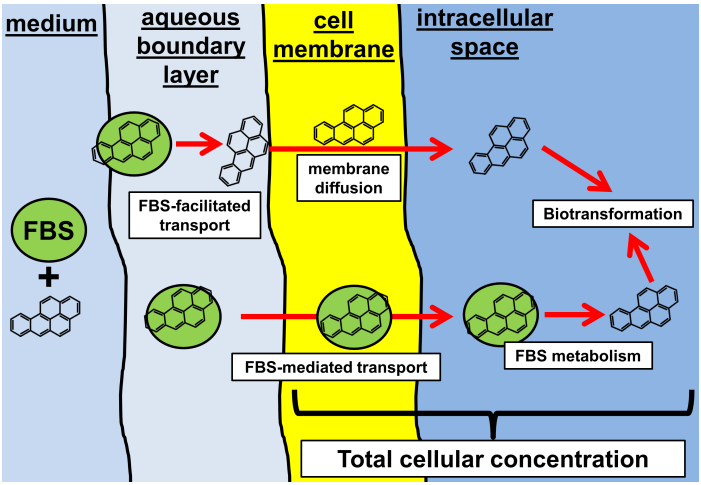

Figure 5: Active and passive transport mechanisms that are potentially involved in the kinetics and extent of chemical uptake into *in vitro* cells, leading to time-dependent C_{cell} that was measured as fluorescence intensity in the cells in *Publication* 2.

(Huber et al. 2015). Targeting of ion channels was recently discussed as suitable measure to increase the bioavailability of pharmaceuticals, particularly anion-permeable ion channels (Leanza et al. 2016). The occurrence of ion channels and their affinity to the evaluated chemicals could explain the rapid accumulation of the partially and permanently charged chemicals observed in *Publication* 2. The presence of membrane proteins that transport organic chemicals over the cell membrane in *in vivo* cells was already subject to numerous pharmacological studies (e.g., Tóth et al. 2014). It can be assumed that the relevance of membrane transporters on the chemical uptake in *in vivo* cells resembles their impact on *in vitro* bioavailability. *In vitro* transporter bioassays that assess whether new pharmaceutical drugs are transported into the cells by certain membrane proteins have already been developed (Volpe 2016). For TMA-DPH[+], active transport was evident in *Publication* 2, because similar C_{cell} were measured at different C_{free} indicating that the observed C_{cell} did not result from thermodynamic equilibrium but might be increased due to of a larger contribution of active transport at

higher FBS contents (Figure 6B). However, whether this phenomenon was caused by active transport, by membrane proteins, and/or FBS-mediated transport could not be clarified by the fluorescence microscopy method applied in *Publication* 2.

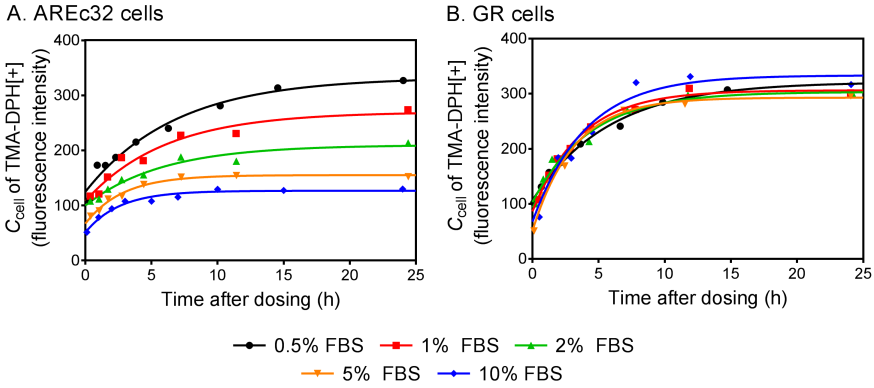

Figure 6: Time-dependent C_{cell} and corresponding first-order uptake kinetic fits of TMA-DPH[+] in the A. AREc32 and B. GR cells at 0.5% (black dots), 1% (red squares), 2% (green triangles), 5% (orange triangles), and 10% FBS content (blue diamonds) in the medium. C_{cell} was measured as fluorescence intensity in the cells (FI_{cell}) as described in *Publication* 2.

The type and quantity of active membrane transporters is expected to differ between different *in vitro* cell lines and their ability to carry organic chemicals could greatly vary, hence, occurrence and quantity of membrane transporters might lead to different C_{cell} dependent on the applied cell line and the chemical(s) tested, which would explain why similar C_{cell} of TMA-DPH[+] at different C_{free} was only observed for GR cells (Figure 6B), whereas C_{cell} in the AREc32 was decreased by a factor of 3 when changing the medium FBS content from 0.5% to 10% (Figure 6A), as expected based on the mass balance model. This observation indicates that active transport was significantly involved in the overall transport process for the GR cells while being of lesser relevance for the AREc32 cells. Although the data and derived first-order uptake kinetics gave extensive insight into the complexity of cellular uptake of organic chemicals, it needs to be identified which

transport processes are decisive for the overall uptake into *in vitro* cells, requiring to distinguish between active and passive transport processes in future projects. The large difference in $t_{95\%}$ between the chemicals could hinder the quantitative comparison of effects of single chemicals and mixtures that include both neutral and ionizable chemicals. Cell assays that were developed to assess chronic exposure can be more sensitive to charged chemicals as the time for the charged species to enter the cells is lower compared to the overall test duration. However, an AUC analysis of $\mathrm{FI}_{\mathrm{cell}}(t)$ illustrated that, for the evaluated bioassays setup, exposure over time was reduced by <20% for eight of the ten evaluated chemicals (Table 3 in *Publication* 2), indicating that the mass balance model from *Publication* 1, which assumes instantaneous equilibrium between medium and cells should still predict accurate C_{cell}, provided the accuracy of the model input parameters. The experiments in *Publication* 2 confirmed that the FBS in the medium has a high influence on the extent of cellular uptake (i.e., C_{cell}), but also on the kinetics of cellular uptake ($t_{95\%}$), which should be considered when changing the FBS content of an assay medium and when comparing the effect data of assays that applied different FBS contents.

2.4 *Publication* 3: Application of experimental polystyrene partition constants and diffusion coefficients to predict the sorption of neutral organic chemicals to multiwell plates in *in vivo* and *in vitro* bioassays

The application of *in vitro* cell-based bioassays to HTS formats favors the use of multiwell plates to enable the simultaneous measurement of multiple chemicals. 1536-well plates with medium volumes of 5-6 µL were used for the Tox21 reporter gene assays. The chemical sorption to the plastic material of multiwell plates was discussed as possible depletive chemical loss process in earlier studies on *in vitro* exposure (Kramer et al. 2012, Armitage et al. 2014, Groothuis et al. 2015). However, mechanistic data that quantitatively parameterize the sorption of organic chemicals to multiwell plate plastics were missing, hampering the inclusion of this process into existing exposure models. The most common multiwell plate material is polystyrene, a glassy, inflexible plastic that is persistent against most hydrophilic organic solvents. For cell culture purposes, polystyrene is often cross-linked with carboxyl and amine groups (TC-treated) and/or surface-coated with biopolymers for improved cell attachment (Ryan 2008). Neutral organic chemicals can diffuse into the polystyrene and accumulate into it to a considerable extent, as was already demonstrated by comparing the toxicity observed in *in vivo* assays when applying plastic multiwell plates and glass vials (Riedl and Altenburger 2007, Schreiber et al. 2008). Because of the reported low diffusion coefficients of neutral organic chemicals in polystyrene (log D_{PS} ≈ -13 to -19 m^2 s^{-1}) (Gavara et al. 1996, Begley et al. 2005, Bernardo 2012), sorption of organic chemicals in *in vitro* cell-based bioassays was expected to be time-dependent, necessitating the consideration of kinetics when including the process into the *in vitro* exposure framework. As was measured for PDMS and low density polyethylene (LDPE), we expected a correlation of D_{PS} with the molecular weight of the chemical. Sorption of the charged species of ionizable chemicals was expected to be negligible due to the lack of ionic interactions reported for polyacrylate and ethylene-vinyl acetate (Broeders et al. 2011, Oemisch et al. 2014). The high sorptive ca-

pacity of the FBS in the medium of *in vitro* cell-based bioassays raised the assumption in *Publication* 1 that the medium acts as a chemical reservoir potentially compensating for chemical depletion by multiwell plate sorption, which was supported by the stable C_{medium} measured in *Publication* 2 and the *in vitro* exposure study from Kramer et al. (2012). In *Publication* 3 we aimed to investigate to which extent the medium compensates for multiwell plate sorption at different medium FBS contents and in various multiwell plates applied in HTS platforms (96-, 384-, and 1536-well plates). *Publication* 3 provides experimentally determined D_{PS} and $K_{PS/w}$ of 22 neutral organic chemicals with heterogenous properties that cover a wide range of hydrophobicity (log K_{ow} 1.98-8.68) and molecular weight (154-396 g mol^{-1}). The data was applied to a kinetic model that predicts the depletion of C_{medium} by multiwell plate sorption based on the polystyrene surface area in the well, the medium volume, and the partition constant between polystyrene and medium ($K_{PS/medium}$). In order to emphasize the role of FBS, we compared the findings for *in vitro* cell-based bioassays to the FET assay that applies colloid-free aqueous medium. For *in vitro* cell-based bioassays, chemical partitioning to the polystyrene of multiwell plate represents a process of lower relevance compared to bioassays that apply colloid-free aqueous media (Figure 5 in *Publication* 3). Due to the increased affinity of the chemicals to the medium, partitioning into the polystyrene is expected to be considerably reduced since the chemical gradient between medium and polystyrene, expressed as $K_{PS/medium}$, is much lower compared to the gradient building up in aqueous media ($K_{PS/w}$) (Figure 6 in *Publication* 3). An AUC analysis was performed to quantitatively describe the time-dependent depletion of neutral organic chemicals in the medium by multiwell plate sorption. The results show that for *in vitro* assays in 96-well and 384-well plates that apply 200 µL and 40 µL medium, exposure is expected to decrease by <20% when applying 0.5% FBS (Figure 5 in *Publication* 3), confirming that chemical depletion by multiwell plate sorption has a lower impact on the medium exposure compared to assays that apply colloid-free media, such as the FET assay (Figure 4 in *Publication* 3). C_{medium} was expected to be reduced to a greater extent in higher tier

multiwell plates, such as for 4.7% in 96-well plates compared to 15.8% in 1536-well plates for chemical with a log K_{ow} 3 when applying 0.5% FBS. As hypothesized, increasing the FBS content in the medium from 0.5% to 10% decreased the depletion of C_{medium} from 15.8% to 8.5% in 1536-well plates due to the higher amount of sorptive proteins and lipids in the medium at 10% medium FBS. Predicted depletion of C_{medium} was generally highest for chemicals with a log K_{ow} between 3-4 because of the slope of 0.56 for the correlation between log K_{ow} and log $K_{PS/w}$, which is considerably lower compared to the almost 1:1 correlation between $K_{lip/w}$ and log K_{ow} (Endo et al. 2011). For lipophilic chemicals with log $K_{lip/w} > 4$, the depletion of C_{medium} by multiwell plate sorption is expected to decrease because of their relatively higher sorptive affinity to medium lipids (Figure 6 in *Publication* 3). The hypotheses drawn in *Publications* 1 and 2 were confirmed: First, the larger volume of medium used in lower tier multiwell plates (e.g., 200 µL in 96-well plates) compared to the 6 µL used in 1536-well plates reduces the polystyrene surface area to medium volume ratio thus decreasing the proportion of C_{medium} sorbed to the well plate after a certain time frame. Second, with increasing FBS, the percentage depletion by multiwell sorption decreased due to the larger amount of proteins and lipids in the medium. The results emphasize that chemical sorption to the polystyrene of multiwell plates can be neglected when applying higher medium FBS contents and low- or middle-tier multiwell plates (96- or 384-well plates). Contrarily, 0.5% medium FBS in 1536-well plates with 5-6 µL medium volume can lead to considerable chemical losses foremost when simultaneous depletion occurs by cellular uptake and volatilization, which could have represented a source of uncertainty in the modeling of the Tox21 *in vitro* effect data with the mass balance model in *Publication* 1. The database of $K_{PS/w}$ and D_{PS} and associated predictive models that were reported in *Publication* 3 can be applied by external users to evaluate the relevance of multiwell plate sorption in both *in vitro* and *in vivo* bioassays, either prospective for improved dosing or retrospective for increased interpretability of chemical exposure by AUC analyses. The generated knowledge on polystyrene sorption is not only important for the exposure assessment in bioassays, but also for the

packaging industry and of relevance for environmental chemical transport modeling considering the large amounts of polystyrene present in the environment as macro- and microplastics (Song et al. 2015).

2.5 Combined model results

This chapter provides a general impression of the complexity of chemical partitioning in cell-based bioassays and how differences in the experimental setup of the assays can influence bioavailability. Therefore, the models described in chapter 2.1 were combined to predict the chemical partitioning of ten neutral organic chemicals between the medium, the cells, the air and the multiwell plastic after the typical 24-hour assay duration (Figure 7).

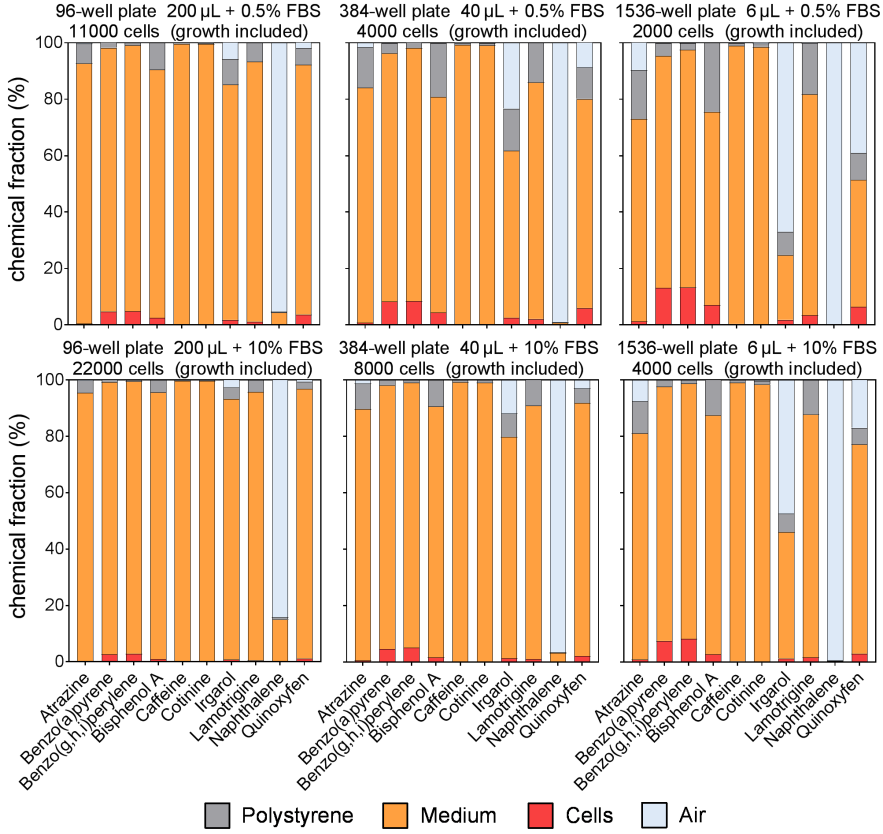

Figure 7: Chemical partitioning of ten neutral organic chemicals between the assay compartments multiwell plate plastic (polystyrene), medium, air and cells after the common assay duration of 24 hours given different experimental setups.

The chemicals were selected because they cover a large range of hydrophobicity (log K_{ow}) and Henry law constant (i.e., tendency to partition to the air). Different experimental setups were tested: The typical multiwell plate formats with 96-, 384- and 1536-wells and corresponding medium volumes of 200, 40, and 6 µL. The generic medium reported in *Publication* 1 was used, which is composed of a basic medium supplemented with 0.5% and 10% FBS, representing the typical range of % FBS supplemented to the medium of mammalian cell-based bioassays. An air volume of 1 L was assumed, which is discussed in detail in chapter 2.8. Standard cell numbers of the generic cell from *Publication* 1 were used including cell growth rates at the corresponding medium FBS content after 24 hours that were measured by bright-field microscopy in *Publication* 2. Most of the evaluated organic chemicals are predicted to sorb to the medium to the largest extent (>80%), confirming that the medium is the major determinant for chemical partitioning and bioavailability in cell-based bioassays, even when combined depletion by chemical partitioning to polystyrene, the air and the cells occurred during the 24-hour assay duration (Figure 7). Naphthalene represented an exception, which was predicted to predominantly partition to the air compartment in all evaluated setups. With increasing well number in the plate and correspondingly decreasing medium volumes (200 µL in 96-well plates compared to 6 µL in 1536-well plates), the depletion of C_{medium} by partitioning to the other compartments increases. Chemical partitioning to the medium was considerably lower at 0.5% FBS compared to 10%, such as for lamotrigine with f_{medium} of 78% at 0.5% and 86% at 10% medium FBS, demonstrating again that the extent of chemical partitioning to the medium correlates with the applied medium FBS content (Gülden and Seibert 1997, Gülden et al. 2002). Although most chemicals were predicted to partition predominantly to the medium, chemical partitioning between the assay compartments still differed between the evaluated chemicals. The hydrophilic chemicals caffeine and cotinine were predicted to partition to the medium by >99% independent on the multiwell plate and medium setup, whereas the hydrophobic benzo(a)pyrene and benzo(g,h,i)perylene were predicted to partition to a higher extent to the cells, particularly in low medium

volumes with 0.5% FBS (maximum of 13% in 1536-well plates). The moderately hydrophobic bisphenol A and lamotrigine were predicted to sorb to the polystyrene to a higher extent than the other chemicals tested, due to the nonproportional sorption affinities to polystyrene and the medium, as discussed in chapter 2.4. The combined model results presented in Figure 7 emphasize the complexity of chemical partitioning in *in vitro* cell assays and the necessity to experimentally parameterize *in vitro* exposure model to accurately predict C_{free} and C_{cell}.

2.6 Serum-mediated passive dosing

The generated knowledge in the *Publications* 1-3 leads to important conclusions regarding the factors that influence bioavailability in *in vitro* cell-based bioassays: The medium is the major determinant for chemical partitioning within the assay because it represents the dominant sorptive sink. Because of the high sorptive capacity of the medium, it is only marginally depleted by cellular uptake, sorption to multiwell plates, and volatilization, leading to stable exposure conditions in the medium and consequently to stable C_{free}. Due to the analogy to conventional passive dosing, in which chemical exposure is kept constant by redelivery from a chemical-saturated polymer (Smith et al. 2010), the term serum-mediated passive dosing (SMPD) was introduced in *Publication* 2. The assumption of proportional C_{medium} and C_{free} requires that the kinetics of chemical resorption from medium proteins and lipids are faster than the depletive process in order to keep C_{free} virtually constant. Literature suggests that resorption of chemicals that are reversibly bound to proteins and lipids is relatively fast, such as in the range of minutes for BSA (Kramer et al. 2007, Krause et al. 2018), which is fast in relation to the slow depletion by sorption to multiwell plates and cellular uptake, for which partitioning kinetics were in the range of several hours (chapters 2.3 and 2.4). The suitability of SMPD to stabilize C_{medium} was experimentally confirmed in *Publications* 2 and 3 for a set of heterogenous neutral and ionizable chemicals. Similar C_{free} after 0 and 24 hours were recently measured by *in situ* SPME measurements for a small set of neutral and ionizable chemicals in the AREc32 assay applying 10% FBS (Henneberger et al. 2018b), verifying the suitability of the chemical reservoir in the medium to stabilize C_{free} over the entire assay duration for these chemicals. Increasing the medium FBS content from 0.5% to 10% considerably increases the amount of sorptive proteins in the medium, such as by a factor of 4.4 for a 6 µL medium in 1536-well plates leading to an increased C_{medium}, as exemplarily shown for B(a)P[N] for which an increased $\text{FI}_{\text{medium}}$ of 2 was measured at 10% FBS compared to 0.5% FBS in 96-wells with 200 µL medium (Figure 8B). These additional sorptive proteins increase the capacity of the chemical reservoir in the medium, enhancing its ability

to compensate depletive processes. However, they also decrease the C_{cell} of chemicals and thus the sensitivity of the assay, as exemplarily shown for B(a)P[N] in Figure 8A, for which a reduction in FI_{cell} of a factor of 4 was measured when increasing the medium FBS content from 0.5% to 10%.

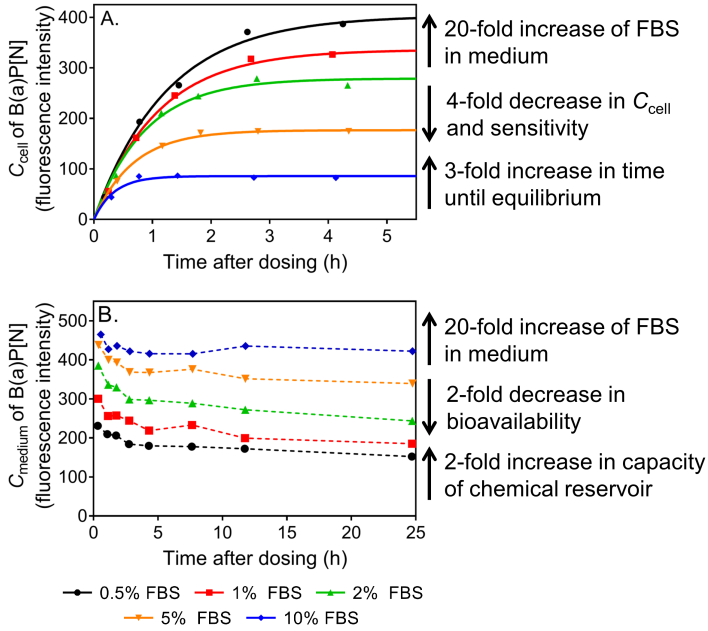

Figure 8: A. C_{cell} of B(a)P[N] and B. C_{medium} of B(a)P[N] at 0.5% (black dots), 1% (red squares), 2% (green triangles), 5% (orange triangles), and 10% FBS content (blue diamonds) in the medium, as well as resulting consequences for the applicability of SMPD, test sensitivity, and kinetics of cellular uptake. C_{cell} and C_{medium} were measured as fluorescence intensity in the cells and medium (FI_{medium}, FI_{cell}) as described in *Publication* 2.

Provided that the chemical partitioning to the medium constituents can be accurately quantified by mass balance modeling, the chemical reservoir in the medium represents a suitable tool to stabilize bioavailability in the assay. As shown in Figures 7 and 8, the applicability of SMPD is strongly dependent on the medium FBS content and the applied multiwell plate format, as well as the physicochemical properties of the chemical. C_{medium} can be de-

pleted to a considerable extent (> 20%) when applying low medium FBS contents in low medium wells (5-6 µL), as was done in the Tox21 reporter gene assays. Interestingly, chemicals with a log K_{ow} of 3-4 such as bisphenol A that are relatively sensitive to polystyrene sorption ($K_{PS/medium(0.5\%FBS)}$= 27.3) while partitioning to the cells to considerable extent (log $K_{cell/w}$ of generic cell = 2.23), could not be controlled by SMPD when applying low medium FBS contents. Volatile chemicals with a log $D_{air/medium}$ of <-6 are not applicable to SMPD in multiwell plates, which is discussed in detail in chapter 2.8.

2.7 Relevance of kinetics

The model results and the experimental data generated in *Publications* 1-3 generally support the application of the mass balance model that assumes equilibrium between cells and medium while not considering the kinetics of cellular uptake and neglecting multiwell plate sorption. Figure 9 illustrates the relevance of kinetics for the external exposure (C_{medium}) and cellular exposure (C_{cell}) of B(a)P[N] based on the AUC of both $C_{\text{medium}}(t)$ and $C_{\text{cell}}(t)$ compared to the maximum C_{medium} and C_{cell} that would result from instantaneous partitioning between medium and cells and constant chemical concentrations the medium. The results emphasize that the temporal change in C_{medium} due to cellular uptake, multiwell plate sorption, and other depletive processes is negligible with 2.4% reduced AUC exposure in the medium, thus stable chemical bioavailability in the exposure medium is assured during the 24-hour assay duration by SMPD. Likewise, for the two assay setups and ten neutral and ionizable chemicals evaluated in *Publication* 2, experimentally determined C_{medium} remained relatively constant over the entire test duration (<20% reduced C_{medium} over 24 hours). These findings support the quantification of C_{free} by the mass balance model published in *Publication* 1. The relevance of cellular uptake kinetics and cell growth is also small with only 5.4% reduced cellular AUC exposure during

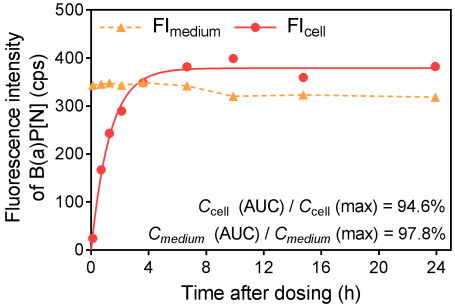

Figure 9: C_{cell} and C_{medium} as well as corresponding AUC of B(a)P[N] over time in the GR assay applying medium supplemented with 0.5% FBS. C_{cell} and C_{medium} were measured as fluorescence intensities in the cells and medium ($\text{FI}_{\text{medium}}$, FI_{cell}) as described in *Publication* 2.

the 24 hours, and <20% reductions were measured for eight of ten chemicals in the GR cells. With increasing duration of the *in vitro* cell-based bioassays, the relevance of the cellular uptake kinetics will decrease. Contrarily, the amount of chemicals that sorb to the polystyrene of multiwell plates and the relevance of the process will increase with the duration of the assay. The evaluation of the kinetics generally emphasized that for the evaluated chemicals and bioassay setups, the equilibrium mass balance model leads to realistic and reliable C_{cell} and C_{free}. Still, we have identified chemicals for which a continuous increase in C_{cell} occurred even after 24 hours ($t_{95\%}$ up to 50 hours, see Table 2 in *Publication* 2), which necessitates the inclusion of cellular uptake kinetics into the model in such scenarios. The inclusion of kinetic processes into exposure considerations should generally be favored to increase the accuracy of the predicted exposure data, provided that the necessary input data to run the kinetic models are available (eqs. 12 and 16). In the experiments and model approaches that were performed within the framework of the thesis, we identified processes and chemicals that exceed the applicability domain of SMPD, which are discussed in the following chapter 2.8.

2.8 Sources of uncertainty

Volatilization

A complex process influencing bioavailability in *in vitro* cell assays is the chemical partitioning to the air compartment. Because common multiwell plates that are applied in HTS are only sealed with a plastic lid or a breathable foil, chemical partitioning into the air is not limited to the small headspace above the medium in the well (Schreiber et al. 2008), which complicates the estimation of V_{air} and integration of air partitioning into the mass balance model. Because of the large volume of air that is available for chemical partitioning, the partitioning of chemicals to the air compartment is expected to be time-dependent, hence, the equilibrium assumption in the mass balance model could not hold. Because of these uncertainties, air partitioning was neglected in the mass balance model presented in *Publication* 1 and it was stated that chemicals with an $K_{\mathrm{air/w}} > 0.03$ are not applicable to *in vitro* cell-based bioassays based on an estimated headspace volume of 10 mL. However, measured C_{medium} of the semi-volatile PAHs phenanthrene and anthracene in *Publication* 3 indicated that this cut-off might underestimate the extent of loss. Despite their relatively low $D_{\mathrm{air/w}}$ of 0.002 and 0.003 at 37 °C (PP-LFER database, Ulrich et al. 2017), phenanthrene and anthracene were depleted more than predicted by the kinetic exposure model while including chemical partitioning to the medium, the cells and the multiwell plate (Figure 10). This discrepancy was most probably not caused by pipetting errors because the samples that served as 100% recovery controls were pipetted into the extraction vials by the same procedure as the samples (see section 3.4 of *Publication* 3). The higher depletion of phenanthrene and anthracene (16% and 12% after 24 hours) than predicted by the kinetic model was probably caused by chemical volatilization. Applying the degree of depletion by air partitioning after 24 hours into eq. 8 (calculation of f_{air}) indicates a headspace volume V_{air} in the range of 1 L, questioning the 10 mL that were assumed in *Publication* 1. The chemical depletion by volatilization emphasizes that not only the headspace right above the medium is available for partitioning, but that volatile chemicals

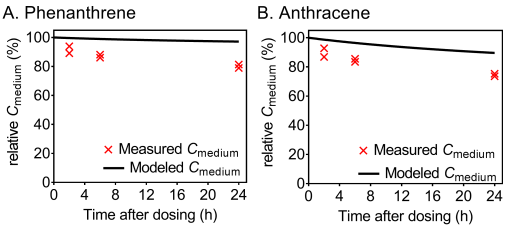

Figure 10: C_{medium} measured by liquid-liquid extraction and modeled by the kinetic model from *Publication* 3 (eq. 16). The measured C_{medium} is lower compared to the predicted C_{medium}, probably because of chemical volatilization.

can be potentially emitted into the headspace of the whole cell incubator. Figure 10 indicates that chemical air partitioning exceeds the 24-h assay duration, suggesting ongoing partitioning kinetics that are not adequately reflected by an equilibrium mass balance model. The experiments presented in Figure 10 applied 96-well plates with medium volumes of 200 µL and 10% medium FBS. Figure 11 predicts the chemical fractions of the 55 neutral organic study chemicals in such an assay system after applying their corresponding $D_{\text{air/medium}}$ in the mass balance model assuming an air volume of 1 L.

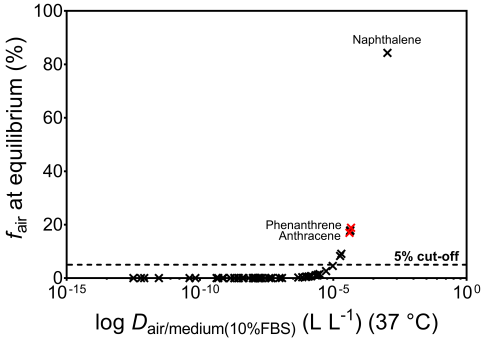

Figure 11: Predicted chemical fraction in the air (f_{air}) at equilibrium in a cell-based bioassay performed in 96-well plates, a medium volume of 200 µL supplemented with 10% FBS and an air volume of 1 L. $D_{\text{air/w}}$ of the chemicals were derived from the PP-LFER database (Ulrich et al. 2017).

Although the $D_{\mathrm{air/w}}$ of all evaluated chemicals but naphthalene is <0.02, seven of the 55 neutral organic chemicals are expected to be >5% depleted from the medium by air partitioning. Naphthalene was depleted by 84% after 24 hours with an $D_{\mathrm{air/w}}$ of 0.03, confirming the model results in Figure 7. Besides phenanthrene and anthracene, chlorpyrifos, 2-(methylthio)benzothiazole, diazinon, and PCB 52 were depleted by >5% over the 24-hour assay duration. Interestingly, some chemicals with relatively low log $D_{\mathrm{air/w}}$ such as diazinon with -3.77 were considerably depleted (17.9%) while other chemicals with higher log $D_{\mathrm{air/w}}$ such as -2.99 of 4-nonylphenol were less depleted (0.6%). This phenomenon results from the higher sorption of 4-nonylphenol to the medium (log $D_{\mathrm{medium(10\%FBS)/w}}$ = 2.93) compared to diazinon (log $D_{\mathrm{medium(10\%FBS)/w}}$ = 0.59), eventually resulting in higher $D_{\mathrm{air/medium(10\%FBS)}}$ for diazinon than 4-nonylphenol. These predictions demonstrate that SMPD is capable of compensating air partitioning to a considerable extent. For the evaluated medium composition and volume, the 5% cut-off corresponds to an log $D_{\mathrm{air/medium(10\%FBS)}}$ of -5 . With decreasing medium volume and medium FBS content, the influence of air partitioning on C_{medium} increases, as was indicated in Figure 7. Note that the predictions and corresponding cut-off presented in Figure 11 assume a 1 L headspace volume, that was in turn estimated based on the experimentally quantified C_{medium} of three chemicals. Further data is needed in order to adequately assess the relevance of volatilization in cell-based bioassays. Still, a log $D_{\mathrm{air/medium}}$ of <-6 can be used as approximate cut-off to ensure that air partitioning is negligible when assessing bioavailability in cell-based bioassays. These results demonstrate that air partitioning can lead to considerable chemical losses from the medium, particularly due to the 37 °C assay temperature that increases the log $D_{\mathrm{air/w}}$ compared to room temperature. Because not only the headspace above the medium is saturated with chemicals, chemical exchange between single wells could lead to uncertainties when testing several volatile chemicals in one plate. It is not advisable to perform *in vitro* assays with volatile chemicals using open well plates, and alternative methods targeting volatile chemicals were developed (Aufderheide et al. 2002, Pariselli et al. 2009), such as the control

of exposure and saturation of the headspace by hanging droplets in closed glass vials (Liu et al. 2013) and the usage of a headspace-free test system (Stalter et al. 2013). Because this thesis targets the application of *in vitro* cell-based bioassays in HTS format applying standardized multiwell plates, non-volatile chemicals were prioritized.

Erroneous model parameters

Independent experimental determination of the protein and lipid concentrations of basic medium and FBS showed that the basic medium also consists of small amounts of proteins and lipids, such as 0.86 mL proteins and 0.19 mL lipids per liter DMEM Glutamax (Supporting Information of *Publication* 1). However, it is likely that polar, non-sorptive constituents of the basic medium containing C=C double bonds, such as large vitamins and hormones, were reactive in the SPV-method leading to a higher apparent lipid concentration and an overestimated sorptive capacity of the basic medium. This assumption was supported by the larger decrease in C_{cell} of B(a)P[N] at higher FBS contents measured in *Publication* 2 than predicted by the model in *Publication* 1, indicating that the sorption of B(a)P[N] to the basic medium is overestimated by the model. This observation was recently confirmed by experimental determination of basic medium-water distribution ratios $D_{\mathrm{DMEM/w}}$ (Henneberger et al. 2018a), which were considerably lower than predicted based on the protein and lipid concentrations of the basic media reported in *Publication* 1. The protein and lipids contents of the basic media can represent a source of uncertainty in determining the $D_{\mathrm{medium/w}}$ (eq. 6). Non-linear sorption isotherms can lead to erroneous predictions by the mass balance model as it assumes that the different distribution ratios ($D_{\mathrm{cell/w}}$, $D_{\mathrm{medium/w}}$, $D_{\mathrm{PS/w}}$) are independent of the chemical concentration, hence excluding saturation of the sorption phases. The saturation of the albumin that is the most frequent protein in FBS, was observed for anions at concentrations in the medium that fall into the concentration range typically tested in concentration-response experiments (Henneberger et al. 2018a). Anion saturation of the medium FBS can already occur at low concentrations due to their high sorptive affinity to proteins compared

to lipids. The saturation of the medium would result in C_{free} exceeding the predictions by the mass balance model that does not factor in saturation of medium constituents. Chemical saturation of the polystyrene is not expected up to a molar fraction of the chemical >0.1 in the polymer (Bernardo 2012), which is not reached with typical concentration-response testing. Experimental $D_{\text{cell/w}}$ of anions that were determined within this recent study were also substantially lower compared to $D_{\text{cell/w}}$ derived by eq. 7 (Henneberger et al. 2018a), questioning either the measured phase volumes by the Lowry assay and SPV-method or the applied surrogates for proteins (BSA) and lipids (lip). Because measured $D_{\text{cell/w}}$ agreed with predicted values for neutral and cationic chemicals, it can be assumed that chemical sorption of anions to cellular proteins is not adequately reflected by their interaction with BSA. Studies reported that partitioning of anions to BSA can depend on the chemicals' 3D-structure and is not the result of non-specific interactions (Henneberger et al. 2016), as is the case for neutral chemicals (Endo and Goss 2011). The usage of BSA as surrogate for cellular proteins could lead to inaccurate model predictions since the cells are expected to be composed of structural proteins rather than functional proteins like BSA. Particularly for anions, predicted C_{cell} could be overestimated by the mass balance model because of their complex interactions with proteins. The availability of partition constants to structural proteins is still scarce, hampering the inclusion of structural proteins as surrogates for cellular proteins in the model so far.

Abiotic degradation

In cases of rapid abiotic degradation in the medium, C_{medium} could considerably decrease within the assay duration. Photolysis of chemicals that are sensitive to light, such as PAHs for which photolysis was already reported (Lampi et al. 2006, Willis and Oris 2014). The amount of chemicals that are photolysed during the assay duration depends on the light sensitivity of the chemical and the intensity of the light. Because *in vitro* assay plates are typically incubated in the dark, photolysis is considered to have a minor impact. However, chemical dosing is commonly performed at daylight, which

could represent a source of uncertainty for chemicals that are rapidly degraded by photolysis. Depletion in C_{medium} could further result from chemical reactions involving nucleophiles, such as the breakage of ester bonds by hydrolysis (Schwarzenbach 2016). The conversion rates of a chemical by nucleophilic substitution can considerably increase with temperature. An increase of the temperature by 10 °C can lead to an increase in the reaction rate by a factor of 3-5 (Schwarzenbach 2016). *In vitro* assays are typically carried out at physiological temperature (37 °C), at which hydrolysis reactions should play a minor role for the majority of chemicals. However, some chemical structures are sensitive to certain types of nucleophiles, such as the unimolecular nucleophilic substitution of chemicals with a tertiary alcohol group by chlorinated nucleophiles with potential half times of the degraded chemicals of 23 seconds (Schwarzenbach 2016). Such rapid reactions could lead to a considerable depletion of C_{medium}, because the decrease in C_{free} would lead to a rapid resorption of FBS bound chemicals, decreasing C_{total} over time. For both photolysis and hydrolysis reactions, the degradation products can have different physicochemical properties compared to the parent chemical therefore exhibiting altered chemical partitioning between the assay compartments and potentially a different affinity to the target receptor. Chemicals that are not stable in *in vitro* assay media are generally hard to test, and it should be questioned whether in makes sense to test these chemicals in the chemical risk assessment framework. Chemicals that are unstable under such controlled conditions are presumably not stable *in vivo* and in the environment, making it senseless to assess their effects. In fact, it would make more sense to identify their degradation products in the environment and measure corresponding effects in order to assess the risk of the parent chemical, as was done for methyl triclosan, the degradation product of triclosan (Lozano et al. 2013).

Biotransformation

Bacterial contamination and a potential metabolic turnover of chemical by bacteria should be prevented in *in vitro* assays because the bacterial contamination can negatively affect the cells. In *Publication* 2, we measured

rapid and considerable reductions in C_{cell} of B(a)P[N] when using AREc32 cells. Since these reductions were not measured for GR cells using the same medium composition and multiwell plates (Figure 12), cellular biotransformation appears to be most reasonable.

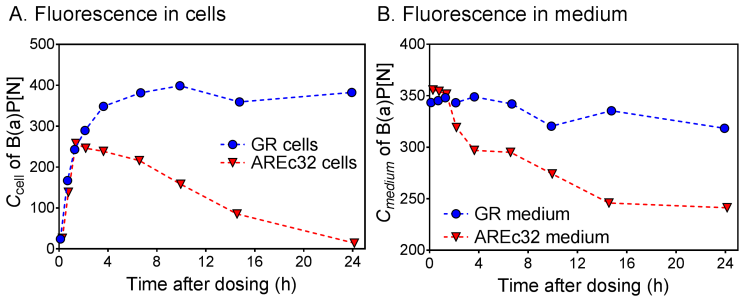

Figure 12: A. C_{cell} and B. C_{medium} of B(a)P[N] in the cells and medium of the GR (blue circles) and AREc32 assays (red triangles) measured as fluorescence intensity in the cells and media (FI_{cell}, $\text{FI}_{\text{medium}}$).

The metabolic turnover was that high that C_{medium} was considerably reduced. Biotransformation of B(a)P[N] is a well-known process in *in vivo* and *in vitro* hepatocytes (Diamond et al. 1980), however, the results of *Publication* 2 suggest that other cell lines are likewise capable of degrading B(a)P[N], despite existing literature suggests that AREc32 are not capable of metabolism of B(a)P[N] (Ding et al. 2009). Cellular biotransformation should generally be interpreted as part of the biological response by the cells to chemical stress. It is not advisable to counteract biotransformation by passive dosing from a saturated polymer as both the parent chemical as well as the transformation product(s) can contribute to the measured effects on the cellular level. For instance, biotransformation of B(a)P[N] results in the transformation product benzo(a)pyrene-7,8-dihydrodiol-9,10-epoxide, which is reactive and genotoxic to a higher extent than its parent chemical (Madureira et al. 2014). A redelivery of B(a)P[N] after its degradation would increase the concentration of the epoxide metabolite even further without decrease in the concentration of B(a)P[N], which would in the end result in a mixture effect of both the parent chemical and its transforma-

tion product for which the corresponding equilibrium concentration would be determined by the transformation rate of the applied cell line.

3 Relevance

3.1 Smart dosing strategies

The first step to face the challenge of implementing *in vitro* cell-based bioassays into chemical risk assessment is to improve the chemical dosing for increased reliability of *in vitro* effect data and prevention of experimental artifacts that can lead to false results. This section demonstrates how to improve chemical dosing in cell-based bioassays considerably with minimum effort. The smart usage of available information on the assay system and test chemicals is crucial to accurately plan the chemical dosing before running an assay. The non-consideration of chemical and/or system associated limitations and uncertainties can lead to poor data quality or, in the worst case, to data that cannot be interpreted.

Prediction of $C_{\mathbf{free}}$ by simplified mass balance modeling

As was discussed in section 2.5, the medium of *in vitro* cell assays represents the major determinant for chemical partitioning within the test system, thus, the most relevant parameter that needs to be known is the composition of the medium, in particular the medium FBS content, which is proportional to the amount of sorptive medium proteins and lipids. The application of higher medium FBS contents favors the suitability of SMPD to stabilize exposure, which is advisable when optimizing an *in vitro* cell-based bioassay. Provided that C_{medium} and thus C_{free} remains stable by SMPD, C_{free} can be approximated by a simple mass balance that accounts only for binding to FBS while neglecting other depletive processes.

$$C_{\mathrm{free}} = C_{\mathrm{free}} \cdot \left(1 + D_{\mathrm{BSA/w}} \cdot \frac{V_{\mathrm{proteins,\%FBS}}}{V_{\mathrm{w,medium}}} + D_{\mathrm{BSA/w}} \cdot \frac{V_{\mathrm{lipids,\%FBS}}}{V_{\mathrm{w,medium}}}\right)^{-1} \cdot \frac{V_{\mathrm{assay}}}{V_{\mathrm{w,medium}}} \tag{17}$$

With rising medium volume and medium FBS content and hence a larger chemical reservoir in the medium, the accuracy of calculated C_{free} by eq.

17 is expected to increase. By that means, a defined C_{free} can be adjusted in the medium without the need to parameterize the other assay compartments. It is expected to be sufficiently accurate to use the protein and lipid concentrations of the FBS types that were reported in *Publication* 1. Note that FBS is a natural product with varying protein and lipid concentrations between different lots, therefore it is advisable to measure protein and lipid concentrations of each fresh FBS lot to prevent systematic errors. Still, modeling C_{free} by eq. 17 and literature data on the composition of the FBS is already a step forward compared to the usage of C_{nom} for chemical dosing.

Calculation of maximum medium concentrations

Since C_{free} is expected to be proportional to C_{medium}, the maximum medium concentration $C_{\mathrm{medium,sat}}$ needs to be calculated for the preparation of the dosing solution to measure the full dose-response curve. To achieve that, the $D_{\mathrm{medium/w}}$ needs to be predicted (eq. 6). $D_{\mathrm{medium/w}}$ is practically the factor of how much the maximum medium concentration exceeds the maximum concentration in pure water $C_{\mathrm{w,sat}}$ through the presence of medium proteins and lipids. The maximum medium concentration can be calculated by multiplying $C_{\mathrm{w,sat}}$ with $D_{\mathrm{medium/w}}$ (eq. 17).

$$C_{\mathrm{medium,sat}} = C_{\mathrm{w,sat}} \cdot D_{\mathrm{medium/w}} \tag{18}$$

This simple calculation allows the prevention of chemical precipitation in the dosing solution while simultaneously applying the highest possible C_{medium}. This means that in many cases, it can be worked without solvents, or the solvents are evaporated in a dosing vial and the chemical is solubilized by the medium components without adding potentially toxic solvents. The preparation of the dosing solutions in advance without directly pipetting solvent stocks into the wells of the plates ensures a well-mixed situation at the start of the cell assays while preventing the occurrence of solvent-related effect artifacts, such as the increased toxicity due to dimethyl sulfoxide droplets (Tanneberger et al. 2010).

Preventing cytotoxicity interference

As was discussed in Judson et al. (2016), cytotoxicity can interfere with the sensitive endpoints evaluated in the cell-based bioassay, such as the interaction of the chemical with a certain receptor. Cellular cytotoxicity results from chemical concentrations in the cell membrane exceeding 300 mmol L^{-1} that is expected to cause disturbance of the cell membrane integrity. This threshold was measured for isolated cell membranes (Escher and Schwarzenbach 2002) and corresponds to the 0.1 to 1 mol L^{-1} lipid threshold observed for aquatic organisms (McCarty and Mackay 1993). The cytotoxicity burst is one of the major experimental artifacts that can interfere with specific endpoints in cell-based bioassays (Fay et al. 2018). At cytotoxic concentrations, the cells activate several signaling pathways, amongst others potentially the evaluated specific effect. Analysis of the Tox21 *in vitro* effect data revealed that for a large proportion of the chemicals that were active in the reporter gene assays (Figure 7 in *Publication* 1), cytotoxicity could have interfered with the assessed endpoints, as is exemplarily demonstrated for the chemicals active in the oxidative stress response assay (Tox21_ARE_bla_agonist assay) (Figure 13). For the chemicals that lie within the range of critical membrane concentration for baseline toxicity, such as B(a)P[N] and prazepam, activation in the assay could have resulted from nonspecific effects that also led to reporter gene activation. The activity of these chemicals in the assay can thus be considered as false positive as they are not the result of specific reporter binding but nonspecific reporter gene activation.

As demonstrated by Figure 13, cytotoxicity can be directly related to the chemicals $D_{\mathrm{lip/w}}$ that determines the affinity to membrane lipids and thus the resulting membrane concentration. An optimal chemical dosing would cover both the concentration range in which the specific effect can occur as well as the concentration range that causes cytotoxicity. The resulting EC_{50} values for the specific effects should be derived independent of cytotoxicity, therefore, only concentrations that are 10 times lower than the critical membrane concentration should be included in the dose-response curve. By combining the C_{free} from eq. 17 and the $D_{\mathrm{lip/w}}$ of the chemical, the

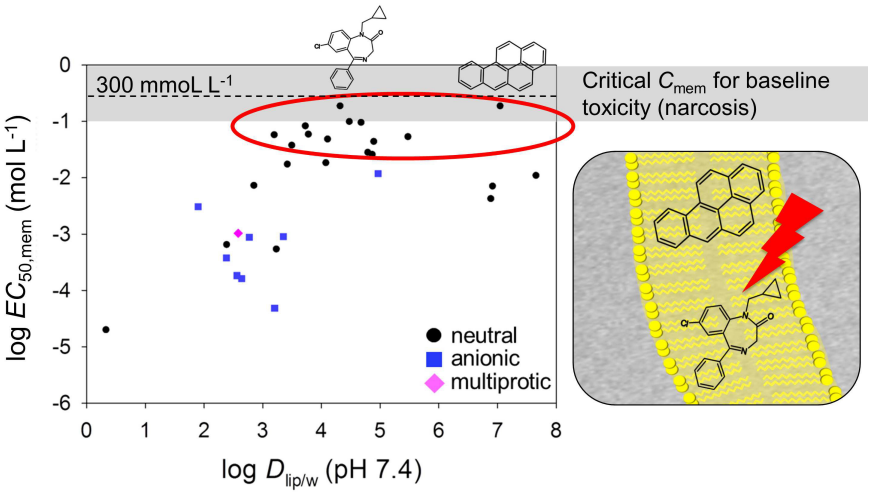

Figure 13: How quantifying EC_{mem} of existing *in vitro* effect data can discriminate whether a measured specific effect is reliable or induced by cytotoxicity burst. In the Tox21 oxidative stress response assay displayed here (Tox21_ARE_bla_agonist), EC_{mem} of a large proportion of the active neutral chemicals are near the critical membrane concentration ($EC_{\text{mem}} > 300$ mmol L^{-1}), thus measured specific effects might be the result of interfering cytotoxicity.

concentration in the membrane can be predicted and adjusted to target and/or prevent cytotoxic concentrations (eq. 19).

$$C_{\text{mem}} = C_{\text{free}} \cdot D_{\text{lip/w}} \tag{19}$$

Prediction of C_{cell} by simplified mass balance modeling

Because C_{free} does not directly inform about the extent of chemical partitioning into the cells without knowledge of the $D_{\text{cell/w}}$, it is required to parameterize the cells when aiming to adjust desired C_{cell} to be used as representative exposure metric. The $D_{\text{cell/w}}$ is driven by the water, protein, and lipid concentrations of the respective cell lines (eq. 7). In order to approximate C_{cell}, the generic cell reported in *Publication* 1 and the corresponding $D_{\text{cell/w}}$ of the chemicals can be used in combination with C_{free} from eq. 17

(eq. 20).

$$C_{\text{cell}} = C_{\text{free}} \cdot D_{\text{cell/w}} \tag{20}$$

Derivation of required chemical and system parameters

For many chemicals, the input parameters that are needed to perform the presented calculations (eqs. 17-20) are available in the literature or predictive methods exist, hence, no experiments are needed to increase the quality of chemical dosing by the simplified methods. The database on sorptive phases in both the medium and cells is already comprehensive and will continue to grow in the next years. For the quantification of chemical partitioning between assay compartments and corresponding phases, the K_{ow}, the $K_{\text{BSA/w}}$, and the $K_{\text{lip/w}}$ are required. BSA and lip are biological matrices that are of relevance for various applications, therefore, a large database already exists and the availability of experimental data is growing. If no experimental data is available, the relevant partition constants can be calculated by different prediction methods that were calibrated by experimental data, such as QSARs, PP-LFER (Endo and Goss 2014), as well as 3D-models like 3D-QSARs (Linden et al. 2017) and COSMOmic (Bittermann et al. 2014). The simplest method of lowest effort is the prediction of partition constants from the log K_{ow}, for which QSARs exist for $K_{\text{BSA/w}}$ (Endo et al. 2011), $K_{\text{lip/w}}$ (Endo and Goss 2011), and $K_{\text{PS/w}}$ (*Publication* 3) (eqs. 21-23).

$$\log K_{\text{BSA/w}} = 0.71 \cdot \log K_{\text{ow}} + 0.42 \tag{21}$$

$$\log K_{\text{lip/w}} = 1.01 \cdot \log K_{\text{ow}} + 0.12 \tag{22}$$

$$\log K_{\text{PS/w}} = 0.56 \cdot \log K_{\text{ow}} - 0.05 \tag{23}$$

Predictions by the PP-LFER database (Ulrich et al. 2017) should be favored over predictions from the log K_{ow}, provided that PP-LFER descriptors are available or reliably predictable. The database provides chemical partitioning data for approximately 3,700 chemicals to various biological, artificial, and natural matrices and polymers. It is easily accessible and user-friendly. PP-LFERs multiply the chemicals' polarizability/dipolarity parameter (S),

effective hydrogen (H)-bond acidity (A) and basicity (B), molar volume (V) and hexadecane-air partition constant (L) by experimentally determined system descriptors, as is shown for $K_{\mathrm{BSA/w}}$ and $K_{\mathrm{lip/w}}$ (eqs. 24 and 25) (Endo and Goss 2011, Endo et al. 2011).

$$\log K_{\mathrm{BSA/w}} = 0.35 + 0.28 \cdot L - 0.46 \cdot S + 0.2 \cdot A - 3.18 \cdot B + 1.84 \cdot V \qquad (24)$$

$$\log K_{\mathrm{lip/w}} = 0.53 + 0.49 \cdot L - 0.93 \cdot S + 0.18 \cdot A - 3.75 \cdot B + 1.73 \cdot V \qquad (25)$$

The presented QSARs (eq. 21-23) and PP-LFERs (eqs. 24 and 25) are only valid for neutral chemicals and the neutral fraction of ionizable chemicals. The speciation of an ionizable chemical can affect the chemical partitioning between phases, because both the neutral and charged species can exhibit a different sorption affinity to certain phases. In order to apply equations 21-23, the octanol-water distribution ratio D_{ow} (pH 7.4) for ionizable chemicals can be predicted by eq. 26.

$$D_{\mathrm{ow}}(\mathrm{pH\ 7.4}) = \alpha_{\mathrm{neutral}} \cdot K_{\mathrm{ow}}(\mathrm{neutral}) + \alpha_{\mathrm{ion}} \cdot K_{\mathrm{ow}}(\mathrm{ion}) \qquad (26)$$

Because the chemical partitioning of the charged species into octanol is negligible ($\log K_{\mathrm{ow}}$ (ion) = 0), the equation can be simplified (eq. 27).

$$D_{\mathrm{ow}}(\mathrm{pH\ 7.4}) = \alpha_{\mathrm{neutral}} \cdot K_{\mathrm{ow}}(\mathrm{neutral}) \qquad (27)$$

Partitioning of the charged species to the biomatrices BSA and lip can be predicted by 3D-QSARs and COSMOmic, as was done in *Publication* 1. The predicted data have shown great agreement with experimental values (Bittermann et al. 2014, Linden et al. 2017), however, the software is not openly accessible and the use requires adequate training. Alternatively, the $D_{\mathrm{lip/w}}$ can be estimated by assuming that the sorption affinity of α_{ion} is 10 times lower than of the $\alpha_{\mathrm{neutral}}$(eq. 28) (Bittermann et al. 2016).

$$D_{\mathrm{lip/w}}(\mathrm{pH\ 7.4}) = \alpha_{\mathrm{neutral}} \cdot \log K_{\mathrm{lip/w}}(\mathrm{neutral}) + \alpha_{\mathrm{ion}} \cdot \frac{\log K_{\mathrm{lip/w}}(\mathrm{neutral})}{10} \qquad (28)$$

Chemical partitioning of α_{ion} to BSA can be complex and dependent on 3D interactions between the ion and the biomolecule as was shown for anions (Henneberger et al. 2016), which could lead to considerable uncertainties when deriving $D_{\text{BSA/w}}$ by simple QSARs. A general observation after compiling the dataset on of >99% were between 10 and 100 times higher than the $K_{\text{BSA/w}}$ of neutral chemicals, whereas for cations, the sorption affinity was generally equal or lower, suggesting to use eq. 29 for anions and eq. 30 for cations in order to roughly estimate $D_{\text{BSA/w}}$.

$$\begin{aligned}\text{anion } D_{\text{BSA/w}}(\text{pH 7.4}) = \alpha_{\text{neutral}} \cdot K_{\text{BSA/w}}(\text{neutral}) + \\ \alpha_{\text{ion}} \cdot K_{\text{BSA/w}}(\text{neutral}) \cdot 50\end{aligned} \tag{29}$$

$$\text{cation } D_{\text{BSA/w}}(\text{pH 7.4}) = K_{\text{BSA/w}}(\text{neutral}) \tag{30}$$

Please be aware that equations 28-30 should only be applied for rough estimations in order to adjust chemical dosing, whereas the values should not be used for analysis of effect data.

3.2 Maximizing data quality

In vitro exposure modeling opens up several possible ways to interpret the data and link it to different exposure metrics relevant for environmental and human risk assessment. As demonstrated in *Publication* 1, existing databases in which *in vitro* exposure was not considered during the dosing process can be reanalyzed, provided that the minimum information on the experimental setups of the cell assays is available, as discussed in chapter 3.1. In order to make *in vitro* effect data suitable for reliable extrapolation to various exposure scenarios, the accuracy of exposure modeling should be maximized. Therefore, the comprehensive mass balance model that includes chemical partitioning to all relevant assay compartments is to be preferred and optimally parameterized with experimental values. For further increase in accuracy, the equilibrium mass balance model can be extended for kinetic processes, such as the kinetic models that were experimentally calibrated in *Publications* 2 and 3. By that means, users can assess the temporal change in both the external exposure ($C_{\mathrm{medium}} \sim C_{\mathrm{free}}$) and the cellular exposure ($C_{\mathrm{cell}}(t)$). The experimental determination of medium water, proteins and lipid concentrations by the Lowry assay and SPV-method can be performed without much efforts, whereas the likewise determination for the cells is time- and material-consuming because a sufficient number of cells needs to be cultivated and freeze dried. The use of BSA and lip as surrogates can lead to uncertainties when modeling the intracellular chemical partitioning of complex chemicals such as anions, because the cellular protein-chemical interaction might not be adequately represented (chapter 2.8). An alternative approach is given by the determination of the cell and medium volumes and corresponding analytical measurement of $D_{\mathrm{cell/w}}$ and $D_{\mathrm{medium/w}}$, which would reduce the risk of erroneous model predictions. Measurement of sorption isotherms can prevent the uncertainty of non-linear sorption, meaning that due to saturation of medium proteins and lipids, the $D_{\mathrm{medium/w}}$ are reduced at high chemical concentrations. This results in C_{free} exceeding the predictions by the mass balance model that does not factor in saturation of medium constituents. The saturation of albumin, the most frequent protein contained in the medium FBS (Gstraunthaler and Lindl 2013), was recently

verified for anion concentrations that fall into the concentration range typically tested in dose-response experiments (Henneberger et al. 2018a). Anion saturation of the medium proteins can occur at relatively low concentrations due to their high $D_{\mathrm{BSA/w}}$ compared to their relatively low $D_{\mathrm{cell/w}}$. In order to prove the applicability of SMPD to stabilize the C_{free} and to validate the predicted C_{free} by the mass balance model, *in situ* SPME measurements can be performed. As discussed in chapter 2.8, there are processes and chemicals that do not fall into the applicability domain of SMPD, therefore, SPME can be used to assess the kinetics of C_{free} and/or the percentage of depletion caused, such as in the case of rapid biotransformation of B(a)P[N] in AREc32 cells. Measurements with SPME are complicated by the small medium volumes applied for *in vitro* HTS, requiring to use SPME fibers with low volumes that do not deplete the medium to a significant degree. Although *in vitro* miniaturized SPME is a promising tool to measure the C_{free} directly in the assay medium, routine measurements are still not feasible for HTS. SPME can complement the *in vitro* exposure model framework by applying proof-of-principle measurements for new, unknown chemicals to assess the suitability of SMPD, the validity of model outputs, and derive chemical parameters required for the models, such as $D_{\mathrm{cell/w}}$ and $D_{\mathrm{medium/w}}$ (Henneberger et al. 2018a).

3.3 Extrapolation of *in vitro* effect data

Application to QIVIVE models

A key objective of implementing *in vitro* cell assays in chemical risk assessment is the ability to extrapolate effects measured *in vitro* to the whole organism level (QIVIVE) (Wetmore 2015). Reliable prediction of *in vivo* effects from *in vitro* data would be a crucial step forward in the effort to reduce, refine, and replace animal testing. Quantitative understanding of *in vitro* exposure by model approaches such as presented in this thesis does not only improve the quality, reliability and comparability of *in vitro* effect data, it also enables the direct linkage to exposure concentrations within the human body (Wetmore et al. 2012). The key parameter of QIVIVE is C_{unbound} (eq. 1), which is, similar to C_{free} in *in vitro* systems, strongly dependent on the presence of the plasma proteins and lipids in combination with the sorptive affinity of the chemicals to these biomolecules. Due to the parallels between the *in vivo* cell-plasma and the *in vitro* cell-medium exposure scenarios, both concepts can be compared directly by relating *in vitro* EC_{free} to predicted steady-state C_{unbound} that are expected to result from average exposure (Figure 14). The ratio of C_{unbound} to EC_{free} can be used as metric to quantify the hazard potential of a chemical. A ratio of >1 would mean that the average steady-state C_{unbound} exceeds the concentrations that lead to considerable effects, which should generally be counteracted in a HHRA framework because the extent of exposure to the chemical is likely to alter biological pathways. A ratio <1 means that the exposure in the human body does not exceed toxic values such as the 50% effect concentration ($EC_{50,\mathrm{free}}$). Nevertheless, a ratio of >0.01 can be interpreted as potential risk of chemical exposure to the health of a population.

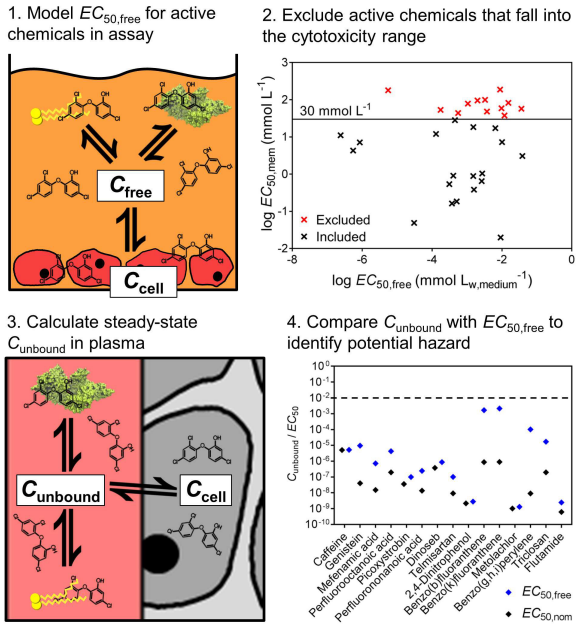

Figure 14: Possible framework on how to use *in vitro* effect data that is linked to modeled C_{free} in a QIVIVE approach. The hazard potential of the chemicals is evaluated by comparing $EC_{50,\text{free}}$ directly to the calculated steady-state C_{unbound} that is expected for 95% of the population in the U.S. [data from https://comptox.epa.gov/dashboard/, accessed on 8 August 2018].

Figure 14 presents the described framework and the application to the Tox21 oxidative stress response assay (Tox21_ARE_bla_agonist). $EC_{50,\text{nom}}$ of the active chemicals were gathered from the database and modeled to $EC_{50,\text{free}}$ by the mass balance model of *Publication* 1. To ensure that the measured chemical effects were not the result of interfering cytotoxicity, a threshold of $EC_{50,\text{mem}} = 30$ mmol L^{-1} was set and active chemicals that exceeded the threshold were excluded from the subsequent extrapolation approach. Data on the f_{unbound} of the chemicals, the intrinsic metabolic clearance rate, and the average total exposure (in mg per kg per hour) representative for 95% of the U.S. citizens were gathered from the U.S. EPA chemical dashboard. With these input parameters, C_{unbound} was calculated by eq. 1. As illus-

trated in Figure 14, the predicted C_{unbound} of the active chemicals in the Tox21 ARE assay did not exceed the measured $EC_{50,\text{free}}$ and they did not exceed the threshold of 0.01. However, there are chemicals with a ratio of >0.001, such as benzo(k)fluoranthene with a ratio of 0.0021. Given that the effect data in the Tox21 *in vitro* database is expressed as 50% effect concentrations, it is possible that for benzo(k)fluoranthene, the C_{unbound} exceeds biological pathway altering doses (BPAD), i.e. the dose that can lead to a significant change of a signaling pathway in the human body (Judson et al. 2011). The relatively high ratio of benzo(k)fluoranthene indicates that measures should be considered to decrease the exposure of U.S. citizens in the future. The modeling of $EC_{50,\text{free}}$ was crucial in the case of benzo(k)fluoranthene given that the application of $EC_{50,\text{nom}}$ would result into a ratio of $8.9 \cdot 10^{-7}$ because of the decrease in bioavailability of benzo(k)fluoranthene due to its high sorptive affinity to medium proteins ($\log D_{\text{BSA/w}} = 5.40$) and lipids ($\log D_{\text{lip/w}} = 6.92$). The non-consideration of the *in vitro* bioavailability can eventually lead to a large underestimation of the potential risk that the present exposure poses to human. This is particularly relevant for chemicals that are bound to a large extent, whereas the QIVIVE result of less sorptive chemicals such as caffeine ($\log D_{\text{BSA/w}} = 1.31$, $\log D_{\text{lip/w}} = 0.33$) is not considerably affected on whether $EC_{50,\text{nom}}$ or $EC_{50,\text{free}}$ are used for the extrapolation (Figure 14). An import prerequisite for using the presented QIVIVE approach are comparable kinetics of cellular uptake *in vitro* and *in vivo*. The direct comparison of C_{cell} *in vitro* to C_{cell} *in vivo* would require similar or at least comparable uptake kinetics in both systems. It can be assumed that HSA-mediated and HSA-facilitated transport are of comparable relevance *in vivo* as FBS-mediated and FBS-facilitated transport are *in vitro*. However, this hypothesis needs to be evaluated in future studies. The occurrence and quantity of ion channels and membrane transporters is expected to be dependent on the corresponding cell, which should be considered when applying the QIVIVE concept presented in Figure 14. Mimicking *in vivo* uptake kinetics in *in vitro* test systems would optimally involve the use of human cell lines with similar composition and metabolic activity as well as medium FBS contents similar to the HSA content in plasma.

The QIVIVE framework presented in Figure 14 is a simple tool to identify possible hazards resulting from chemical exposure. In the given example, average exposure concentrations expected in U.S. citizens were used, but the approach can be modified to evaluate peak exposure concentrations, such as by accidental exposure at work. The relevance of chronic exposure that is commonly given in the realistic exposure scenario compared to the acute effects in 24-hour cell-based bioassays should be addressed in the future by linking the approach to time-resolved AOPs and PBPKs. The framework is dependent on the quality of the modeled *in vitro* exposure data, the predicted exposure concentrations, and the calculated steady-state C_{unbound}. A major challenge in the future is the experimental validation of the $C_{\mathrm{free}} \sim C_{\mathrm{unbound}}$ assumption that underlies the framework, as well as to identify possible sources of uncertainty. The inclusion of kinetic processes into the *in vitro* exposure framework would enhance the accuracy of modeled C_{free}, thus increasing the suitability of *in vitro* cell-based bioassays to predict effects in human.

Comparability between *in vitro* and *in vivo* bioassays in ecotoxicological applications

Figure 15 emphasizes the considerable differences in the experimental setup of different *in vivo* and *in vitro* bioassays, but also the setup differences that were already applied for the same bioassay. Considering that chemical effect characterization in ERA is often based on testing the effects on different organisms or different cell lines, these differences can lead to considerably altered C_{free} and thus altered apparent effects between the bioassays, hampering the quantitative comparison of effects measured in different *in vitro* and *in vivo* bioassays.

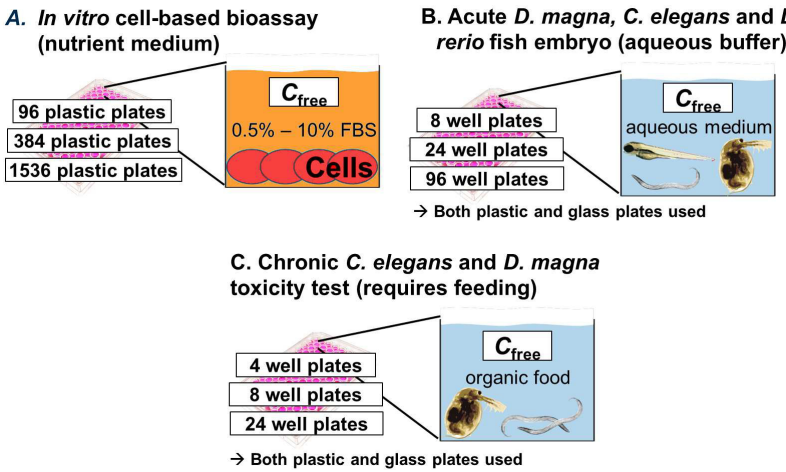

Figure 15: How *in vitro* and *in vivo* bioassays differ regarding the composition of the bioassay media and the usage of different well plate formats.

As shown in chapter 2.5, the medium composition of *in vitro* assays has a huge influence on C_{free}, and similar effects of sorptive colloids on the chemical bioavailability in other bioassays can be expected, such as for the chronic *Caenorhabditis elegans* toxicity test (Fischer et al. 2016), in which the range of applied food contents in the medium can alter the C_{free} by a factor of 40. The application of higher tier plates with lower medium volume generally increased the impact of multiwell plate sorption on C_{free}, which should be considered when comparing effect data generated in different multiwell plates or when comparing the effects with effect concentrations generated in glass vials (Figure 15). The influence of the chemical sorption to multiwell plates was recognized for aqueous *in vivo* bioassays, such as a decrease of >90% in C_{medium} of phenanthrene measured in the FET assay (Schreiber et al. 2008), or EC_{50} of 4-nitrotoluene that were reduced by 36% in plastic multiwell plates compared to glass plates (Gellert and Stommel 1999). The exposure framework that was presented for *in vitro* cell-based bioassays in this thesis can be extended to *in vivo* bioassays in order to achieve comparable exposure conditions and an improved comprehensive effect assessment of single chemicals and their mixtures. Application of mass balance mod-

els that predict the sorptive capacity in the medium combined with the kinetic model predicting multiwell plate sorption presented in *Publication* 3 can enhance the quality of chemical dosing in other bioassays in which chemical losses are expected to likewise influence bioavailability. By that means, effect concentrations that are based on measured or modeled C_{free} ($EC_{50,\mathrm{free}}$) generated in different bioassays would be comparable, leading to an increased reliability of chemical effect characterization and reducing the risk of a misevaluation of the hazard risk of chemicals and their mixtures.

4 Outlook

4.1 Future applicability of *in vitro* assays under consideration of exposure

Complementing *in vitro* cell-based bioassays by exposure models will increase their interpretability and applicability in chemical risk assessment, as measured effects can be linked to actual exposure concentrations, increasing the predictive significance of the assays. So far, lack of sensitivity of the assay due to the colloid-rich *in vitro* assay media was criticized. Contrarily, the thesis' results emphasize that the medium stabilizes chemical exposure in the test systems, (i) enabling the application of mass balance models that assume chemical equilibrium between the assay compartments and (ii) increasing the comparability between chemicals as kinetics do not lead to unsystematic differences between chemicals and bioassays. These are great advantages compared to *in vivo* bioassays that lack a natural passive dosing system. In *in vivo* bioassays, kinetics such as transport over the ABL and resulting organism-medium equilibrium partitioning as well as well plate sorption not only lead to considerably reduced C_{free} but also a time-dependent decrease in C_{free}, hampering the discrimination of toxicokinetic and toxicodynamics. Although cellular uptake was particularly delayed for ionizable chemicals, as well as plastic sorption was continuously depleting C_{medium}, overall time-dependent medium and cell exposure was stable throughout the assay duration. This enables the direct comparison to steady-state exposure scenarios such as in the human body. The thesis' findings, conclusions and developed models support the implementation of *in vitro* cell-based bioassays in the regulatory risk assessment of chemicals.

4.2 Environmental samples

Environmental samples are composed of numerous chemicals with various physicochemical properties, complicating the correction of differences in chemical bioavailability. An ideal chemical dosing of environmental samples would thus depend on preserving the chemical composition and con-

centrations of the sample. After applying an environmental sample into the cell-based bioassays by solvent spiking, the chemicals are expected to partition between the medium components, other assay compartments, and the cells according to their affinity to the phases. Because the chemicals likewise exhibit this partitioning between water, organic carbon, and biota in the environment, it can be expected that the original mixture composition of an environmental sample remains relatively similar to the resulting composition in the cells, considering the linear difference of C_{nom} in the environment, C_{nom} in the *in vitro* assay, and resulting C_{cell} (Jahnke et al. 2016). As discussed in chapter 1, C_{cell} represents a suitable metric to quantify the total cellular dose, particularly for chemicals and mixtures that exhibit several MoA, which is to be expected for environmental samples. It is thus not necessarily required to account for differences in C_{free} between the chemicals in environmental samples following the assumption that the cellular dose *in vitro* reflects the internal concentration of organisms in the environment the samples were taken. In order to roughly model the C_{free} of chemicals in an environmental sample, chromatographic fractionation of the chemicals into groups of hydrophobicity can be performed, such as by C18 HPLC columns, which is usually done in the field of effect-directed analysis to reduce the complexity of chemical mixtures (Brack 2003, Hecker and Hollert 2009). The resulting chemical fractions can be sorted by their log K_{ow} range and corresponding ranges of C_{free} could subsequently be modeled by eq. 17. This procedure would increase the informative value of the effect data that was measured for each chemical fraction, because differences in effects do not result from differences in bioavailability but rather the potency of the chemical fraction.

4.3 Upcoming challenges

The thesis' results demonstrate that SMPD is a suitable tool to stabilize exposure in cell-based bioassays. However, scenarios that exceed the applicability domain were identified, foremost processes that rapidly decrease the C_{medium}, such as cellular biotransformation. For these scenarios, experimental determination of C_{free} by miniaturized SPME methods could represent a

suitable alterative tool, but also complementary to *in vitro* exposure modeling. The implementation of non-depletive *in situ* SPME techniques into robotic platforms that perform HTS is technically challenging and requires standardized protocols to ensure that simultaneous measurements of exposure concentrations and effects do not conflict with each other. SPME can be applied to generate a larger experimental database on chemical partition constants to structural proteins, opening up the inclusion of structural proteins as surrogates for cellular proteins into the mass balance model. A more detailed parameterization and discrimination of different cellular lipids (storage lipids, phospholipids, cholesterol) by applying new analytical lipid determination methods could further increase the accuracy of the cell parameterization, hence leading to more realistic C_{cell} predictions. Quantification of the intracellular chemical partitioning of fluorophores by extension of the fluorescence microscopy method to cell organelle stains can be applied to compare the chemical concentrations in different organelles with the concentrations that were predicted to evaluate the suitability of the mass balance model to predict intracellular chemical partitioning. The experimental determination of cellular uptake kinetics indicated that different transport mechanisms contribute to the overall cellular uptake of neutral and ionizable chemicals. The measurement of membrane permeability by the developed fluorescence microscopy method could be achieved by measuring the accumulation in artificial liposomes that previously incorporated surrogate proteins such as BSA and structural proteins to mimic the intracellular composition of *in vitro* cells. This experimental setup would also allow to quantify the influence of FBS-facilitated transport over the ABL at different medium FBS contents. Active transport by carrier proteins and FBS endocytosis could be addressed by chemical inhibition of carrier proteins prior to measurement of uptake kinetics (McGeoch et al. 1978, Chen et al. 2014), provided that the integrity of the cellular membranes remain unchanged by the additional chemical exposure. Chemical biotransformation of B(a)P[N] by the AREc32 cells was observed in *Publication* 2, which needs to be verified by detection of B(a)P[N] metabolites such as benzo(a)pyrene-7,8-dihydrodiol-9,10-epoxide in the medium and/or cells

of the assay (Madureira et al. 2014). To achieve this, the medium could be gathered and extracted by a hydrophobic solvent (e.g., n-heptane) following analytical quantification by mass spectrometry. The effects in AREc32 cells that resulted from exposure to both the parent chemical and the metabolite can be compared to effects exhibited by exposure to the metabolite(s) to evaluate the assumption that the toxicity of B(a)P[N] mainly results from bioactivation by the cytochrome P450 complex and the reactive and genotoxic effects of the epoxide-metabolite (Arlt et al. 2008). *Publication* 3 provides a decent database on $K_{\mathrm{PS/w}}$ and D_{PS} of neutral organic chemicals. While the correlation between log $K_{\mathrm{PS/w}}$ and log K_{ow} was evident, no relations to physicochemical properties could be identified for D_{PS}. The database was sufficiently heterogenous to calibrate the predictive model on multiwell plate sorption, and the generation of further datapoints could eventually pave the way to parameterize PP-LFERs for both $K_{\mathrm{PS/w}}$ and D_{PS}, which are expected to be of high interest for the plastic research field and would increase the applicability domain of the developed predictive model even further. The assumption that charged chemicals do not partition into polystyrene needs to be verified and the potential role of polylysine coatings that might represent an additional sorptive sink for anions due to its charged hydrophilic amino groups at pH 7.4 needs to the investigated (Ryan 2008). The experimental setup for measuring $K_{\mathrm{PS/w}}$ proved to be suitable for long-term experiments because the total concentration in the test vials remained constant over 700 hours. The setup can be adapted to parameterize the sorption of neutral organic chemicals to other glassy polymers with low diffusion coefficients, such as expected for graphene or polytetrafluoroethylene. The next step in the process of implementing the *in vitro* exposure framework in chemical risk assessment is the application in the QIVIVE framework. Therefore, a completely experimentally parameterized kinetic exposure model needs to be set up in order to evaluate the relationship between C_{free} and C_{unbound} and to identify similarities and/or deviations traced back to differences in kinetics, medium compositions, and cell morphology between *in vitro* and *in vivo*.

5 References

Ali, R., Trump, S., Lehmann, I., and Hanke, T. (2015) Live cell imaging of the intracellular compartmentalization of the contaminate benzo[a]pyrene. *Journal of Biophotonics* 8, 361-371.

Ankley, G. T., Bennett, R. S., Erickson, R. J., Hoff, D. J., Hornung, M. W., Johnson, R. D., Mount, D. R., Nichols, J. W., Russom, C. L., Schmieder, P. K., Serrrano, J. A., Tietge, J. E., and Villeneuve, D. L. (2010) Adverse outcome pathways: a conceptual framework to support ecotoxicology research and risk assessment. *Environmental Toxicology and Chemistry* 29, 730-741.

Arlt, V. M., Stiborova, M., Henderson, C. J., Thiemann, M., Frei, E., Aimova, D., Singh, R., Gamboa da Costa, G., Schmitz, O. J., Farmer, P. B., Wolf, C. R., and Phillips, D. H. (2008) Metabolic activation of benzo[a]pyrene *in vitro* by hepatic cytochrome P450 contrasts with detoxification *in vivo*: experiments with hepatic cytochrome P450 reductase null mice. *Carcinogenesis* 29, 656-665.

Armitage, J. M., Wania, F., and Arnot, J. A. (2014) Application of mass balance models and the chemical activity concept to facilitate the use of *in vitro* toxicity data for risk assessment. *Environmental Science & Technology* 48, 9770-9779

Attene-Ramos, M. S., Miller, N., Huang, R., Michael, S., Itkin, M., Kavlock, R. J., Austin, C. P., Shinn, P., Simeonov, A., Tice, R. R., and Xia, M. (2013) The Tox21 robotic platform for the assessment of environmental chemicals - from vision to reality. *Drug Discovery Today* 18, 716-723.

Aufderheide, M., Knebel, J. W., and Ritter, D. (2002) A method for the *in vitro* exposure of human cells to environmental and complex gaseous mixtures: application to various types of atmosphere. *Alternatives to Laboratory Animals* 30, 433-441.

Bean, B. P. (1992) Pharmacology and electrophysiology of ATP-activated ion channels. *Trends in Pharmacological Science* 13, 87-90.

Bean, R. C., Shepherd, W. C., and Chan, H. (1968) Permeability of lipid bilayer membranes to organic solutes. *Journal of General Physiology* 52, 495-508.

Begley, T., Castle, L., Feigenbaum, A., Franz, R., Hinrichs, K., Lickly, T., Mercea, P., Milana, M., O'Brien, A., Rebre, S., Rijk, R., and Piringer, O. (2005) Evaluation of migration models that might be used in support of regulations for food-contact plastics. *Food Additives & Contaminants* 22, 73-90.

Bernardo, G. (2012) Diffusivity of alkanes in polystyrene. *Journal of Polymer Research* 19:9836.

Bittermann, K., Spycher, S., Endo, S., Pohler, L., Huniar, U., Goss, K.-U., and Klamt, A. (2014) Prediction of phospholipid-water partition coefficients of ionic organic chemicals using the mechanistic model COSMOmic. *Journal of Physical Chemistry B* 118, 14833-14842.

Blacquière, T., Smagghe, G., van Gestel, C. A. M., and Mommaerts, V. (2012) Neonicotinoids in bees: a review on concentrations, side-effects and risk assessment. *Ecotoxicology* 21, 973-992.

Brack, W. (2003) Effect-directed analysis: a promising tool for the identification of organic toxicants in complex mixtures? *Analytical and Bioanalytical Chemistry* 377, 397-407.

Broeders, J. J. W., Blaauboer, B. J., and Hermens, J. L. M. (2011) Development of a negligible depletion-solid phase microextraction method to determine the free concentration of chlorpromazine in aqueous samples containing albumin. *Journal of Chromatography A* 1218, 8529-8535.

Brown, R. P., Delp, M. D., Lindstedt, S. L., Rhomberg, L. R., and Beliles, R. P. (1997) Physiological parameter values for physiologically based pharmacokinetic models. *Toxicology and Industrial Health* 13, 407-484.

Capuzzi, S. J., Politi, R., Isayev, O., Farag, S., and Tropsha, A. (2016) QSAR modeling of Tox21 challenge stress response and nuclear receptor signaling toxicity assays. *Frontiers in Environmental Science* 4, 2296-665.

Carson, R. (1962). Silent spring. Boston, MA, USA, Houghton Mifflin Company. ISBN: 0046442249065.

Cavero, I., and Guillon, J. M. (1993) Membrane ion channels and cardiovascular ATP-sensitive K+ channels. *Cardiologia* 38, 445-452.

Chen, Y., Scully, M., Petralia, G., and Kakkar, A. (2014) Binding and inhibition of drug transport proteins by heparin: a potential drug transporter modulator capable of reducing multidrug resistance in human cancer cells. *Cancer Biology & Therapy* 15, 135-145.

Court, G. S., Davies, L. S., Focardi, S., Bargargli, R., Fossi, C., Leonzio, C., and Marili, L. (1997) Chlorinated hydrocarbons in the tissues of South Polar Skuas (*Catharacta maccormicki*) and Adelie Penguins (*Pygoscelis adeliea*) from Ross Sea, Antarctica. *Environmental Pollution* 97, 295-301.

Davies, B., and Morris, T. (1993) Physiological parameters in laboratory animals and humans. *Pharmacological Research* 10, 1093-1095.

Dewailly, E., Ayotte, P., Bruneau, S., Laliberte, C., Muir, D. C. G., and Norstrom, R. J. (1993) Inuit exposure to organochlorines through the aquatic food-chain in arctic Quebec. *Environmental Health Perspectives* 101, 618-620.

Diamond, L., Kruszewski, F., Aden, D. P., Knowles, B. B., and Baird, W. M. (1980) Metabolic activation of benzo[a]pyrene by a human hepatoma cell line. *Carcinogenesis* 1, 871-875.

Ding, S. H., Vardy, A., Elcombe, C. R., and Wolf, C. R. (2009) An *in vitro* model for the prediction of chemical metabolism and toxicity. *Toxicology* 262, 23-23.

Dulbecco, R., and Freeman, G. (1959) Plaque production by the polyoma virus. *Virology* 8, 396-397.

Elmore, S. A., Ryan, A. M., Wood, C. E., Crabbs, T. A., and Sills, R. C. (2014) FutureTox II: Contemporary concepts in toxicology: "Pathways to prediction: *in vitro* and in silico models for predictive toxicology". *Toxicologic Pathology* 42, 940-942.

Embry, M. R., Belanger, S. E., Braunbeck, T. A., Galay-Burgos, M., Halder, M., Hinton, D. E., Léonard, M. A., Lillicrap, A., Norberg-King, T., and Whale, G. (2010) The fish embryo toxicity test as an animal alternative method in hazard and risk assessment and scientific research. *Aquatic Toxicology* 97, 79-87.

Endo, S., Escher, B. I., and Goss, K. U. (2011) Capacities of membrane lipids to accumulate neutral organic chemicals. *Environmental Science & Technology* 45, 5912-5921.

Endo, S., and Goss, K. U. (2011) Serum albumin binding of structurally diverse neutral organic compounds: Data and models. *Chemical Research in Toxicology* 45, 2293-2301.

Endo, S., and Goss, K.-U. (2014) Applications of polyparameter linear free energy relationships in environmental chemistry. *Environmental Science & Technology* 48 (21), 12477-12491.

Escher, B., and Schwarzenbach, R. P. (2002) Mechanistic studies on baseline toxicity and uncoupling as a basis for modeling internal lethal concentrations in aquatic organisms. *Aquatic Sciences* 64, 20-35.

Escher, B. I., and Hermens, J. L. M. (2004) Internal exposure: Linking bioavailability to effects. *Environmental Science & Technology* 38, 455A-462A.

Escher, B. I., Bramaz, N., Mueller, J. F., Quayle, P., Rutishauser, S., and Vermeirssen, E. L. M. (2008) Toxic equivalent concentrations (TEQs) for baseline toxicity and specific modes of action as a tool to improve interpretation of ecotoxicity testing of environmental samples. *Journal of Environmental Monitoring* 10, 612-621.

Escher, B., and Leusch, F. (2012) Bioanalytical tools in water quality assessment. London, UK, IWA Publishing. ISBN: 9781843393689.

Fay, K. A., Villeneuve, D. L., Swintek, J., Edwards, S. W., Nelms, M. D., Blackwell, B. R., and Ankley, G. T. (2018) Differentiating pathway-specific from nonspecific effects in high-throughput toxicity data: A foundation for prioritizing Adverse Outcome Pathway development. *Toxicological Sciences* 163, 500-515.

Fischer, F., Böhm, L., Höss, S., Möhlenkamp, C., Claus, E., Düring, R.-A., and Schäfer, S. (2016) Passive dosing in chronic toxicity tests with the nematode *Caenorhabditis elegans*. *Environmental Science & Technology* 50, 9708-9716.

Frings, C. S., and Dunn, R. T. (1970) A colorimetric method for determination of total serum lipids based on sulfo-phospho-vanillin reaction. *American Journal of Clinical Pathology* 53, 89-91.

Gavara, R., Hernandez, R. J., and Giacin, J. (1996) Methods to determine partition coefficient of organic compounds in water/polystyrene systems. *Journal of Food Science* 61, 947-952.

Gellert, G., and Stommel, A. (1999) Influence of microplate material on the sensitivity of growth inhibition tests with bacteria assessing toxic organic substances in water and waste water. *Environmental Toxicology* 14, 424-428.

Ghafourian, T., and Amin, Z. (2013) QSAR models for the prediction of plasma protein binding. *Bioimpacts* 3, 21-27.

Gibbons, G. F., Khurana, R., Odwell, A., and Seelaender, M. C. L. (1994) Lipid balance in HepG2 cells - Active synthesis and impaired mobilization. *Journal of Lipid Research* 35, 1801-1808.

Groothuis, F. A., Heringa, M. B., Nicol, B., Hermens, J. L. M., Blaauboer, B. J., and Kramer, N. I. (2015) Dose metric considerations in *in vitro* assays to improve quantitative *in vitro-in vivo* dose extrapolations. *Toxicology* 332, 30-40.

Gstraunthaler, G., and Lindl, T. (2013) Zell- und Gewebekultur: Allgemeine Grundlagen und spezielle Anwendungen. Heidelberg, Germany. Springer Spektrum. ISBN: 978-3-642-35997-2

Gülden, M., and Seibert, H. (1997) Influence of protein binding and lipophilicity on the distribution of chemical compounds in *in vitro* systems. *Toxicology In Vitro* 11, 479-483.

Gülden, M., Morchel, S., and Seibert, H. (2001) Factors influencing nominal effective concentrations of chemical compounds *in vitro*: cell concentration. *Toxicology In Vitro* 15, 233-243.

Gülden, M., Morchel, S., Tahan, S., and Seibert, H. (2002) Impact of protein binding on the availability and cytotoxic potency of organochlorine pesticides and chlorophenols *in vitro*. *Toxicology* 175, 201-213.

Gülden, M., and Seibert, H. (2005) Impact of bioavailability on the correlation between *in vitro* cytotoxic and *in vivo* acute fish toxic concentrations of chemicals. *Aquatic Toxicology* 72, 327-337.

Hecker, M., and Hollert, H. (2009) Effect-directed analysis (EDA) in aquatic ecotoxicology: state of the art and future challenges. *Environmental Science and Pollution Research* 16, 607-613.

Henneberger, L., Goss, K.-U., and Endo, S. (2016) Equilibrium sorption of structurally diverse organic ions to bovine serum albumin. *Environmental Science & Technology* 50, 5119-5126.

Henneberger, L., Mühlenbrink, M., Fischer, F. C., and Escher, B. I. (2018a) Using C18-coated solid phase microextraction fibers for the quantification of partitioning of organic acids to biological materials. Manuscript in preparation.

Henneberger, L., Mühlenbrink, M., Fischer, F. C., and Escher, B. I. (2018b) Using a combination of serum-mediated passive dosing and SPME measurements for controlling the dose of chemicals in *in vitro* bioassays. Manuscript in preparation.

Heringa, M. B., Schreurs, R., van der Saag, P. T., van der Burg, B. and Hermens, J. L. M. (2003) Measurement of free concentration as a more intrinsic dose parameter in an *in vitro* assay for estrogenic activity. *Chemical Research In Toxicology* 16, 1662-1663.

Heringa, M. B., Schreurs, R., Busser, F., Van Der Saag, P. T., Van Der Burg, B., and Hermens, J. L. M. (2004) Toward more useful *in vitro* toxicity data with measured free concentrations. *Environmental Science & Technology* 38, 6263-6270.

Huang, R. L., Xia, M. H., Cho, M. H., Sakamuru, S., Shinn, P., Houck, K. A., Dix, D. J., Judson, R. S., Witt, K. L., Kavlock, R. J., Tice, R. R., and Austin, C. P. (2011) Chemical genomics profiling of environmental chemical modulation of human nuclear receptors. *Environmental Health Perspectives* 119, 1142-1148.

Huang, R., Sakamuru, S., Martin, M. T., Reif, D. M., Judson, R. S., Houck, K. A., Casey, W., Hsieh, J.-H., Shockley, K. R., Ceger, P., Fostel, J., Witt, K. L., Tong, W., Rotroff, D. M., Zhao, T., Shinn, P., Simeonov, A., Dix, D. J., Austin, C. P., Kavlock, R. J., Tice, R. R., and Xia, M. (2014) Profiling of the Tox21 10K compound library for agonists and antagonists of the estrogen receptor alpha signaling pathway. *Scientific reports* 4, 5664-5664.

Huber, S. M., Butz, L., Stegen, B., Klumpp, L., Klumpp, D. and Eckert, F. (2015) Role of ion channels in ionizing radiation-induced cell death. Biochimica et Biophysica Acta (BBA) - *Biomembranes* 1848, 2657-2664.

Judson, R. S., Kavlock, R. J., Setzer, R. W., Hubal, E. A. C., Martin, M. T., Knudsen, T. B., Houck, K. A., Thomas, R. S., Wetmore, B. A., and Dix, D. J. (2011) Estimating toxicity-related biological pathway altering doses for high-throughput chemical risk assessment. *Chemical Research in Toxicology* 24: 451-462.

Judson, R., Houck, K., Martin, M., Richard, A. M., Knudsen, T. B., Shah, I., Little, S., Wambaugh, J., Setzer, R. W., Kothya, P., Phuong, J., Filer, D., Smith, D., Reif, D., Rotroff, D., Kleinstreuer, N., Sipes, N., Xia, M. H., Huang, R. L., Crofton, K., and Thomas, R. S. (2016) Analysis of the effects of cell stress and cytotoxicity on *in vitro* assay activity across a diverse chemical and assay space. *Toxicological Sciences* 152, 323-339.

Kelly, B. C., and Gobas, F. (2003) An arctic terrestrial food-chain bioaccumulation model for persistent organic pollutants. *Environmental Science & Technology* 37, 2966-2974.

Kiersch, K., Jandl, G., Meissner, R., and Leinweber, P. (2010) Small scale variability of chlorinated POPs in the river Elbe floodplain soils (Germany). *Chemosphere* 79, 745-753.

Knudsen, T. B., Keller, D. A., Sander, M., Carney, E. W., Doerrer, N. G., Eaton, D. L., Fitzpatrick, S. C., Hastings, K. L., Mendrick, D. L., Tice, R. R., Watkins, P. B., and Whelan, M. (2015) FutureTox II: *in vitro* data and in silico models for predictive toxicology. *Toxicological Sciences* 143, 256-267.

Kramer, N. I., van Eijkeren, J. C. H., and Hermens, J. L. M. (2007) Influence of albumin on sorption kinetics in solid-phase microextraction: consequences for chemical analyses and uptake processes. *Analytical Chemistry* 79, 6941-6948.

Kramer, N. I., Busser, F. J. M., Oosterwijk, M. T. T., Schirmer, K., Escher, B. I., and Hermens, J. L. M. (2010) Development of a partition-controlled dosing system for cell assays. *Chemical Research in Toxicology* 23, 1806-1814.

Kramer, N. I., Krismartina, M., Rico-Rico, A., Blaauboer, B. J. and Hermens, J. L. M. (2012) Quantifying processes determining the free concentration of phenanthrene in basal cytotoxicity assays. *Chemical Research in Toxicology* 25, 436-445.

Krause, S., Ulrich, N. and Goss, K. U. (2018) Desorption kinetics of organic chemicals from albumin. *Archives of Toxicology* 92, 1065-1074.

Lai, Y. (2013). 8 - Drug transporters in drug discovery and development. Transporters in Drug Discovery and Development. Y. Lai, Woodhead Publishing: 633-674.

Lampi, M. A., Gurska, J., McDonald, K. I., Xie, F., Huang, X. D., Dixon, D. G., and Greenberg, B. M. (2006) Photoinduced toxicity of polycyclic aromatic hydrocarbons to Daphnia magna: ultraviolet-mediated effects and the toxicity of polycyclic aromatic hydrocarbon photoproducts. *Environmental Toxicology and Chemistry* 25, 1079-1087.

Leanza, L., Managò, A., Zoratti, M., Gulbins, E., and Szabo, I. (2016) Pharmacological targeting of ion channels for cancer therapy: *in vivo* evidences. *Biochimica et Biophysica Acta (BBA) - Molecular Cell Research* 1863, 1385-1397.

Linden, L., Goss, K. U., and Endo, S. (2017) 3D-QSAR predictions for alpha-cyclodextrin binding constants using quantum mechanically based descriptors. *Chemosphere* 169, 693-699.

Liu, F. F., Peng, C., Escher, B. I., Fantino, E., Giles, C., Were, S., Duffy, L., and Ng, J. C. (2013) Hanging drop: an *in vitro* air toxic exposure model using human lung cells in 2D and 3D structures. *Journal of Hazardous Materials* 261, 701-710.

Lowry, O. H., Rosebrough, N. J., Farr, A. L., and Randall, R. J. (1951) Protein measurement with the Folin phenol reagent. *Journal of Biological Chemistry* 193, 265-275.

Lozano, N., Rice, C. P., Ramirez, M., and Torrents, A. (2013) Fate of triclocarban, triclosan and methyltriclosan during wastewater and biosolids treatment processes. *Water Research* 47, 4519-4527.

Madureira, D. J., Weiss, F. T., Van Midwoud, P., Helbling, D. E., Sturla, S. J., and Schirmer, K. (2014) Systems toxicology approach to understand the kinetics of benzo(a)-pyrene uptake, biotransformation, and DNA adduct formation in a liver cell model. *Chemical Research in Toxicology* 27, 443-453.

Margot, J., Rossi, L., Barry David, A., and Holliger, C. (2015) A review of the fate of micropollutants in wastewater treatment plants. *Wiley Interdisciplinary Reviews: Water* 2, 457-487.

McCarty, L. S., and Mackay, D. (1993) Enhancing ecotoxicological modeling and assessment. *Environmental Science & Technology* 27, 1719-1728.

McGeoch, J., Falconer Smith, J., Ledingham, J., and Ross, B. (1978) Inhibition of active-transport sodium-potassium-A.T.P.ase by myeloma protein. *Lancet* 2, 17-18.

Meyer, T., and Wania, F. (2007) What environmental fate processes have the strongest influence on a completely persistent organic chemical's accumulation in the Arctic? *Atmospheric Environment* 41, 2757-2767.

OECD (2004). Test No. 202: *Daphnia sp.* Acute Immobilisation Test.

OECD (2011). Test No. 201: Freshwater Alga and Cyanobacteria Growth Inhibition Test.

Oemisch, L., Goss, K.-U., and Endo, S. (2014) Ion exchange membranes as novel passive sampling material for organic ions: Application for the determination of freely dissolved concentrations. *Journal of Chromatography A* 1370, 17-24.

Pariselli, F., Sacco, M. G., and Rembges, D. (2009) An optimized method for *in vitro* exposure of human derived lung cells to volatile chemicals. *Experimental and Toxicologic Pathology* 61, 33-39.

Pérez-Maldonado, I. N., Trejo, A., Ruepert, C., Jovel, R. d. C., Méndez, M. P., Ferrari, M., Saballos-Sobalvarro, E., Alexander, C., Yáñez-Estrada, L., Lopez, D., Henao, S., Pinto, E. R., and Díaz-Barriga, F. (2010) Assessment of DDT levels in selected environmental media and biological samples from Mexico and Central America. *Chemosphere* 78, 1244-1249.

Poulin, P., and Haddad, S. (2015) Albumin and uptake of drugs in cells: additional validation exercises of a recently published equation that quantifies the albumin-facilitated uptake mechanism(s) in physiologically based pharmacokinetic and pharmacodynamic modeling research. *Journal of Pharmaceutical Sciences* 104, 4448-4458.

Poulin, P., Burczynski, F. J. and Haddad, S. (2016) The Role of Extracellular Binding Proteins in the Cellular Uptake of Drugs: Impact on Quantitative *in vitro*-to-*in vivo* Extrapolations of Toxicity and Efficacy in Physiologically Based Pharmacokinetic-Pharmacodynamic Research. *Journal of Pharmaceutical Sciences* 105, 497-508.

Rand, G. (1995). Fundamentals of aquatic toxicology: Effects, environmental fate, and risk assessment. Boca Raton, FL, USA, CRC Press. ISBN 1-56032-091-5.

Riedl, J., and Altenburger, R. (2007) Physicochemical substance properties as indicators for unreliable exposure in microplate-based bioassays. *Chemosphere* 67, 2210-2220.

Rule, A. D., Gussak, H. M., Pond, G. R., Bergstralh, E. J., Stegall, M. D., Cosio, F. G., and Larson, T. S. (2004) Measured and estimated GFR in healthy potential kidney donors. *American Journal of Kidney Diseases* 43, 112-119.

Ryan, J. A. (2008) Evolution of Cell Culture Surfaces. *BioFiles* 3.8, 21.

Schreiber, R., Altenburger, R., Paschke, A., and Küster, E. (2008) How to deal with lipophilic and volatile organic substances in microtiter plate assays. *Environmental Toxicology and Chemistry* 27, 1676-1682.

Seibert, H., Morchel, S., and Gülden, M. (2002) Factors influencing nominal effective concentrations of chemical compounds *in vitro*: medium protein concentration. *Toxicology In Vitro* 16, 289-297.

Shukla, S. J., Huang, R. L., Sommons, S. O., Tice, R. R., Witt, K. L., vanLeer, D., Rabamabhardan, R., Austin, C. P. and Xia, M. H. (2012) Profiling environmental chemicals for activity in the andioxidant response element signaling pathway using a high-throughput screening approach. *Environmental Health Perspectives* 120, 1150–1156.

Smith, K. E. C., Oostingh, G. J., and Mayer, P. (2010) Passive dosing for producing defined and constant exposure of hydrophobic organic compounds during *in vitro* toxicity tests. *Chemical Research in Toxicology* 23, 55-65.

Song, Y. K., Hong, S. H., Jang, M., Han, G. M., and Shim, W. J. (2015) Occurrence and distribution of microplastics in the sea surface microlayer in Jinhae Bay, South Korea. *Archives of Environmental Contamination and Toxicology* 69, 279-287.

Stadnicka-Michalak, J., Tanneberger, K., Schirmer, K., and Ashauer, R. (2014) Measured and modeled toxicokinetics in cultured fish cells and application to *in vitro-in vivo* toxicity extrapolation. *PLOS ONE* 9(3): e92303.

Stalter, D., Dutt, M., and Escher, B. I. (2013) Headspace-free setup of *in vitro* bioassays for the evaluation of volatile disinfection by-products. *Chemical Research in Toxicology* 26, 1605–1614.

Schwarzenbach, R. P., Gschwend, P. M., and Dieter M. Imboden (2016) Environmental Organic Chemistry, 3rd Edition. Wiley, NJ, USA. ISBN: 978-1-118-76723-8.

Tanneberger, K., Rico-Rico, A., Kramer, N. I., Busser, F. J. M., Hermens, J. L. M., and Schirmer, K. (2010) Effects of solvents and dosing procedure on chemical toxicity in cell-based *in vitro* assays. *Environmental Science & Technology* 44, 4775-4781.

Tarazona, J. V., Court-Marques, D., Tiramani, M., Reich, H., Pfeil, R., Istace, F., and Crivellente, F. (2017) Glyphosate toxicity and carcinogenicity: a review of the scientific basis of the European Union assessment and its differences with IARC. *Archives of Toxicology* 91, 2723-2743.

ter Laak, T. L., ter Bekke, M. A., and Hermens, J. L. M. (2009) Dissolved organic matter enhances transport of PAHs to aquatic organisms. *Environmental Science & Technology* 43, 7212-7217.

Tóth, B., Krajcsi, P. and Magnan, R. (2014). Chapter 56 - Membrane transporters and transporter substrates as biomarkers for drug pharmacokinetics, pharmacodynamics, and toxicity/adverse events. Biomarkers in Toxicology. R. C. Gupta. Boston, MA, USA, Academic Press: 947-963.

Ulrich, N., Endo, S., Brown, T. N., Watanabe, N., Bronner, G., Abraham, M. H., Goss, K.-U. (2017) UFZ-LSER database v 3.2.1, Leipzig, Germany, Helmholtz Centre for Environmental Research-UFZ. [accessed on 10.08.2018].

U.S. EPA (2000) Supplementary guidance for conducting health risk assessment of chemical mixtures.

Van den Berg, M., Birnbaum, L. S., Denison, M., De Vito, M., Farland, W., Feeley, M., Fiedler, H., Hakansson, H., Hanberg, A., Haws, L., Rose, M., Safe, S., Schrenk, D., Tohyama, C., Tritscher, A., Tuomisto, J., Tysklind, M., Walker, N., and Peterson, R. E. (2006) The 2005 World Health Organization reevaluation of human and mammalian toxic equivalency factors for dioxins and dioxin-like compounds. *Toxicological Sciences* 93, 223-241.

Verhaar, H. J. M., Ramos, E. U., and Hermens, J. L. M. (1996) Classifying environmental pollutants 2. Separation of class 1 (baseline toxicity) and class 2 ('polar narcosis') type compounds based on chemical descriptors. *Journal of Chemometrics* 10, 149-162.

Villeneuve, D. L., Blankenship, A. L., and Giesy, J. P. (2000) Derivation and application of relative potency estimates based on *in vitro* bioassay results. *Environmental Toxicology and Chemistry* 19, 2835-2843.

Volpe, D. A. (2016) Transporter assays as useful *in vitro* tools in drug discovery and development. *Expert Opinion on Drug Discovery* 11, 91-103.

Wang, X. J., Hayes, J. D., and Wolf, C. R. (2006) Generation of a stable antioxidant response element-driven reporter gene cell line and its use to show redox-dependent activation of nrf2 by cancer chemotherapeutic agents. *Cancer Research* 66, 10983-10994.

Wetmore, B. A., Wambaugh, J. F., Ferguson, S. S., Sochaski, M. A., Rotroff, D. M., Freeman, K., Clewell, H. J., III, Dix, D. J., Andersen, M. E., Houck, K. A., Allen, B., Judson, R. S., Singh, R., Kavlock, R. J., Richard, A. M., and Thomas, R. S. (2012) Integration of dosimetry, exposure, and high-throughput screening data in chemical toxicity assessment. *Toxicological Sciences* 125, 157-174.

Wetmore, B. A. (2015) Quantitative *in vitro*-to-*in vivo* extrapolation in a high-throughput environment. *Toxicology* 332, 94-101.

Williams, G. M., Aardema, M., Acquavella, J., Berry, S. C., Brusick, D., Burns, M. M., de Camargo, J. L. V., Garabrant, D., Greim, H. A., Kier, L. D., Kirkland, D. J., Marsh, G., Solomon, K. R., Sorahan, T., Roberts, A., and Weed, D. L. (2016) A review of the carcinogenic potential of glyphosate by four independent expert panels and comparison to the IARC assessment. *Critical Reviews in Toxicology* 46, 3-20.

Willis, A. M., and Oris, J. T. (2014) Acute photo-induced toxicity and toxicokinetics of single compounds and mixtures of polycyclic aromatic hydrocarbons in zebrafish. *Environmental Toxicology and Chemistry* 33, 2028-2037.

The following Appendix includes the three Publications.

EBERHARD KARLS
UNIVERSITÄT
TÜBINGEN

Mathematisch-Naturwissenschaftliche Fakultät

Erklärung nach § 5 Abs. 2 Nr. 8 der Promotionsordnung der Math.-Nat. Fakultät
-Anteil an gemeinschaftlichen Veröffentlichungen-
Nur bei kumulativer Dissertation erforderlich!

Declaration according to § 5 Abs. 2 No. 8 of the PromO of the Faculty of Science
-Share in publications done in team work-

Name: Fabian Christoph Fischer

List of Publications

1. Fischer, F. C., Henneberger, L., König, M., Bittermann, K., Linden, L., Goss, K.-U. and Escher, B. I. (2017) Modeling Exposure in the Tox21 *in Vitro* Bioassays. *Chemical Research in Toxicology* 30, 1197-1208.
2. Fischer, F. C., Abele, C., Droge, S. T. J., Henneberger, L., König, M., Schlichting, R., Scholz, S. and Escher, B. I. (2018) Cellular uptake kinetics of neutral and charged chemicals in *in vitro* assays measured by fluorescence microscopy. *Chemical Research in Toxicology* 31(8), 646-657.
3. Fischer, F. C., Cirpka, O., Goss, K. U., Henneberger, L. and Escher, B. I. (2018) Application of experimental polystyrene partition constants and diffusion coefficients to predict the sorption of organic chemicals to well plates in *in vivo* and *in vitro* bioassays. *Environmental Science & Technology* 52(22), 13511-13522.

Nr.	**Accepted for publication yes/no**	**Number of all authors**	Position of the candidate in list of authors	Scientific ideas of candidate (%)	Data generation by candidate (%)	Analysis and Interpretation by candidate (%)	Paper writing by candidate (%)
			Optional, the declaration of the own share can also be done in words, please add an extra sheet.				
1	yes	7	1	60%	70%	80%	70%
2	yes	8	1	80%	80%	90%	80%
3	yes	5	1	80%	90%	60%	90%

I certify that the above statement is correct.

Date, Signature of the candidate

I/We certify that the above statement is correct.

Date, Signature of the doctoral committee or at least of one of the supervisors

Publication I

Modeling exposure in the Tox21 *in vitro* bioassays

Fabian C. Fischer[1], Luise Henneberger[1], Maria König[1], Kai Bittermann[2], Lukas Linden[2], Kai-Uwe Goss[2], Beate I. Escher[1]*

[1] Helmholtz Centre for Environmental Research - UFZ, Department Cell Toxicology, Permoserstraße 15, 04318 Leipzig, Germany

[2] Helmholtz Centre for Environmental Research - UFZ, Department Analytical Environmental Chemistry, Permoserstraße 15, 04318 Leipzig, Germany

Address correspondence to: fabian.fischer@ufz.de

Published in Chemical Research in Toxicology, DOI: acs.chemrestox.7b00023

Chemical Research in Toxicology

ACS Editors' Choice

Article

pubs.acs.org/crt

Modeling Exposure in the Tox21 *in Vitro* Bioassays

Fabian C. Fischer,*[,†] Luise Henneberger,[†] Maria König,[†] Kai Bittermann,[‡] Lukas Linden,[‡] Kai-Uwe Goss,[‡] and Beate I. Escher[†]

[†]Department Cell Toxicology, Helmholtz Centre for Environmental Research - UFZ, Permoserstraße 15, 04318 Leipzig, Germany

[‡]Department Analytical Environmental Chemistry, Helmholtz Centre for Environmental Research - UFZ, Permoserstraße 15, 04318 Leipzig, Germany

Supporting Information

ABSTRACT: High-throughput *in vitro* bioassays are becoming increasingly important in the risk characterization of anthropogenic chemicals. Large databases gather nominal effect concentrations (C_{nom}) for diverse modes of action. However, the biologically effective concentration can substantially deviate due to differences in chemical partitioning. In this study, we modeled freely dissolved (C_{free}), cellular (C_{cell}), and membrane concentrations (C_{mem}) in the Tox21 GeneBLAzer bioassays for a set of neutral and ionogenic organic chemicals covering a large physicochemical space. Cells and medium constituents were experimentally characterized for their lipid and protein content, and partition constants were either collected from the literature or predicted by mechanistic models. The chemicals exhibited multifaceted partitioning to proteins and lipids with distribution ratios spanning over 8 orders of magnitude. Modeled C_{free} deviated over 5 orders of magnitude from C_{nom} and can be compared to *in vivo* effect data, environmental concentrations, and the unbound fraction in plasma, which is needed for the *in vitro* to *in vivo* extrapolation. C_{cell} was relatively constant for chemicals with membrane lipid−water distribution ratios of 1000 or higher and proportional to C_{nom}. Representing a sum parameter for exposure that integrates the entire dose from intracellular partitioning, C_{cell} is particularly suitable for the effect characterization of chemicals with multiple target sites and the calculation of their relative effect potencies. Effective membrane concentrations indicated that the specific effects of very hydrophobic chemicals in multiple bioassays are occurring at concentrations close to baseline toxicity. The equilibrium partitioning model including all relevant system parameters and a generic bioassay setup is attached as an excel workbook to this paper and can readily be applied to diverse *in vitro* bioassays.

1. INTRODUCTION

In vitro cell bioassays present a simple, fast and cost-efficient tool for the effect characterization of chemicals. Particularly when run in high-throughput screening (HTS) format, *in vitro* bioassays will meet the high demands of effect data for the increasing number and variety of anthropogenic chemicals. The dose metric in *in vitro* testing is typically the nominal concentration (C_{nom}). However, only the freely dissolved concentration (C_{free}) is available for uptake and thus driving effects.[1] C_{free} should be quantified for interassay comparison and interpretation of *in vitro* effect data and for subsequent use in the quantitative *in vitro* to *in vivo* extrapolation (QIVIVE).[2−4] The total cellular concentration (C_{cell}) is directly related to C_{free} by the cell−water partition constant ($K_{cell/w}$) under equilibrium conditions and can serve as a proxy for the biological dose of chemicals.[5,6]

In *in vitro* bioassays, C_{free} can be depleted by sorption to medium constituents, such as the proteins and lipids from the medium.[7,8] Continuous reduction can be caused by evaporation,[9] partitioning into plate materials,[10] and degradation processes.[11] The relative importance of these processes depends on the bioassay setup and the physicochemical properties of the tested chemical.[12,13] These differences may result in a large and nonproportional deviation of C_{free} from C_{nom} and hence to reduced sensitivity of and low comparability between *in vitro* bioassays.

Recent studies demonstrated the variability of *in vitro* bioavailability as a result of chemical equilibrium partitioning between medium constituents and cells in different bioassay formats.[8,13] These studies normalized C_{cell} to the total cellular lipid content leading to underestimated C_{cell} of hydrophilic chemicals and chemicals that exhibit high protein sorption, such as anions.[14] Relevant partition constants were predicted by the chemicals' octanol−water partition constants (K_{ow}). However, the sorption of chemicals to biomolecules such as serum proteins can be very complex and dependent on various molecular interactions between the chemical and the sorbent, in

Received: January 27, 2017
Published: March 19, 2017

DOI: 10.1021/acs.chemrestox.7b00023
Chem. Res. Toxicol. 2017, 30, 1197−1208

particular for ionogenic organic chemicals (IOCs), leading to high errors in the prediction of partition constants via K_{ow}.[14,15]

A large *in vitro* database is available on the iCSS ToxCast Dashboard (https://actor.epa.gov/dashboard) provided by the US EPA, in which data from ToxCast (https://www.epa.gov/chemical-research/toxicity-forecasting) and Tox21 (https://www.epa.gov/chemical-research/toxicology-testing-21st-century-tox21) are collected. While ToxCast included more than 700 bioassays, the number of chemicals was limited to ∼1800. In contrast, in Tox21, ∼10,000 chemicals (Tox21 10K library) were tested in ∼50 *in vitro* bioassays covering various steps of the cellular signaling pathway.[16] Reporter gene assays based on various nuclear receptors and transcription factors are included in Tox21, and experiments were performed in HTS format in 1536 well plates using robotic systems.[16] In the iCSS ToxCast Dashboard, measured toxicity is expressed as 50% activity concentration (AC50), hereinafter referred to as 50% effect concentration (EC50). The use of 1536 well plates and the very small medium volumes of 5−6 μL hampered the analytical quantification of C_{free} and C_{cell}; thus, all reported effect data are based on C_{nom}.

As representative examples of the Tox21 bioassays, we chose 26 bioassays of the GeneBLAzer platform,[17−19] which use various human cell lines with reporter genes for diverse receptors. The cells constitutively coexpress a fusion protein of the ligand binding domain of the human nuclear receptor or transcription factor (DNA-binding domain).[17] Upon ligand binding, the fusion protein translocates to the nucleus and binds to the Upstream Activator Sequence (UAS) which controls the transcription of β-lactamase. The amount of β-lactamase is quantified via the changing fluorescence property of a specific substrate that is transformed by β-lactamase.[17]

This study aimed (i) at modeling 50% effective freely dissolved, cellular and membrane concentrations ($EC50_{free}$, $EC50_{cell}$, $EC50_{mem}$) of 100 neutral, anionic, cationic, and multiprotic (multiple acid and base functional groups) river pollutants with heterogeneous physicochemical properties and multiple modes of action[20] that have been comprehensively assessed with the Tox21 GeneBLAzer assays and (ii) to discuss the utility of the different dose metrics. As the basis for our model, relevant system parameters such as water, protein, and lipid contents in the assay media and cells were determined by experiment. Bovine serum albumin (BSA) and phospholipid liposomes (lip) were used in the modeling approach as surrogates for assay proteins and lipids, respectively. For both sorptive matrices, several databases of experimental partition constants are available in the literature,[14,15,21−23] and validated prediction approaches have been developed.[15,24−26] These were used to derive speciation-corrected distribution ratios at pH 7.4 between both surrogates and water ($D_{BSA/w}$, $D_{lip/w}$). We hypothesized that the chemicals would exhibit multifaceted partitioning between and within the medium and the cells dependent on the physicochemical properties of the chemicals and the assay setup, leading to a large variability in exposure between different chemicals and bioassays. This diversity could have hampered the risk prioritization within the Tox21 program because the differences in the EC50 could be due to both, differences in exposure and differences in the reporter gene construct of the particular cell line. Here, we address the former point, the variability in exposure and the insufficiency of nominal concentrations as a dose metric. Experimental determination of assay parameters as well as the use of state-of-the-art methods for the prediction of partition constants will enhance the precision and accuracy of model outputs while extending their domain of applicability to complex chemicals such as IOCs. Linking effect data to C_{free} and C_{cell} would improve the comparability between different *in vitro* bioassays, the analysis and interpretation of *in vitro* effect data, as well as its suitability for the QIVIVE.[4,27]

2. THEORY

As described by Armitage et al.,[13] the partition properties of *in vitro* assays can be defined by the composition and volumes of their system compartments, such as the medium, cells, headspace, and well plate materials as well as the respective partition constants for the chemicals of interest. Since we assume equilibrium, kinetic processes such as evaporation, diffusion into well plate materials, cellular uptake kinetics, and degradation were neglected for this study.

Quantifying evaporative losses from the well would only be possible in closed systems with a defined headspace volume, which generally hampers *in vitro* toxicity testing of volatile chemicals in unsealed HTS plate format. Therefore, only nonvolatile chemicals (air−water partition constant ≤0.03) were chosen for this study. The binding to plate material may be an important and time-dependent influencing factor in aqueous media with low organic matter content, e.g., in the *Aliivibrio fischeri*,[28] the *Danio rerio* fish embryo,[9] and the algae toxicity test, for which considerable losses are generally expected to occur for neutral chemicals with a log K_{ow} > 3.[10] Availability of partition constants and diffusion coefficients to polystyrene is relatively low, impeding the integration of sorption to plate materials into the model so far.

Preliminary experiments showed that equilibrium partitioning kinetics between the medium and the cells can be slow and different between neutral chemicals and IOCs,[29] which can lead to an underestimation of C_{cell} for a large period of the test duration. Because of this variability, equilibrium might not be achieved within the typical assay duration of up to 24 h, requiring modeling approaches to quantify exposure over time in future studies.

Proteins and lipids are the major sorptive colloids for organic chemicals in *in vitro* bioassays.[12,30] Thus, we define that the medium and the cells are composed of their respective volumes of proteins ($V_{protein}$ in L, density 1.36 kg L^{-1}), lipids (V_{lipid} in L, density 1.0 kg L^{-1}), and water (V_w in L, density 1.0 kg L^{-1}) (eqs 1 and 2) and that components with a low sorptive capacity such as carbohydrates are neglected.

$$V_{medium} = V_{protein,medium} + V_{lipid,medium} + V_{w,medium} \quad (1)$$

$$V_{cell} = V_{protein,cell} + V_{lipid,cell} + V_{w,cell} \quad (2)$$

Assuming equilibrium state and similar physical conditions (pH) between and within the medium and the cells results in equal medium and intracellular C_{free} as well as defined C_{cell}, as illustrated in Figure 1.

BSA and lip were used as surrogates for all medium and cellular proteins and lipids, respectively. However, given that both medium and, foremost, cells are composed of innumerable proteins and lipids of variable structure, this could represent a source of uncertainty. The distribution ratios between medium and water ($D_{medium/w}$, $L_w\ L_{medium}^{-1}$) as well as cells and water ($D_{cell/w}$, $L_w\ L_{cell}^{-1}$) are given as a function of their respective volume fractions (*VF*) of proteins, lipids, and water and the chemicals $D_{BSA/w}$ and $D_{lip/w}$ (eqs 3 and 4).

DOI: 10.1021/acs.chemrestox.7b00023
Chem. Res. Toxicol. 2017, 30, 1197−1208

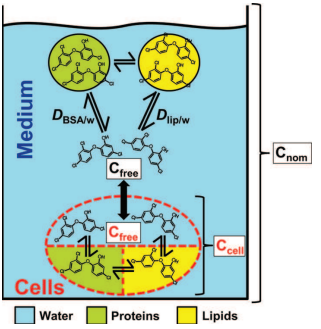

Figure 1. Mass balance model used for this study. The chemical partitioning was calculated from the distribution ratios between medium and cells at a medium pH of 7.4. Both compartments are composed of water, proteins, and lipids. Proteins and lipids are represented by BSA and lip.

$$D_{medium/w}\ (\text{pH } 7.4) = VF_{protein,medium} \times D_{BSA/w} + VF_{lipid,medium} \times D_{lip/w} + VF_{w,medium} \quad (3)$$

$$D_{cell/w}\ (\text{pH } 7.4) = VF_{protein,cell} \times D_{BSA/w} + VF_{lipid,cell} \times D_{lip/w} + VF_{w,cell} \quad (4)$$

$D_{BSA/w}$ ($L_w\ L_{BSA}^{-1}$) and $D_{lip/w}$ ($L_w\ L_{lip}^{-1}$) result from the fraction of neutral and ionized species at medium pH of 7.4 and their associated partition constants (eqs 5 and 6).

$$D_{BSA/w}\ (\text{pH } 7.4) = f_{neutral} \times K_{BSA/w}(\text{neutral}) + f_{ion} \times K_{BSA/w}(\text{ion}) \quad (5)$$

$$D_{lip/w}\ (\text{pH } 7.4) = f_{neutral} \times K_{lip/w}(\text{neutral}) + f_{ion} \times K_{lip/w}(\text{ion}) \quad (6)$$

Chemical partitioning between medium and cells ($D_{medium/cell}$, $L_{cell}\ L_{medium}^{-1}$) was quantified with eq 7.

$$D_{medium/cell}\ (\text{pH } 7.4) = \frac{D_{medium/w}}{D_{cell/w}} \quad (7)$$

The chemical fractions in the cells and the medium were calculated by a mass balance equation (eqs 8 and 9).

$$f_{cell} = \left(1 + D_{medium/cell} \times \frac{V_{medium}}{V_{cell}}\right)^{-1} \quad (8)$$

$$f_{medium} = 1 - f_{cell} \quad (9)$$

Fractions within the two compartments (cells and medium) were calculated by the respective phase volumes (proteins, lipids, and water). For instance, the freely dissolved fraction in the medium ($f_{free,medium}$) and the fraction in cell membranes (f_{mem}) are defined by eqs 10 and 11.

$$f_{free,medium} = \left(1 + D_{BSA/w} \times \frac{V_{protein,medium}}{V_{w,medium}} + D_{lip/w} \times \frac{V_{lipid,medium}}{V_{w,medium}} + D_{cell/w} \times \frac{V_{cell}}{V_{w,medium}}\right)^{-1} \quad (10)$$

Table 1. Assay-Specific Information of the 26 Evaluated Tox21 Reporter Gene Assays of the GeneBLAzer Panel

assay name	biological target	medium information	cell line	cell number
AR BLA agonist ratio	androgen receptor (AR)	6 μL of OptiMEM + 10% d-FBS	HEK293T	2000
AR BLA antagonist ratio	androgen receptor (AR)	5 μL of OptiMEM + 10% d-FBS	HEK293T	2000
AR BLA antagonist viability	cell viability	5 μL of OptiMEM + 10% d-FBS	HEK293T	2000
ER BLA agonist ratio	estrogen receptor (ER)	6 μL of DMEM phenol-red free +2% cs-FBS	HEK293T	5000
ER BLA antagonist ratio	estrogen receptor (ER)	5 μL of DMEM phenol-red free +2% cs-FBS	HEK293T	5000
ER BLA antagonist viability	cell viability	5 μL of DMEM phenol-red free +2% cs-FBS	HEK293T	5000
GR BLA agonist ratio	glucocorticoid receptor (GR)	6 μL of OptiMEM + 1% d-FBS	HEK293T	1500
GR BLA antagonist ratio	glucocorticoid receptor (GR)	5 μL of OptiMEM + 1% d-FBS	HEK293T	1500
GR BLA antagonist viability	cell viability	5 μL of OptiMEM + 1% d-FBS	HEK293T	1500
PPARG BLA agonist ratio	peroxisome proliferator-activated receptor γ (PPARG)	6 μL of DMEM phenol-red free + 1% cs-FBS	HEK293H	3000
PPARG BLA antagonist ratio	peroxisome proliferator-activated receptor γ (PPARG)	6 μL of DMEM phenol-red free + 1% cs-FBS	HEK293H	3000
PPARG BLA antagonist viability	cell viability	6 μL of DMEM phenol-red free + 1% cs-FBS	HEK293H	3000
ARE BLA agonist ratio	nuclear factor: (erythroid-derived 2)-like 2	5 μL of DMEM GlutaMAX + 1% FBS	HepG2	2000
ARE BLA agonist viability	cell viability	5 μL of DMEM GlutaMAX + 1% FBS	HepG2	2000
P53 BLA p1−5 ratio	nuclear factor: tumor protein p53	5 μL of OptiMEM + 0.5% d-FBS	HCT 116	4000
P53 BLA p1−5 viability	cell viability	5 μL of OptiMEM + 0.5% d-FBS	HCT 116	4000
NFKB BLA agonist ratio	nuclear factor: kappa light polypeptide gene	6 μL of OptiMEM + 10% d-FBS	ME-180	2000
NFKB BLA agonist viability	cell viability	6 μL of OptiMEM + 10% d-FBS	ME-180	2000

DOI: 10.1021/acs.chemrestox.7b00023
Chem. Res. Toxicol. 2017, 30, 1197−1208

$$f_{mem} = \left(1 + \frac{1}{D_{lip/w}} \times \frac{V_{w,cell}}{V_{lipid,cell}} + \frac{D_{BSA/w}}{D_{lip/w}} \times \frac{V_{protein,cell}}{V_{lipid,cell}} + \frac{D_{medium/w}}{D_{lip/w}} \times \frac{V_{medium}}{V_{lipid,cell}}\right)^{-1} \quad (11)$$

$(E)C_{free}$ in the medium (mol $L_{w,medium}^{-1}$) can thereof be calculated by multiplying the free fraction in the medium ($f_{free,medium}$) with $(E)C_{nom}$ (mol L_{total}^{-1}) and the ratio of the system volume (V_{system}, L_{total}) to the water phase volume of the medium ($V_{w,medium}$, $L_{w,medium}$).

$$(E)C_{free} = (E)C_{nom} \times f_{free,medium} \times \frac{V_{system}}{V_{w,medium}} \quad (12)$$

$(E)C_{cell}$ (mol L_{cell}^{-1}) can be derived by multiplying $(E)C_{free}$ (mol $L_{w,medium}^{-1}$) with $D_{cell/w}$ (L_w L_{cell}^{-1}).

$$(E)C_{cell} = (E)C_{free} \times D_{cell/w} \quad (13)$$

$(E)C_{mem}$ (mol L_{mem}^{-1}) is the product of f_{mem}, $(E)C_{nom}$ (mol L_{total}^{-1}), and the quotient of the system volume (V_{system}, L_{total}) with the lipid volume of the cells ($V_{lipid,cell}$, L_{mem}), assuming that all cellular lipids are membrane lipids.

$$(E)C_{mem} = (E)C_{nom} \times f_{mem} \times \frac{V_{system}}{V_{lipid,cell}} \quad (14)$$

3. MATERIALS AND METHODS

3.1. System Parameters. The information on the experimental setup of the selected GeneBLAzer assays was gathered from the iCSS ToxCast Dashboard (https://actor.epa.gov/dashboard/, accessed on June 15, 2016). They were performed in 1536 well plate format with medium volumes of 5−6 μL and a maximum of 1 vol % of dimethyl sulfoxide. All cells were adherent. The end points, either binding to nuclear receptors or transcription factor activity measured as a fluorescence signal produced by GAL4 β-lactamase inducible reporter technology or cell viability based on luciferase-coupled ATP quantification, were quantified after 24 h of chemical exposure.

3.1.1. Determination of Water, Protein, and Lipid Contents of Cells and Media. In the 26 evaluated Tox21 GeneBLAzer assays (Table 1), either Opti Minimum Essential Medium (OptiMEM) or Dulbecco's Modified Eagle Medium (DMEM, phenol-red free or GlutaMAX) were used as basic medium with fetal bovine serum as supplement, either untreated (FBS), charcoal stripped (cs-FBS), or dialyzed (d-FBS). We used the cell lines HEK293T (ER alpha Griptite, CN: K1393), HEK293H (PPAR gamma-UAS-*bla*, CN: K1419), HepG2 (ARE-*bla*, CN: K1208), HCT116 (p53RE-*bla*, CN: K1202), and ME-180 (HRE-*bla*, CN: K1202) for the quantification of cell parameters. All medium constituents and cells were purchased from Thermo Fisher Scientific (Waltham, MA, USA).

To determine the water content of the cell lines, a defined number of cells (3−8 million cells) of each cell line was washed once with phosphate buffered saline (8% NaCl in H_2O, 0.2% KCl in H_2O, 1.442% Na_2HPO_4 in H_2O, and 0.25% KH_2PO_4 in H_2O, v/v 1:1:1:1), gathered in a microtube and centrifuged. The cell number was quantified with the automated cell counter CASY MODEL TT (Roche Innovatis, Reutlingen, Germany). Wet weight of the cell pellet was measured. Subsequently, the cells were freeze-dried for at least 24 h, and their dry weight was measured. The water content of the cells was defined as the difference between wet and dry weights.

The protein contents of cells and media were quantified with the Lowry assay.[31] The cells were homogenized for 1 min by ultrasonic treatment (Sonoplus 2070, Bandelin, Berlin, Germany). Both the homogenized cells and medium constituents were diluted in bidistilled water yielding protein concentrations that fell into the range of the BSA calibration (0.1−1 mg mL^{-1}, Carl Roth GmbH + Co. KG, Karlsruhe, Germany). In a 96-well plate (clear, flat bottom, Corning, Lowell, MA, USA), 200 μL of Lowry reagent (1% $CuSO_4$ in H_2O, 2% K−Na-tartrate in H_2O, 2% Na_2CO_3 in H_2O, v/v 0.5:0.5:25) was added to 20 μL of BSA standard or sample. The well plate was shaken on a vortex mixer (VXR basic, IKA, Staufen, Germany) for 5 min at 900 rpm. Twenty microliters of a 1 M Folin−Ciocalteu reagent (Sigma-Aldrich, Munich, Germany) was added to each well. After 30 min at 900 rpm, the color intensity at 750 nm was measured in an UV/Vis plate reader (F200 Infinite Pro, TECAN, Männedorf, Switzerland), whereby 16 measurements were automatically performed at different positions in the well. The protein content of the samples was then quantified by the resulting linear regression equation of the BSA calibration series.

Lipids in the cells and media constituents were extracted according to a modified Bligh−Dyer method without use of chlorinated solvents.[32,33] Briefly, 2-propanol (99% purity, Merck KGaA, Darmstadt, Deutschland) and cyclohexane (99% purity, Merck) were added to samples of homogenized cells in bidistilled water and single medium constituents yielding a volume ratio of 8:10:11. The tubes were then vortexed for 30 s, sonicated for 5 min in a water bath at room temperature and centrifuged at 2000 rpm for 5 min (Centrifuge 5804, Eppendorf, Hamburg, Germany). The resulting upper cyclohexane layer was removed from the tubes and gathered. The extraction was repeated once with 1 mL of cyclohexane. The lipid contents of the extracts were subsequently determined with three different methods. The total lipid content in the extract was determined gravimetrically. Lipids were further quantified by a modified sulfo-phosphovanillin method via the number of double bonds on the fatty acids.[34] The extracts were transferred to 1.5 mL HPLC vials and dried under nitrogen, followed by the addition of 0.2 mL 95% concentrated sulfuric acid (Merck) and heating at 100 °C for 10 min. After adding 0.8 mL of phosphoric acid-vanillin reagent (0.2 g vanillin (Sigma-Aldrich) in 80 mL of H_2O and 20 mL of 85% phosphoric acid (Merck)) and 10 min of incubation at room temperature, absorbance was measured at 530 nm. Triolein (Sigma-Aldrich), 1-palmitoyl-2-oleoyl-*sn*-glycero-3-phosphocholine (POPC, Avanti Polar Lipids, Alabaster, AL, USA), and cholesterol (Sigma-Aldrich) were used as calibration standards (0−100 μg). Since the lipid compositions of cells and media are unknown, the mean value of the three calibrations with three different calibration standards was finally used for quantification. The total organic phosphorus content (TOP) of the extracts was determined in addition to estimate the phospholipid content as representative of membrane lipids. For the TOP measurements, the cyclohexane extracts were gathered in 250 mL round flasks and evaporated in a rotary evaporator (RE 121, Büchi, Essen, Germany) to form thin lipid films for improved formation of membrane lipid vesicles. After adding 8 mL of bidistilled water and resuspension in an ultrasonic bath for 5 min, the TOP was determined by inductively coupled plasma atomic emission spectroscopy. The phospholipid concentration in POPC equivalents (C_{POPC}) was calculated based on the molecular weight of phosphorus (M_P = 31 g mol^{-1}) and POPC (M_{POPC} = 760 g mol^{-1}):

$$C_{POPC} = \frac{C_P}{\frac{M_P}{M_{POPC}}} \quad (15)$$

The sulfo-phosphovanillin method was found to be most suitable for the lipid determination of *in vitro* test media and cells due to the small amounts of lipids that rendered the gravimetric method unreliable. The values from the sulfo-phosphovanillin method were used for modeling. A discussion on the different lipid determination methods can be found in the Supporting Information (section S1).

All results from the water, protein and lipid determinations can be found in the Supporting Information (Table S1).

3.2. Chemical Descriptors. The 100 chemicals cover a wide range of physicochemical properties. The hydrophobicity of the neutral species of the chemicals spans almost 9 orders of magnitude with log K_{ow} ranging from 0.07 to 8.48 (Table S3) with water solubility differing from easily soluble (e.g., caffeine with 200 g L^{-1}) to almost insoluble in

DOI: 10.1021/acs.chemrestox.7b00023
Chem. Res. Toxicol. 2017, 30, 1197−1208

Table 2. System Parameters of Two Reporter Gene Assays of the GeneBLAzer Panel[a]

androgen receptor (AR) assay			antioxidant response element (ARE) assay		
medium			medium		
volume	6 μL		volume	5 μL	
medium	OptiMEM + 10% d-FBS		medium	DMEM GlutaMAX + 1% FBS	
V_{water}	5.97×10^{-03} μL	99.45%	V_{water}	4.99×10^{-03} μL	99.84%
$V_{protein}$	3.12×10^{-05} μL	0.52%	$V_{protein}$	6.90×10^{-06} μL	0.14%
V_{lipid}	1.66×10^{-06} μL	0.03%	V_{lipid}	1.04×10^{-06} μL	0.02%
cells			cells		
cell line	HEK293T		cell line	HepG2	
cell number	2000		cell number	2000	
V_{water}	1.32×10^{-05} μL	90.57%	V_{water}	5.31×10^{-06} μL	87.35%
$V_{protein}$	1.23×10^{-06} μL	8.43%	$V_{protein}$	5.75×10^{-07} μL	9.46%
V_{lipid}	1.46×10^{-07} μL	1.00%	V_{lipid}	1.94×10^{-07} μL	3.19%

[a]The water, protein, and lipid contents of the cells and media were experimentally determined as described in section 3.1. The characteristics of all other assays are described in Table S2.

water (e.g., indeno(1,2,3-c,d)pyrene with 0.01 μg L^{-1}). Four chemicals are permanently charged, and 46 chemicals are ionizable, of which 31 are >99% ionized in water at medium pH of 7.4, 16 are present with a fraction of the neutral species ≤98%, and 6 are multiprotic (forming dicationic, dianionic, and zwitterionic species).

The partition constants that were used to calculate the distribution ratio of the chemicals were preferably experimental values from the literature. If no experimental data were available, partition constants for the neutral and ionic species were modeled as described in the following sections. The complete data set including all relevant physicochemical properties and distribution ratios D for the chemicals at pH 7.4 is provided in the Supporting Information (Table S3).

3.2.1. PP-LFERs to Predict Partition Constants of Neutral Species. For neutral chemicals and the neutral fraction of IOCs, the polyparameter linear free energy relationships (PP-LFERs) shown in eqs 16[15] and 17[23] were used to predict $K_{BSA/w}$ and $K_{lip/w}$.

$$\log K_{BSA/w} = 0.35 + 0.28 \times L - 0.46 \times S + 0.2 \times A - 3.18 \times B + 1.84 \times V \quad (16)$$

$$\log K_{lip/w} = 0.53 + 0.49 \times L - 0.93 \times S - 0.18 \times A - 3.75 \times B + 1.73 \times V \quad (17)$$

The capital letters describe the properties of the chemical, wherein S is the dipolarity/polarizability parameter, A is the solute's H-bond acidity, B is the solute's H-bond basicity, V is the molar volume, and L is the logarithm of the hexadecane-air partition constant. These chemical descriptors are multiplied with system descriptors that depend on the difference in chemical properties between two sorbates and are derived from multiple linear regression analysis against experimental partition constants. Experimental substance and system descriptors were obtained from the UFZ-LSER database,[35] and missing substance descriptors were calculated using the Absolv module available in ACD/Laboratories.[36]

3.2.2. 3D-QSARs. A 3D quantitative structure-activity relationship (3D-QSAR) model was used to predict $K_{BSA/w}$ for those ions that have no reported experimental values on partition constants or fraction bound in plasma.[37] Two experimental data sets of 83 neutral chemicals[15] and 45 anionic chemicals[14] were used to construct a 3D-QSAR model with open3DQSAR.[38] The detailed procedure is reported elsewhere[39] and shall be explained here only briefly. The basis for the calculation is the COSMO-RS theory[40] and the representation of chemicals through their polarized surface (sigma surface). The sigma surface is used for the alignment[41] of the 3D-QSAR model, and the model is calibrated in the same way as it was done in a previous publication for various data sets.[37] After model calibration, $K_{BSA/w}$ could be estimated with a RMSE of 0.63 ± 0.10 and R^2 of 0.52 ± 0.15 for the 128 chemicals of the data set.[39]

3.2.3. COSMOmic. In those cases where no experimental values were available for $K_{lip/w}$ of ions, we used COSMOmic for prediction.[24,42] COSMOmic is a mechanistic, quantum mechanistically based model, which extends the Conductor-like Screening Model for Real Solvents (COSMO-RS)[40] in order to describe anisotropic micelle or lipid bilayer systems.[24] The implementation of the membrane bilayer potential enables the calculation of $K_{lip/w}$ of charged organic chemicals[42] both more reliably and in a more mechanistically based manner using other models.[26] COSMOmic accounts for the anisotropy of a phospholipid bilayer by virtually slicing the bilayer into consecutive layers and successively calculating the Gibbs free energy of the chemicals between a bulk water layer and each phospholipid layer. Thereby, the different contributions of the depth-dependent chemical environments of a phospholipid bilayer can be taken into account.

3.3. Tox21 Data Extraction. We extracted $EC50_{nom}$ from the iCSS ToxCast Dashboard (https://actor.epa.gov/dashboard, accessed on January 27, 2017) for the active chemicals in the selected bioassays. Between 2 and 31 chemicals were active in 25 of the 26 selected assays, and the literature $EC50_{nom}$ values are compiled in Table S4.

4. RESULTS AND DISCUSSION

4.1. System Parameters of the Tox21 GeneBLAzer Reporter Gene Battery. As is common for human cell-based bioassays, the media used in the Tox21 GeneBLAzer battery are consistently composed of a basic medium amended with a defined amount of FBS. The experimental quantification of protein, lipid, and water volumes revealed that protein and lipid contents of the three different basic media (OptiMEM, DMEM GlutaMAX, and phenol-red free DMEM) varied by 46 and 18%, respectively. Variability among FBS, d-FBS, and cs-FBS was 17% in terms of protein and 5% in terms of lipid content. Cellular water, protein, and lipid contents of the five cell lines differed by 52%, 41%, and 20% from the average.

The experimental setup regarding basic medium, FBS content, as well as used cell line and cell number varied considerably between the assays (Table 1). For example, the androgen receptor (AR) assay was performed in OptiMEM with a d-FBS content of 10%, whereas DMEM GlutaMAX with only 1% FBS was used in the antioxidant response element (ARE) assay (Table 2). The medium made up >99% of the total volume in all evaluated assays, and both, the medium and the cells, were predominantly composed of water with minor volume contributions of proteins and lipids (Table S2). Proteins and lipids are considered the main sorptive phases in *in vitro* bioassays. The proportion of proteins and lipids were

DOI: 10.1021/acs.chemrestox.7b00023
Chem. Res. Toxicol. 2017, 30, 1197−1208

consistently higher in the cells (AR assay: $VF_{protein,cell}$ = 8.43%; $VF_{lipid,cell}$ = 1.00%) compared to the medium (AR assay: $VF_{protein,medium}$ = 0.52%; $VF_{lipid,medium}$ = 0.03%) (Table 2), whereby the volume of proteins was higher than the volume of lipids in the medium (AR assay: 17.3:1) and in the cells (AR assay: 8.4:1).

These differences led to a 4.5 times higher protein and a 1.6 times higher lipid content in the AR medium than in the ARE medium. The bioassays were also performed with different cell lines. In the AR assay, HEK293T cells derived from a human embryonic kidney were used, whereas the human liver cancer cell line HepG2 was used in the ARE assay (Table 2). Although having a 2.4 times higher total volume and being composed of 2.5 times and 2.1 times more water and proteins, respectively, the VF_{lipid} of the HEK293T cells was measured to be 3.2 times lower compared to that of the HepG2 cells. HepG2 cells synthesize fatty acids during cultivation which explains their high lipid content.[43] The system parameters of all evaluated GeneBLAzer assays with associated volumes of water, proteins, and lipids can be found in Table S2.

4.2. Chemical Partitioning. The sorption affinities to BSA and liposomes vary by orders of magnitude between the chemicals, with log $D_{BSA/w}$ and log $D_{lip/w}$ ranging from −0.2 up to 6.5 and −0.4 up to 8 (Figure 2), respectively. Even very

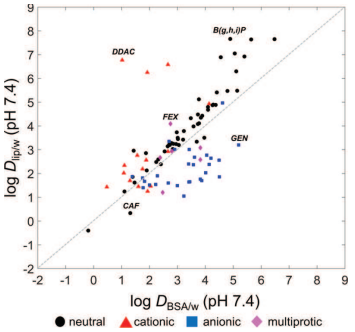

Figure 2. $D_{lip/w}$ and $D_{BSA/w}$ of neutral, cationic, anionic, and multiprotic chemicals at a medium pH of 7.4. Didecyldimethylammonium chloride (DDAC), caffeine (CAF), fexofenadine (FEX), genistein (GEN), and benzo(g,h,i)perylene (B(g,h,i)P) are emphasized as examples.

hydrophilic chemicals such as caffeine (CAF, log $D_{lip/w}$ = 0.33) sorb considerably to BSA (log $D_{BSA/w}$ = 1.31), while polycyclic aromatic hydrocarbons such as benzo(g,h,i)perylene (B(g,h,i)-P) show very high sorption affinity to both surrogates (log $D_{BSA/w}$ = 4.89, log $D_{lip/w}$ = 7.66).

For the neutral chemicals ($f_{neutral}$ > 98%), there is an apparent correlation between log $D_{BSA/w}$ and log $D_{lip/w}$ with binding to liposomes a factor of up to 1000 times stronger than that to BSA. Although most of the investigated anionic chemicals (f_{anion} ≥ 2%) show higher affinity to proteins compared to phospholipids, e.g., genistein (GEN) (f_{anion} = 0.61, log $D_{BSA/w}$ = 5.19, log $D_{lip/w}$ = 3.20), there are also exceptions, such as pentobarbital (f_{anion} = 0.16, log $D_{BSA/w}$ = 1.38, log $D_{lip/w}$ = 1.68). Most of the considered cations are predominantly available in the water phase of the medium, but quaternary ammonium cations with long carbon chains, such as didecyldimethylammonium chloride (DDAC) (f_{cation} = 1, log $D_{BSA/w}$ = 1.02, log $D_{lip/w}$ = 6.77), are >99% bound to lipids, probably as a result of structural similarities to phospholipids that make up liposomes.[23]

The distribution ratios for the 100 chemicals illustrate the complexity of chemical partitioning to proteins and lipids, which emphasizes that their derivation by log K_{ow} correlation can lead to a high uncertainty and inaccuracy.[14,23,26] Using prediction methods such as PP-LFERs, COSMOmic, and 3D-QSARs that include several chemical properties and even 3D interactions can substantially improve the quality of predicted partition constants compared to predictions via log K_{ow}.

4.3. Freely Dissolved Concentration as the *in Vitro* Dose Metric. A key objective of *in vitro* effect testing is the comparison and extrapolation of observed effects to realistic exposure scenarios, e.g., in the environment. C_{free} serves as most appropriate dose metric for this purpose since it is safe to assume that the target site concentration is in equilibrium with C_{free} in the vicinity of the target site in most scenarios. C_{free} can thus be used as an indicator of whether an effect is to be expected.[6,8,12,13,44] In other words, if an assay shows an effect at a given C_{free}, then we can expect to measure the same effects at equal C_{free} in any other exposure scenario.

As shown for the AR assay for a constant C_{nom} of 10 μM (Figure 3A), modeled C_{free} can differ considerably and

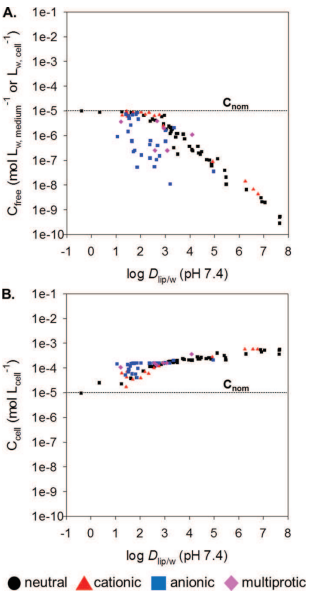

Figure 3. Modeled freely dissolved (A) and cellular (B) concentrations of neutral, cationic, anionic, and multiprotic chemicals in the AR assay based on a nominal concentration of 10 μM, sorted by chemicals' $D_{lip/w}$ at medium pH 7.4. Note that chemicals could have been sorted just as well by $D_{BSA/w}$.

DOI: 10.1021/acs.chemrestox.7b00023
Chem. Res. Toxicol. 2017, 30, 1197−1208

nonproportionally from C_{nom} with a deviation of up to 5 orders of magnitude for very hydrophobic chemicals. There are also large deviations of C_{free} from C_{nom} for anionic chemicals with log $D_{lip/w}$ < 3, confirming that C_{nom} is not suitable as an approximation for C_{free} in the Tox21 GeneBLAzer assays.

Modeling C_{free} by our approach can substantially increase the comparability within the Tox21 GeneBLAzer battery, to other *in vitro* constructs, and to *in vivo* systems, for which controlling and measuring C_{free} is progressively becoming the norm.[7,45−47] Since environmental monitoring of chemicals is increasingly based on C_{free} measured by, e.g., *in situ* passive sampling devices,[48,49] modeled C_{free} can directly be compared to environmental concentrations. C_{free} represents the most appropriate input parameter for the QIVIVE since it can directly be related to the unbound fraction in plasma.[4,27]

4.4. Cellular Concentration as the *in Vitro* Dose Metric. The toxic effects of a chemical most probably result from complex combinations of specific (e.g., hormone receptor binding), reactive, and baseline effects. As discussed in earlier studies, internal effect concentrations (IEC) can serve as proxy for the biologically effective dose in whole organisms.[5,50,51] Analogous to this concept, C_{cell} represents a sum parameter that integrates the entire intracellular dose from partitioning into different biological targets, e.g., suitable to describe exposure to electrophilic chemicals that can react with biological nucleophiles located in different cell organelles[52] or to evaluate baseline toxicity based on membrane concentrations.[53]

At a constant C_{nom} in the AR assay, C_{cell} is fairly constant for chemicals with log $D_{lip/w}$ > 3, and there is only a narrow gap of 1 order of magnitude between C_{nom} and C_{cell} (Figure 3B). This finding is relevant considering the approach to characterize the *in vitro* toxicity of chemicals and mixtures based on relative effect potencies (REP), which relate the effect of a chemical to a potent reference chemical.[54,55] Because of the systematic difference between C_{nom} and C_{cell}, the REP values in *in vitro* assays when derived from C_{nom} and C_{cell} are very similar for a given chemical across a large chemical space. Thus, the approach remains valid for *in vitro* systems even though bioavailability can vary greatly. The WHO toxic equivalency factors (TEF) are consensus values for comparison of the potency of dioxin-like chemicals,[56,57] and they were derived from measured *in vivo* REPs mainly from mammalian tests using a dose metric of mass per kg body weight, hence a nominal dose. For the derivation of TEF for fish,[57] *in vivo* biomarkers and fish cell lines were used and appear to also have been based on nominal concentrations in most cases. The REP derived from C_{nom} and C_{cell} are thus good proxies for *in vivo* REP and can be used in the future for TEF revisions. The proportionality between C_{nom} and C_{cell} over a wide range of hydrophobicity is given for this particular *in vitro* battery as a result of the colloid-rich medium. C_{cell} deviates nonproportionally from C_{nom} in a colloid-free cell-based system (Figure S3). The same would hold for the cell-free assays that are among the ToxCast assays. For cell-free assays, a simpler model solely based on receptor binding could be invoked, which lies beyond the scope of this study.

4.5. Chemical Partitioning in the Tox21 GeneBLAzer Assays. The dependency of chemical partitioning on the composition of the medium and cells is illustrated in Figure 4. B(g,h,i)P is mainly bound to lipids in medium and cells. Although being >90% available in the water phase of the medium of the AR assay (Figure 4A), within the cells CAF is mainly bound to proteins (Figure 4B). The multimedia

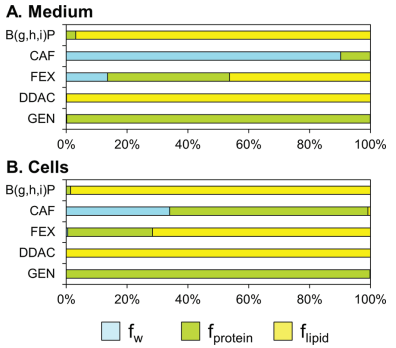

Figure 4. Mass balance of exemplary chemicals in water, proteins, and lipids of (A) the medium and (B) the cells of the AR assay. Note that the mass balance differs considerably between the compartments, as a result of their respective water, lipid, and protein volume fractions (Table 2).

chemical fexofenadine (FEX) is distributed between all phases in the medium but mainly resides in the lipids within the cells.

In contrast, for DDAC and GEN, the distribution does not differ much within the cells and within the medium, caused by the higher sorption affinity of DDAC to lipids compared to proteins (f_{cation} = 1, log $D_{BSA/w}$ = 1.02, log $D_{lip/w}$ = 6.77), and contrarily of GEN to proteins compared to lipids (f_{anion} = 0.61, log $D_{BSA/w}$ = 5.19, log $D_{lip/w}$ = 3.20).

The partitioning of all evaluated chemicals and the resulting large variability in exposure are illustrated for the AR and ARE assays (Figure 5). The medium generally represents the dominant sink for the chemicals in all Tox21 GeneBLAzer assays (>84%, Figure 5A and D). This phenomenon results from the large volume fraction of the medium (>99%) and the fact that the medium makes up a large proportion of total system proteins and lipids, for instance, 96.2% and 91.9% in the AR assay, respectively. This leads to high reductions in the C_{free} of chemicals with high $D_{lip/w}$ and $D_{BSA/w}$ and a large deviation from C_{nom} (Figure 3A).

In the AR medium (Figure 5B), 72 of the 100 chemicals were modeled to partition >70% to proteins and lipids, mainly as a result of the 10% FBS content of the medium leading to a $VF_{protein}$ of 0.52%, whereas only four chemicals are ≥90% freely dissolved in the water phase. In the medium of the ARE assay with 1% FBS and a consequently lower $VF_{protein}$ of 0.14% (Figure 5E), 52 chemicals were bound >70%, whereas 12 were >90% freely available. These findings indicate that C_{free} and thus the measured effects can considerably be reduced in *in vitro* bioassays by the colloid-rich media,[1,30] wherein the degree of reduction highly depends on the FBS content in the medium.

Because of the lower VF_w in the cells (90.6% for AR and 87.4% for ARE) compared to the medium (>99%), the proteins and lipids are the dominant sink for most chemicals in the cells. However, due to the higher volume fraction of lipids (VF_{lipid} = 3.2% in ARE compared to 1.0% in AR), chemical partitioning to the lipid phase of the ARE cells is considerably higher compared to the AR cells (Figure 5C and F).

In the ARE assay with a medium amended with only 1% FBS, the partitioning into the cells becomes more relevant in the

DOI: 10.1021/acs.chemrestox.7b00023
Chem. Res. Toxicol. 2017, 30, 1197−1208

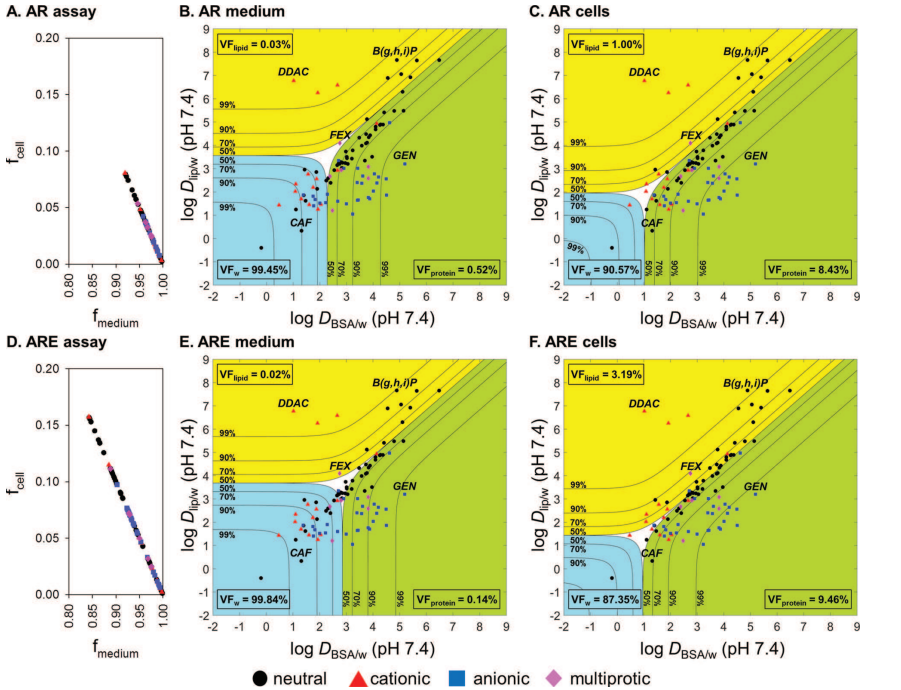

Figure 5. Modeled chemical partitioning of neutral, cationic, anionic, and multiprotic chemicals between cells and medium as well as among lipids (yellow), proteins (green), and water (blue) within the medium and the cells in the AR (A,B,C) and the ARE (D,E,F) assays, based on chemicals' $D_{lip/w}$ and $D_{BSA/w}$ at a medium pH of 7.4. The marked lines indicate the 50%, 70%, 90%, and 99% thresholds that result from the respective phase volume fractions (VF) in cells and medium.

overall mass balance (Figure 5D). Although accounting for only 0.12% of the total system volume, the cells make up 8.0% and 15.8% of total system proteins and lipids (opposed to only 3.8% and 8.1% in the AR assay); thus, particularly chemicals with high $D_{lip/w}$ and $D_{BSA/w}$ partition to a larger proportion into the cells (up to 16%). In contrast, a medium such as the AR medium with 10% FBS is generally less depleted by cellular uptake (<8%, Figure 5A); however, at the same C_{nom}, C_{cell} in the AR assay are lower compared to that of the ARE assay.

4.6. Application of the Model to GeneBLAzer Effect Data. 48 of the 100 evaluated chemicals were active in at least one of the evaluated GeneBLAzer assays, of which 28 are neutral, 13 partially anionic, 1 partially cationic, 1 permanently charged anionic, 2 permanently charged cationic, and 3 multiprotic at medium pH of 7.4. Note that 13 of the chemicals were not tested within the Tox21 GeneBLAzer battery, and 3 were only tested in a subset of the assays. The very hydrophobic neutral polycyclic aromatic hydrocarbons benzo(a)pyrene (B(a)P) and benzo(*b*)fluoranthene as well as the cationic long chain quaternary ammonium compounds DDAC and hexadecyltrimethylammonium were active in various assays, while other chemicals were only active in a single assay, such as CAF (ARE) and indometacin (PPARG). The literature $EC50_{nom}$ and corresponding modeled effect concentrations of all active chemicals in all evaluated bioassays can be found in Table S4.

Figure 6 shows the REP of 6 of the 31 active chemicals in the Tox 21 ARE agonist assay in relation to the highly potent and very hydrophobic reference chemical 2,3,7,8-tetrachlorodibenzodioxin (2,3,7,8-TCDD) (Figure 6A) and the REP with the very hydrophilic chemical CAF as reference (Figure 6B). The REP_{free} based on the $EC50_{free}$ may underestimate the potency of a more hydrophilic chemical if the reference chemical is hydrophobic, whereas the REP_{free} is overestimated for hydrophobic chemicals if the reference chemical is hydrophilic. These differences are caused by the large deviations in chemical partitioning and thus large variety in C_{free} (Figure 3A). Representing a sum parameter for internal exposure, C_{cell} integrates differences in intracellular chemical partitioning between the test chemical and the reference chemical which result from differences in the physicochemical properties, which may span several orders of magnitude, as exemplified by 2,3,7,8-TCDD (log $D_{lip/w}$ = 6.89, Figure 6A) and CAF (log $D_{lip/w}$ = 0.33, Figure 6B). $EC50_{cell}$ thus represents a better input than $EC50_{free}$ for the REP calculations in the same *in vitro* test system. Considering the proportionality of C_{nom} and C_{cell} for

DOI: 10.1021/acs.chemrestox.7b00023
Chem. Res. Toxicol. 2017, 30, 1197−1208

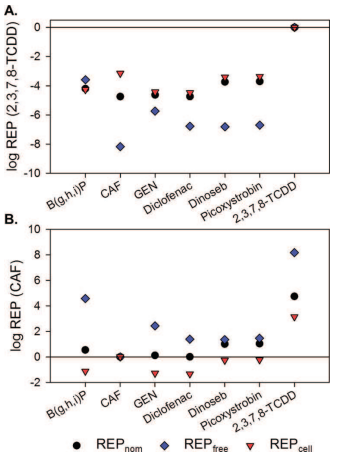

Figure 6. REP of six active chemicals in the ARE agonist assay with (A) 2,3,7,8-tetrachlorodibenzodioxin (2,3,7,8-TCDD) and (B) caffeine (CAF) as reference chemicals on basis of $EC50_{nom}$, $EC50_{free}$, and $EC50_{cell}$.

most of the chemicals (Figure 3B), C_{nom} may thereby serve as proxy for C_{cell} because REP_{nom} is very close to the REP_{cell} independent of the physicochemical properties of the reference chemical (Figure 6).

Baseline toxicity of organic chemicals occurs above a defined membrane concentration of approximately 300 mmol L_{mem}^{-1} in isolated cell membranes[58] and is considered to be related to membrane concentrations of 0.1 to 1 mol L_{lipid}^{-1} in aquatic species.[59,60] Figure 7 shows the EC50 values of agonist chemicals in the ARE assay based on C_{mem}.

Although most of the $EC50_{mem}$ are below the threshold for baseline toxicity, which constitutes the minimum toxicity a chemical can have, particularly neutral hydrophobic chemicals with high log $D_{lip/w}$ are close to the critical membrane concentration for baseline toxicity (prazepam and B(a)P).

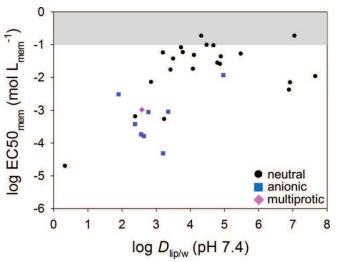

Figure 7. Modeled $EC50_{mem}$ of active neutral, anionic, and multiprotic chemicals in the ARE agonist assay plotted against their $D_{lip/w}$ at pH 7.4. The membrane concentration range of 0.1−1 mol L_{mem}^{-1} is given as a threshold for baseline toxicity (gray shading).[59,60] No cationic study chemicals were active in this bioassay.

Given the fact that the biological target site of the ARE assay is located in the cytosol, measured activities of hydrophobic chemicals might be less specific since concentration−response testing was performed up to cytotoxic concentrations (i.e., critical C_{mem}), also explaining their broad activity in assays indicative of different toxic mechanisms (e.g., B(a)P is active in 10 of the 26 evaluated assays). These results agree with the findings of a recent study by Judson et al.,[61] who revealed that chemicals that tend to cause cytotoxicity within a nominal concentration range of up to 100 μM activated 12% of the evaluated specific end points, whereas chemicals that did not show cytotoxicity within the concentration range were active in only 1.3% of the 815 assays. This phenomenon probably resulted from high C_{mem} since most of the broadly active chemicals are hydrophobic and thus exhibit high sorption to biological membranes, such as 7,12-dimethylbenz(*a*)anthracene (log $K_{lip/w}$ = 6.99). Modeling $EC50_{mem}$ can help to differentiate between chemicals showing specific effects and chemicals for which reported EC50 values might be partly influenced by underlying cytotoxicity. The reported differences in cell sensitivity to chemical-induced cytotoxicity between different cell lines[62] could result from differences in cellular composition resulting in different C_{mem} for similar C_{nom} of the chemical (Figure 5C and F). However, it could also be explained by differences in the medium composition of the considered *in vitro* bioassays.

Most of the target sites in *in vitro* bioassays are located either in the cytosol or in cell compartments such as the nucleus. More detailed modeling of chemical partitioning between different cell compartments could further enhance the interpretability of a cellular response. Further parametrization of compartment-specific proteins and lipids is therefore needed considering the complexity of chemical sorption to biomolecules.[14,15]

4.7. Implication for Chemical Risk Assessment and Future Steps. The protein- and lipid-rich nutrient medium used in cellular assays with mammalian cell lines could have led to a decreased sensitivity of the Tox21 *in vitro* bioassays due to reduced C_{free}. The model output is consistent with the conclusion of earlier studies that C_{nom} is generally not an adequate metric to describe the *in vitro* exposure of most of the evaluated chemicals since they are bound to a large extent even in media with low FBS content.[6,12,13] Given the fact that measured effects were exclusively linked to C_{nom} within the Tox21 program, chemical risk classification and prioritization hence suffers from low comparability between assays at a constant C_{nom} (Figure S4) and particularly to other exposure scenarios, such as *in vivo* toxicity data. Taking into account chemical partitioning by equilibrium model approaches such as those presented here considerably enhances the interpretability of *in vitro* toxicity data, but further refinement of the model, system, and chemical parameters as well as moving from an equilibrium to a kinetically resolved model will further improve the accuracy of the dose descriptors. However, the presented model is already a major leap as compared to purely K_{ow}-based equilibrium partitioning models.

The relative distribution of the chemicals in the Tox21 GeneBLAzer assays shows that chemical partitioning in *in vitro* assays can vary greatly between and within the cells and medium. C_{free} is strongly dependent on (i) the physicochemical properties of all species of the chemicals as well as (ii) the composition of the medium and the cells in terms of volume fractions of lipids, proteins, and water. Inconsistency in basic

DOI: 10.1021/acs.chemrestox.7b00023
Chem. Res. Toxicol. 2017, 30, 1197−1208

medium and FBS content as well as the natural variability of the FBS can thereby lead to highly variable C_{free} between bioassays of a single experimental platform but even more so across different platforms. One should be aware of this variability when comparing effect data of bioassays carried out with different setups or when changing the experimental setup of an assay.

Modeling C_{free}, C_{cell}, and even target site concentrations such as C_{mem} allows evaluation of whether differences in measured toxicity between *in vitro* platforms are the result of intrinsic sensitivity differences of the cell lines, the receptor expression, and/or the reporter gene design or whether they are simply the result of differences in bioavailability. However, in most databases, system parameters are either poorly reported or not available. Clear and traceable information on the system parameters (e.g., medium composition) should always be part of published *in vitro* effect data, in order to allow retrospective bioavailability calculations. Extending the equilibrium model to kinetic processes such as sorption to plate materials, degradation, cellular growth, and uptake kinetics can further improve the accuracy and correctness of the model output.

BSA and liposomes were used as surrogates for all medium and cellular proteins and lipids in order to improve the model over previous K_{ow}-based estimates. Sorption to proteins can be very complex,[63,64] in particular for IOCs for which strong steric and 3D structure effects on BSA sorption were measured for isomeric chemicals.[14] Studies are therefore needed that test the suitability of BSA and liposomes as surrogates for medium and cellular proteins and lipids when testing IOCs. The sorption of a chemical might be considerably different between proteins due to differences in the structure and conformation of binding sites, in particular when comparing serum proteins with structural proteins.[65] In contrast to neutral chemicals, ions are not expected to partition into storage lipids, but some have higher affinity to membrane bilayers. A more detailed parametrization of the medium and cell composition is warranted to find out if a more complex model is required or if the present model is sufficient for routine applications.

The model can readily be used and is included as Supporting Information. We provide experimental data on water, protein, and lipid contents of different media and different cell lines in Table S1, and there is also an average generic set of system parameters that can be applied for cells and media, for which protein and lipid contents have not been characterized. The modified Lowry assay and sulfo-phosphovanillin method are both rapid, robust photometric tests performed in multiwell plate format and can be implemented with low equipment and personnel costs. Considering that FBS is produced from natural blood, meaning its composition can vary considerably, we recommend quantifying proteins and lipids when using a new lot. Cellular composition may differ for similar cell lines of different culture. The partition constants of the study chemicals (log $K_{BSA/w}$ and log $K_{lip/w}$) are gathered in Table S3. Input values needed to perform predictions for neutral organic chemicals via PP-LFERs are moreover freely available for >8,000 chemicals.[35] Although state-of-the-art prediction approaches for ions such as COSMOmic and 3D-QSARs are not that easily accessible so far, there are ongoing efforts to develop user-friendly models for the prediction of IOCs. Considering the complexity of partitioning of ions into complex matrices such as BSA,[14,63,64] we need more experimental data for the mass balance model but also to improve the prediction methods for the binding constants. Methods are needed to robustly measure partition constants of IOCs for the relevant binding matrices, such as third-phase partitioning approaches[66] based on novel sampling devices for IOCs.[67]

■ ASSOCIATED CONTENT

Supporting Information

The Supporting Information is available free of charge on the ACS Publications website at DOI: 10.1021/acs.chemrestox.7b00023.

Model calculations (XLSX)

Experimental data on the system parameters, the relevant partition constants and modeled effect data for the study chemicals were gathered (XLSX)

Utility of the experimental methods used for lipid determination and additional plots (PDF)

■ AUTHOR INFORMATION

Corresponding Author

*Phone: +49 341 235-1512. Fax: +49 341 235-1787. E-mail: fabian.fischer@ufz.de.

ORCID

Fabian C. Fischer: 0000-0002-9511-0506

Beate I. Escher: 0000-0002-5304-706X

Funding

We gratefully acknowledge the financial support and the CEFIC Long-Range Research Initiative (LRI), project ECO30.

Notes

The authors declare no competing financial interest.

■ ACKNOWLEDGMENTS

We thank Cedric Abele and Christin Kühnert for laboratory support. Nils Klüver, Rita Schlichting, Till Luckenbach, and Annika Jahnke are gratefully acknowledged for their critical review of the manuscript. We thank Nadin Ulrich for the persistent upkeep and expansion of the UFZ LSER database. Christoph D. Rummel and Annika Jahnke are acknowledged for assistance with the table of contents graphic. We thank Jessica Hellweg for proofreading and assistance with the MATLAB codes.

■ ABBREVIATIONS

C_{nom}, nominal concentration; C_{free}, freely dissolved concentration; C_{cell}, cellular concentration; C_{mem}, membrane concentration; IOC, ionogenic organic chemicals; K_{ow}, octanol−water partition constant; $D_{lip/w}$, liposome−water distribution ratio; $D_{BSA/w}$, bovine serum albumin−water distribution ratio

■ REFERENCES

(1) Gülden, M., and Seibert, H. (1997) Influence of protein binding and lipophilicity on the distribution of chemical compounds in *in vitro* systems. *Toxicol. In Vitro 11*, 479−483.

(2) Gülden, M., and Seibert, H. (2003) *In vitro−in vivo* extrapolation: estimation of human serum concentrations of chemicals equivalent to cytotoxic concentrations *in vitro*. *Toxicology 189*, 211−222.

(3) Yoon, M., Campbell, J. L., Andersen, M. E., and Clewell, H. J. (2012) Quantitative *in vitro* to *in vivo* extrapolation of cell-based toxicity assay results. *Crit. Rev. Toxicol. 42*, 633−652.

(4) Wetmore, B. A. (2015) Quantitative *in vitro-to-in vivo* extrapolation in a high-throughput environment. *Toxicology 332*, 94−101.

DOI: 10.1021/acs.chemrestox.7b00023
Chem. Res. Toxicol. 2017, 30, 1197−1208

(5) Escher, B. I., and Hermens, J. L. M. (2002) Modes of action in ecotoxicology: Their role in body burdens, species sensitivity, QSARs, and mixture effects. *Environ. Sci. Technol. 36*, 4201−4217.
(6) Escher, B. I., and Hermens, J. L. M. (2004) Internal exposure: Linking bioavailability to effects. *Environ. Sci. Technol. 38*, 455A−462A.
(7) Heringa, M. B., Schreurs, R., Busser, F., Van Der Saag, P. T., Van Der Burg, B., and Hermens, J. L. M. (2004) Toward more useful *in vitro* toxicity data with measured free concentrations. *Environ. Sci. Technol. 38*, 6263−6270.
(8) Kramer, N. I., Krismartina, M., Rico-Rico, A., Blaauboer, B. J., and Hermens, J. L. M. (2012) Quantifying processes determining the free concentration of phenanthrene in basal cytotoxicity assays. *Chem. Res. Toxicol. 25*, 436−445.
(9) Schreiber, R., Altenburger, R., Paschke, A., and Kuster, E. (2008) How to deal with lipophilic and volatile organic substances in microtiter plate assays. *Environ. Toxicol. Chem. 27*, 1676−1682.
(10) Riedl, J., and Altenburger, R. (2007) Physicochemical substance properties as indicators for unreliable exposure in microplate-based bioassays. *Chemosphere 67*, 2210−2220.
(11) Wilk-Zasadna, I., Bernasconi, C., Pelkonen, O., and Coecke, S. (2015) Biotransformation *in vitro*: An essential consideration in the quantitative *in vitro-to-in vivo* extrapolation (QIVIVE) of toxicity data. *Toxicology 332*, 8−19.
(12) Gülden, M., Morchel, S., and Seibert, H. (2001) Factors influencing nominal effective concentrations of chemical compounds *in vitro*: cell concentration. *Toxicol. In Vitro 15*, 233−243.
(13) Armitage, J. M., Wania, F., and Arnot, J. A. (2014) Application of mass balance models and the chemical activity concept to facilitate the use of *in vitro* toxicity data for risk assessment. *Environ. Sci. Technol. 48*, 9770−9779.
(14) Henneberger, L., Goss, K. U., and Endo, S. (2016) Equilibrium sorption of structurally diverse organic ions to bovine serum albumin. *Environ. Sci. Technol. 50*, 5119−5126.
(15) Endo, S., and Goss, K. U. (2011) Serum albumin binding of structurally diverse neutral organic compounds: data and models. *Chem. Res. Toxicol. 24*, 2293−2301.
(16) Attene-Ramos, M. S., Miller, N., Huang, R., Michael, S., Itkin, M., Kavlock, R. J., Austin, C. P., Shinn, P., Simeonov, A., Tice, R. R., and Xia, M. (2013) The Tox21 robotic platform for the assessment of environmental chemicals - from vision to reality. *Drug Discovery Today 18*, 716−723.
(17) Huang, R. L., Xia, M. H., Cho, M. H., Sakamuru, S., Shinn, P., Houck, K. A., Dix, D. J., Judson, R. S., Witt, K. L., Kavlock, R. J., Tice, R. R., and Austin, C. P. (2011) Chemical genomics profiling of environmental chemical modulation of human nuclear receptors. *Environ. Health Persp. 119*, 1142−1148.
(18) Shukla, S. J., Huang, R. L., Sommons, S. O., Tice, R. R., Witt, K. L., vanLeer, D., Rabamabhardan, R., Austin, C. P., and Xia, M. H. (2012) Profiling environmental chemicals for activity in the andioxidant response element signaling pathway using a high-throughput screening approach. *Environ. Health Persp. 120*, 1150−1156.
(19) Huang, R., Sakamuru, S., Martin, M. T., Reif, D. M., Judson, R. S., Houck, K. A., Casey, W., Hsieh, J.-H., Shockley, K. R., Ceger, P., Fostel, J., Witt, K. L., Tong, W., Rotroff, D. M., Zhao, T., Shinn, P., Simeonov, A., Dix, D. J., Austin, C. P., Kavlock, R. J., Tice, R. R., and Xia, M. (2014) Profiling of the Tox21 10K compound library for agonists and antagonists of the estrogen receptor alpha signaling pathway. *Sci. Rep. 4*, 5664−5664.
(20) Busch, W., Schmidt, S., Kuhne, R., Schulze, T., Krauss, M., and Altenburger, R. (2016) Micropollutants in European rivers: A mode of action survey to support the development of effect-based tools for water monitoring. *Environ. Toxicol. Chem. 35*, 1887−99.
(21) Escher, B. I., Berg, M., Muhlemann, J., Schwarz, M. A. A., Hermens, J. L. M., Vaes, W. H. J., and Schwarzenbach, R. P. (2002) Determination of liposome/water partition coefficients of organic acids and bases by solid-phase microextraction. *Analyst 127*, 42−48.
(22) Endo, S., Mewburn, B., and Escher, B. I. (2013) Liposome and protein-water partitioning of polybrominated diphenyl ethers (PBDEs). *Chemosphere 90*, 505−511.
(23) Endo, S., Escher, B. I., and Goss, K. U. (2011) Capacities of membrane lipids to accumulate neutral organic chemicals. *Environ. Sci. Technol. 45*, 5912−5921.
(24) Klamt, A., Huniar, U., Spycher, S., and Keldenich, J. (2008) COSMOmic: A mechanistic approach to the calculation of membrane−water partition coefficients and internal distributions within membranes and micelles. *J. Phys. Chem. B 112*, 12148−12157.
(25) Endo, S., and Goss, K.-U. (2014) Applications of polyparameter linear free energy relationships in environmental chemistry. *Environ. Sci. Technol. 48*, 12477−12491.
(26) Bittermann, K., Spycher, S., and Goss, K.-U. (2016) Comparison of different models predicting the phospholipid-membrane water partition coefficients of charged compounds. *Chemosphere 144*, 382−391.
(27) Wetmore, B. A., Wambaugh, J. F., Ferguson, S. S., Sochaski, M. A., Rotroff, D. M., Freeman, K., Clewell, H. J., III, Dix, D. J., Andersen, M. E., Houck, K. A., Allen, B., Judson, R. S., Singh, R., Kavlock, R. J., Richard, A. M., and Thomas, R. S. (2012) Integration of dosimetry, exposure, and high-throughput screening data in chemical toxicity assessment. *Toxicol. Sci. 125*, 157−174.
(28) Gellert, G., and Stommel, A. (1999) Influence of microplate material on the sensitivity of growth inhibition tests with bacteria assessing toxic organic substances in water and waste water. *Environ. Toxicol. 14*, 424−428.
(29) Abele, C. (2016) Uptake Kinetics of Organic Compounds into Cells Quantified with Fluorescence Microscopy, Bachelor Thesis, University of Tübingen.
(30) Gülden, M., Morchel, S., Tahan, S., and Seibert, H. (2002) Impact of protein binding on the availability and cytotoxic potency of organochlorine pesticides and chlorophenols *in vitro*. *Toxicology 175*, 201−213.
(31) Lowry, O. H., Rosebrough, N. J., Farr, A. L., and Randall, R. J. (1951) Protein measurement with the Folin phenol reagent. *J. Biol. Chem. 193*, 265−75.
(32) Smedes, F. (1999) Determination of total lipid using non-chlorinated solvents. *Analyst 124*, 1711−1718.
(33) Bligh, E. G., and Dyer, W. J. (1959) A rapid method of total lipid extraction and purification. *Can. J. Biochem. Physiol. 37*, 911−917.
(34) Frings, C. S., and Dunn, R. T. (1970) A colorimetric method for determination of total serum lipids based on sulfo-phospho-vanillin reaction. *Am. J. Clin. Pathol. 53*, 89−91.
(35) Endo, S., Brown, T. N., Watanabe, N., Ulrich, N., Bronner, G., Abraham, M. H., and Goss, K.-U. (2015) *UFZ-LSER Database v 3.1 [Internet]*, Helmholtz Centre for Environmental Research-UFZ, Leipzig, Germany, http://www.ufz.de/lserd (accessed on Jan 27, 2017).
(36) ACD/Percepta (2015) *Build 2726*, Advanced Chemistry Development, Inc., Toronto, Canada, http://www.acdlabs.com.
(37) Klamt, A., Thormann, M., Wichmann, K., and Tosco, P. (2012) COSMOsar3D: Molecular field analysis based on local COSMO σ-Profiles. *J. Chem. Inf. Model. 52*, 2157−2164.
(38) Tosco, P., and Balle, T. (2011) Open3DQSAR: a new open-source software aimed at high-throughput chemometric analysis of molecular interaction fields. *J. Mol. Model. 17*, 201−8.
(39) Linden, L., Goss, K. U., and Endo, S. (2017) 3D-QSAR predictions for alpha-cyclodextrin binding constants using quantum mechanically based descriptors. *Chemosphere 169*, 693−699.
(40) Klamt, A. (1995) Conductor-like screening model for real solvents: A new approach to the quantitative calculation of solvation phenomena. *J. Phys. Chem. 99*, 2224−2235.
(41) Thormann, M., Klamt, A., and Wichmann, K. (2012) COSMOsim3D: 3D-similarity and alignment based on COSMO polarization charge densities. *J. Chem. Inf. Model. 52*, 2149−56.
(42) Bittermann, K., Spycher, S., Endo, S., Pohler, L., Huniar, U., Goss, K.-U., and Klamt, A. (2014) Prediction of phospholipid-water

DOI: 10.1021/acs.chemrestox.7b00023
Chem. Res. Toxicol. 2017, 30, 1197−1208

partition coefficients of ionic organic chemicals using the mechanistic model COSMOmic. *J. Phys. Chem. B 118*, 14833−14842.
(43) Gibbons, G. F., Khurana, R., Odwell, A., and Seelaender, M. C. L. (1994) Lipid balance in HepG2 cells - active synthesis and impaired mobilization. *J. Lipid Res. 35*, 1801−1808.
(44) Groothuis, F. A., Heringa, M. B., Nicol, B., Hermens, J. L. M., Blaauboer, B. J., and Kramer, N. I. (2015) Dose metric considerations in *in vitro* assays to improve quantitative *in vitro-in vivo* dose extrapolations. *Toxicology 332*, 30−40.
(45) Bandow, N., Altenburger, R., and Brack, W. (2010) Application of nd-SPME to determine freely dissolved concentrations in the presence of green algae and algae-water partition coefficients. *Chemosphere 79*, 1070−1076.
(46) Smith, K. E. C., Oostingh, G. J., and Mayer, P. (2010) Passive dosing for producing defined and constant exposure of hydrophobic organic compounds during *in vitro* toxicity Tests. *Chem. Res. Toxicol. 23*, 55−65.
(47) Adolfsson-Erici, M., Akerman, G., Jahnke, A., Mayer, P., and McLachlan, M. S. (2012) A flow-through passive dosing system for continuously supplying aqueous solutions of hydrophobic chemicals to bioconcentration and aquatic toxicity tests. *Chemosphere 86*, 593−599.
(48) Zabiegala, B., Kot-Wasik, A., Urbanowicz, M., and Namiesnik, J. (2010) Passive sampling as a tool for obtaining reliable analytical information in environmental quality monitoring. *Anal. Bioanal. Chem. 396*, 273−296.
(49) Booij, K., Robinson, C. D., Burgess, R. M., Mayer, P., Roberts, C. A., Ahrens, L., Allan, I. J., Brant, J., Jones, L., Kraus, U. R., Larsen, M. M., Lepom, P., Petersen, J., Profrock, D., Roose, P., Schafer, S., Smedes, F., Tixier, C., Vorkamp, K., and Whitehouse, P. (2016) Passive sampling in regulatory chemical monitoring of nonpolar organic compounds in the aquatic environment. *Environ. Sci. Technol. 50*, 3−17.
(50) McCarty, L. S., Landrum, P. F., Luoma, S. N., Meador, J. P., Merten, A. A., Shephard, B. K., and van Wezel, A. P. (2011) Advancing environmental toxicology through chemical dosimetry: external exposures versus tissue residues. *Integr. Environ. Assess. Manage. 7*, 7−27.
(51) McCarty, L. S., Mackay, D., Smith, A. D., Ozburn, G. W., and Dixon, D. G. (1993) Residue-based interpretation of toxicity and bioconcentration QSARs from aquatic bioassays - polar narcotic organics. *Ecotoxicol. Environ. Saf. 25*, 253−270.
(52) Schultz, T. W., Carlson, R. E., Cronin, M. T. D., Hermens, J. L. M., Johnson, R., O'Brien, P. J., Roberts, D. W., Siraki, A., Wallace, K. B., and Veith, G. D. (2006) A conceptual framework for predicting the toxicity of reactive chemicals: modeling soft electrophilicity. *Sar Qsar Environ. Res. 17*, 413−428.
(53) Escher, B. I., Eggen, R. I. L., Schreiber, U., Schreiber, Z., Vye, E., Wisner, B., and Schwarzenbach, R. P. (2002) Baseline toxicity (narcosis) of organic chemicals determined by *in vitro* membrane potential measurements in energy-transducing membranes. *Environ. Sci. Technol. 36*, 1971−1979.
(54) Villeneuve, D. L., Kannan, K., Khim, J. S., Falandysz, J., Nikiforov, V. A., Blankenship, A. L., and Giesy, J. P. (2000) Relative potencies of individual polychlorinated naphthalenes to induce dioxin-like responses in fish and mammalian *in vitro* bioassays. *Arch. Environ. Contam. Toxicol. 39*, 273−81.
(55) Escher, B. I., Bramaz, N., Mueller, J. F., Quayle, P., Rutishauser, S., and Vermeirssen, E. L. M. (2008) Toxic equivalent concentrations (TEQs) for baseline toxicity and specific modes of action as a tool to improve interpretation of ecotoxicity testing of environmental samples. *J. Environ. Monit. 10*, 612−621.
(56) Van den Berg, M., Birnbaum, L. S., Denison, M., De Vito, M., Farland, W., Feeley, M., Fiedler, H., Hakansson, H., Hanberg, A., Haws, L., Rose, M., Safe, S., Schrenk, D., Tohyama, C., Tritscher, A., Tuomisto, J., Tysklind, M., Walker, N., and Peterson, R. E. (2006) The 2005 World Health Organization reevaluation of human and mammalian toxic equivalency factors for dioxins and dioxin-like compounds. *Toxicol. Sci. 93*, 223−241.
(57) Van den Berg, M., Birnbaum, L., Bosveld, A. T., Brunström, B., Cook, P., Feeley, M., Giesy, J. P., Hanberg, A., Hasegawa, R., Kennedy, S. W., Kubiak, T., Larsen, J. C., van Leeuwen, F. X., Liem, A. K., Nolt, C., Peterson, R. E., Poellinger, L., Safe, S., Schrenk, D., Tillitt, D., Tysklind, M., Younes, M., Waern, F., and Zacharewski, T. (1998) Toxic equivalency factors (TEFs) for PCBs, PCDDs, PCDFs for humans and wildlife. *Environ. Health Perspect. 106*, 775−792.
(58) Escher, B. I., Schwarzenbach, R. P., and Westall, J. C. (2000) Evaluation of liposome-water partitioning of organic acids and bases. Development of a sorption model. *Environ. Sci. Technol. 34*, 3954−3961.
(59) McCarty, L. S., and Mackay, D. (1993) Enhancing ecotoxicological modeling and assessment. *Environ. Sci. Technol. 27*, 1718−1728.
(60) Escher, B. I., and Schwarzenbach, R. P. (2002) Mechanistic studies on baseline toxicity and uncoupling as a basis for modeling internal lethal concentrations in aquatic organisms. *Aquat. Sci. 64*, 20−35.
(61) Judson, R., Houck, K., Martin, M., Richard, A. M., Knudsen, T. B., Shah, I., Little, S., Wambaugh, J., Setzer, R. W., Kothya, P., Phuong, J., Filer, D., Smith, D., Reif, D., Rotroff, D., Kleinstreuer, N., Sipes, N., Xia, M. H., Huang, R. L., Crofton, K., and Thomas, R. S. (2016) Analysis of the effects of cell stress and cytotoxicity on *in vitro* assay activity across a diverse chemical and assay space. *Toxicol. Sci. 152*, 323−339.
(62) Xia, M., Huang, R., Witt, K. L., Southall, N., Fostel, J., Cho, M. H., Jadhav, A., Smith, C. S., Inglese, J., Portier, C. J., Tice, R. R., and Austin, C. P. (2008) Compound cytotoxicity profiling using quantitative high-throughput screening. *Environ. Health Persp 116*, 284−291.
(63) Fasano, M., Curry, S., Terreno, E., Galliano, M., Fanali, G., Narciso, P., Notari, S., and Ascenzi, P. (2005) The extraordinary ligand binding properties of human serum albumin. *IUBMB Life 57*, 787−796.
(64) Bischel, H. N., Macmanus-Spencer, L. A., Zhang, C., and Luthy, R. G. (2011) Strong associations of short-chain perfluoroalkyl acids with serum albumin and investigation of binding mechanisms. *Environ. Toxicol. Chem. 30*, 2423−30.
(65) Henneberger, L., Goss, K. U., and Endo, S. (2016) Partitioning of Organic Ions to Muscle Protein: Experimental Data, Modeling, and Implications for *in Vivo* Distribution of Organic Ions. *Environ. Sci. Technol. 50*, 7029−7036.
(66) Escher, B. I., Cowan-Ellsberry, C. E., Dyer, S., Embry, M. R., Erhardt, S., Halder, M., Kwon, J. H., Johanning, K., Oosterwijk, M. T. T., Rutishauser, S., Segner, H., and Nichols, J. (2011) Protein and lipid binding parameters in rainbow trout (*Oncorhynchus mykiss*) blood and liver fractions to extrapolate from an *in Vitro* metabolic degradation assay to *in Vivo* bioaccumulation potential of hydrophobic organic chemicals. *Chem. Res. Toxicol. 24*, 1134−1143.
(67) Peltenburg, H., Bosman, I. J., and Hermens, J. L. M. (2015) Sensitive determination of plasma protein binding of cationic drugs using mixed-mode solid-phase microextraction. *J. Pharm. Biomed. Anal. 115*, 534−542.

DOI: 10.1021/acs.chemrestox.7b00023
Chem. Res. Toxicol. 2017, 30, 1197−1208

Publication 2

Cellular uptake kinetics of neutral and charged chemicals in *in vitro* assays measured by fluorescence microscopy

Fabian C. Fischer[1], Cedric Abele[1], Steven T. J. Droge[2], Luise Henneberger[1], Maria König[1], Rita Schlichting[1], Stefan Scholz[3], Beate I. Escher[1,4]*

[1] Helmholtz Centre for Environmental Research - UFZ, Department Cell Toxicology, Permoserstraße 15, 04318 Leipzig, Germany

[2] University of Amsterdam, Institute for Biodiversity and Ecosystem Dynamics, SciencePark 904, 1098 XH Amsterdam, Netherlands

[3] Helmholtz Centre for Environmental Research - UFZ, Department Bioanalytical Ecotoxicology, Permoserstraße 15, 04318 Leipzig, Germany

[4] Eberhard Karls University Tübingen, Environmental Toxicology, Centre for Applied Geoscience, 72074 Tübingen, Germany

*Address correspondence to: fabian.fischer@ufz.de

Published in Chemical Research in Toxicology, DOI: 10.1021/acs.chemrestox.8b00019.

Chemical Research in Toxicology

Article

Cite This: *Chem. Res. Toxicol.* 2018, 31, 646−657

pubs.acs.org/crt

Cellular Uptake Kinetics of Neutral and Charged Chemicals in *in Vitro* Assays Measured by Fluorescence Microscopy

Fabian C. Fischer,*[,†] Cedric Abele,[†] Steven T. J. Droge,[‡] Luise Henneberger,[†] Maria König,[†] Rita Schlichting,[†] Stefan Scholz,[§] and Beate I. Escher[†,∥]

[†]Department of Cell Toxicology, Helmholtz Centre for Environmental Research − UFZ, Permoserstraße 15, 04318 Leipzig, Germany

[‡]Institute for Biodiversity and Ecosystem Dynamics, University of Amsterdam, Science Park 904, 1098 XH Amsterdam, Netherlands

[§]Department of Bioanalytical Ecotoxicology, Helmholtz Centre for Environmental Research − UFZ, Permoserstraße 15, 04318 Leipzig, Germany

[∥]Environmental Toxicology, Centre for Applied Geoscience, Eberhard Karls University Tübingen, 72074 Tübingen, Germany

Supporting Information

ABSTRACT: Cellular uptake kinetics are key for understanding time-dependent chemical exposure in *in vitro* cell assays. Slow cellular uptake kinetics in relation to the total exposure time can considerably reduce the biologically effective dose. In this study, fluorescence microscopy combined with automated image analysis was applied for time-resolved quantification of cellular uptake of 10 neutral, anionic, cationic, and zwitterionic fluorophores in two reporter gene assays. The chemical fluorescence in the medium remained relatively constant during the 24-h assay duration, emphasizing that the proteins and lipids in the fetal bovine serum (FBS) supplemented to the assay medium represent a large reservoir of reversibly bound chemicals with the potential to compensate for chemical depletion by cell uptake, growth, and sorption to well materials. Hence FBS plays a role in stabilizing the cellular dose in a similar way as polymer-based passive dosing, here we term this process as serum-mediated passive dosing (SMPD). Neutral chemicals accumulated in the cells up to 12 times faster than charged chemicals. Increasing medium FBS concentrations accelerated uptake due to FBS-facilitated transport but led to lower cellular concentrations as a result of increased sorption to medium proteins and lipids. *In vitro* cell exposure results from the interaction of several extra- and intracellular processes, leading to variable and time-dependent exposure between different chemicals and assay setups. The medium FBS plays a crucial role for the thermodynamic equilibria as well as for the cellular uptake kinetics, hence influencing exposure. However, quantification of cellular exposure by an area under the curve (AUC) analysis illustrated that, for the evaluated bioassay setup, current *in vitro* exposure models that assume instantaneous equilibrium between medium and cells still reflect a realistic exposure because the AUC was typically reduced less than 20% compared to the cellular dose that would result from instantaneous equilibrium.

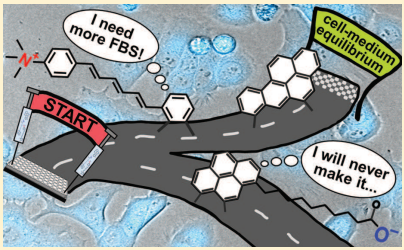

1. INTRODUCTION

The application of *in vitro* cell assays is increasing in chemical risk and hazard assessment of organic chemicals and their mixtures,[1] as well as for monitoring of complex environmental samples.[2] A diverse set of *in vitro* cell assays targeting various cellular signaling pathways has been developed and published.[3] A major challenge of using *in vitro* cell assays for chemical risk and hazard assessment is their need to quantitatively predict effects on the whole organism level, referred to as quantitative *in vitro*−*in vivo* extrapolation (QIVIVE).[4,5] An important first step for QIVIVE is to develop methods to quantify exposure in *in vitro* cell assays.

The bioavailable chemical fraction in *in vitro* systems is best described by the freely dissolved concentration (C_{free}) in the medium, since it represents the chemical concentration available for cellular uptake.[6] In QIVIVE approaches, C_{free} *in vitro* can be directly compared to the unbound concentration in human plasma ($C_{unbound}$),[4,5] enabling the simulation of human exposure in *in vitro* assays. However, it is also well understood that C_{free} does not necessarily relate to the target site concentration, which is the most appropriate metric to interpret effects of single chemicals that act via a specific mode of toxic action (MoA).[7,8] In most cases, the target site of toxic action is either unknown or the concentration is not quantifiable. For a chemical that exhibits several MoA, the internal cellular concentration (C_{cell})

Received: January 31, 2018
Published: June 25, 2018

DOI: 10.1021/acs.chemrestox.8b00019
Chem. Res. Toxicol. 2018, 31, 646−657

Table 1. Physicochemical Properties of the Fluorophores Evaluated in the Study

chemical	abbreviation	CAS Registry No.	log K_{ow} of neutral species (L L^{-1})	mol wt (g mol^{-1})	pK_a	speciation at pH 7.4
3-aminofluoranthene	3-AM-FLA[N]	2693-46-1	4.20[b]	217.27	3.9 (base)[b]	>99.99% neutral
benzo(*a*)pyrene	B(a)P[N]	50-32-8	6.13[a]	252.31		100% neutral
benzo(*g*,*h*,*i*)perylene	B(g,h,i)P[N]	191-24-2	6.63[a]	276.33		100% neutral
3-(dansylamino)phenylboronic acid	3-DAPBA[−]	75806-94-9	3.69[d]	370.23	8.5[b]	7% anionic
1-pyrenedecanoic acid	1-PYR-DEC[−]	64701-47-9	8.64[c]	372.51	4.9[b]	99.7% anionic
2-(fluoranthene-8-carbonyl)benzoic acid	2-FLA-BENZ[−]	351005-20-4	6.63[c]	350.37	3.3[b]	99.99% anionic
9-(methylaminomethyl)anthracene [+]	9-MAMA-ANT[+]	73356-19-1	5.68[c]	221.30	9.7[b]	99.5% cationic
Rhodamine 123	Rhod-123[+]	62669-70-9	4.63[c]	380.83	10.1[b]	99.8% cationic
N,*N*,*N*-trimethyl-4-(6-phenyl-1,3,5-hexatrien-1-yl) phenylammonium *p*-toluenesulfonate	TMA-DPH[+]	115534-33-3		461.60		100% cationic
Rhodamine 110	Rhod-110[Zw]	13558-31-1	5.48[c]	366.80	3.6; 10.9[b]	99.97% zwitterionic

[a]Experimental data from the OPERA report. [b]Predicted by PP-LFER. [c]Predicted by ACD LAB. [d]Predicted by OPERA models: LogP.

represents a good surrogate for exposure because it integrates intracellular chemical distribution.[9,10] Since analytical assessment of *in vitro* exposure *in situ* is challenging due to the small volumes used in high-throughput screening, *in vitro* exposure models have been developed and applied for estimating C_{free} and C_{cell} of neutral[11] and charged[10] chemicals.

In *in vitro* exposure models, C_{cell} can be linked to C_{free} by the cell−water partition constant ($K_{cell/w}$), which is in turn dependent on the volume fraction of cellular proteins, lipids, and water, potentially leading to different C_{cell} between different cells at similar C_{free} and vice versa. In our recent exposure modeling study,[10] we emphasized the role of the fetal bovine serum (FBS) supplemented to the assay medium with FBS concentrations typically varying between 0.5% and 20%. At constant nominal concentration, a higher FBS content resulted in lower C_{free}, due to increased chemical sorption to medium proteins and lipids. However, even at the lowest considered FBS concentration of 0.5%, cellular uptake marginally depleted the medium by a maximum of 16%, leading to the hypothesis that the medium might act as a chemical reservoir compensating for chemical depletion by cellular uptake, growth, plastic sorption, and biotransformation. In this way, C_{free} may be kept virtually constant throughout the incubation period. This can be seen as an analogy to passive dosing, where a polymer is used as chemical reservoir to ensure constant C_{free} throughout the exposure period.[12,13] FBS can thus be considered as a passive dosing device suggesting the term serum-mediated passive dosing (SMPD). However, as for polymer passive dosing, SMPD would require rapid desorption from the medium FBS and fast cellular uptake of the freely dissolved chemicals.

Existing *in vitro* exposure models assume practically instantaneous equilibrium and kinetic processes altering exposure over time have thus so far been neglected. Uptake and elimination kinetics and involved mechanisms in cells, tissues or whole organs are critical in drug discovery, and have been investigated in several pharmacokinetic studies.[14−16] Analogously, kinetic processes may influence chemical exposure leading to altered expression of the cellular response in *in vitro* assays and an inaccurate assessment of the chemicals' potency. *In vitro* studies exist that account for uptake, intracellular partitioning and metabolic stability of nanoparticles,[17] metals,[18] and sparsely, of organic chemicals.[19,20] However, detailed time-dependent exposure studies focusing on exposure kinetics in *in vitro* assays and the relevant processes are scarce.

Earlier studies argued that cellular uptake of neutral chemicals is driven by passive diffusion, whereas charged organic chemicals do not diffuse through biological membranes.[21] In recent pharmacological studies, active transport via ion channels and transport proteins has been addressed for neutral[22] and charged chemicals,[23] whereby the latter mechanism may also work against the chemical gradient. Poulin et al.,[24,25] amongst others, investigated the role of human serum albumin (HSA) in the cellular uptake of drugs in humans. It was discussed that the HSA can transport reversibly bound chemicals over the aqueous boundary layer (ABL) that builds up between the cell surface and its surrounding medium or decrease the thickness of the

DOI: 10.1021/acs.chemrestox.8b00019
Chem. Res. Toxicol. 2018, 31, 646−657

ABL,[26] an idea that was inspired by facilitated transport of pollutants by organic matter.[27,28] The chemicals are desorbed again near the cell membrane due to the concentration gradient resulting from cellular uptake. Co-transport into cells that incorporate HSA by endocytosis could be an additional transport mechanism for charged chemicals, referred to as HSA-mediated transport *in vivo*.[25] Analogous to HSA-facilitated and -mediated transport processes in *in vivo* cells from human plasma,[24] the use of FBS in *in vitro* media might considerably influence cellular uptake.

Live cell imaging has already been applied in studies that have included the measurement of macromolecular interactions in *in vitro* systems, such as for medical applications[29] and in drug development.[30] Synthetic fluorescence stains allow for the discrimination of cell organelles or different types of proteins and lipids.[31] Ali et al.[20] combined fluorescence microscopy with a battery of organelle stains to trace benzo(*a*)pyrene in different compartments of murine hepatoma cells (Hepa1c1c7). Morphological changes of stained cell organelles after chemical exposure were tracked by fluorescence microscopy, and these morphological alterations were proposed as suitable endpoints in chemical effect assessment.[32]

The objective of this study was to develop and apply a method capable of providing real-time *in vitro* exposure quantification by fluorescence microscopy coupled with bright-field image acquisition. We evaluated the uptake kinetics of neutral and charged chemicals (anions, cations, zwitterions) in two reporter gene assays that were derived from the MCF-7 human breast cancer cell line and the HEK293T human embryonic kidney cell line, respectively. We put emphasis on assessing the role of the medium FBS concentration on the extent and kinetics of uptake. We hypothesized that (i) cellular uptake, growth, and further depletive processes can be compensated by SMPD, leading to constant external exposure conditions throughout the assay duration; (ii) cellular uptake of neutral chemicals is faster compared to that of partially or permanently charged chemicals due to higher cell membrane permeability; and (iii) higher medium FBS concentrations lead to accelerated chemical uptake due to FBS-facilitated transport but lower C_{cell} as a result of increased sorption to FBS. Within the exposure model framework,[10,11] we aimed to evaluate if exposure kinetics need to be considered in *in vitro* models or whether the equilibrium assumption in existing mass balance models sufficiently describes routine bioassays with 24 h of cell exposure.

2. MATERIALS AND METHODS

2.1. Chemicals. Ten chemicals that cover a wide range of speciation and hydrophobicity (log K_{ow} = 3.7−8.64) and contain a fluorophore were selected as test chemicals for this study (Table 1). Chemical properties were obtained from experimental data as reported on the U.S. EPA Chemistry dashboard (https://comptox.epa.gov/dashboard) or predicted by polyparameter linear free energy relationships,[33] the software ACD LAB (v. 2015),[34] and the model OPERA (v. 1.02).[35]

All chemicals were purchased from Sigma-Aldrich. Purity was ≥99.0% for Rhod-110[Zw]; ≥98% for 3-AM-FLA[N], B(a)P[N], B(g,h,i)P[N], 3-DAPBA[−], and 1-PYR-DEC[−]; ≥95% for TMA-DPH[+] and 9-MAMA-ANT[+]; and ≥85% for Rhod-123[+] (≤10% water impurity). 2-FLA-BENZ[−] was marked as early discovery product by Sigma; the molecular formula was confirmed by LC-HRMS using an LTQ Orbitrap XL. The protonated molecule $[M^+H]$ was detected at *m/z* 365.1184 ($C_{25}H_{17}O_3$, +3.2 ppm) along with an intense $[M^+H-CH_3]^+$ ion at *m/z* 351.1028 ($C_{24}H_{15}O_3$, +3.6 ppm). All chemical stock solutions were prepared in methanol (GC grade, ≥99% purity, Merck KGaA, Darmstadt, Germany).

2.2. *In Vitro* Cell Assays. Two cell lines were selected. The reporter gene cell line AREc32 for oxidative stress response is derived from the MCF-7 human breast cancer cell line[36] and was originally developed for cancer research[37,38] and has been widely applied for skin sensitization testing[39] and environmental monitoring.[40] The GR-UAS-bla is a reporter gene cell line based on the HEK293T human embryonic kidney cell, which quantifies the glucocorticoid receptor activity via the reporter *β*-lactamase and is part of the Tox21 battery of bioassays.[41]

The cells were cultivated in Dulbecco's Modified Eagle Medium (DMEM GlutaMAX, Thermo Fisher Scientific, Waltham, MA, USA) amended with 10% FBS (Invitrogen GIBCO, Thermo), either untreated FBS (AREc32) or dialyzed FBS (GR-UAS-bla), until a confluency of 70−90% was reached. The cell number was quantified with a cell counter CASY MODEL TT (Roche Innovatis, Reutlingen, Germany). The cells were washed with phosphate buffered saline (PBS, 8% NaCl, 0.2% KCl, 1.442% Na_2HPO4, and 0.25% KH_2PO_4 in H_2O) three times and resuspended in DMEM GlutaMAX amended with 0.5%, 1%, 2%, 5%, or 10% FBS, dependent on the respective experiment (section 2.6). Although the AREc32 and GR assays were optimized and are run routinely with 10% FBS[36] and 2% FBS,[41] respectively, cells displayed no difference in morphology and were growing at all applied FBS concentrations except GR cells which did not grow at 0.5% FBS (Figure S4). A total of 90 μL of cell suspension with 11000 AREc32 cells or 9000−16000 GR-UAS-bla cells were seeded per well of polylysine-coated 96-well polystyrene plates (clear, flat bottom, Corning, Lowell, MA, USA), respectively. Different densities for the GR-UAS-bla cells needed to be seeded for the different FBS concentrations, since cell growth was considerably increased at higher FBS concentrations, which required lower cell density for higher FBS concentrations. This was only a minor issue with AREc32 cells, therefore, one optimized seeding density could be used for all FBS concentrations. The plates were incubated for 24 h at 37 °C and 5% CO_2 for cell adhesion, which proved to be sufficient for adhesion but not for growth as demonstrated in a preliminary experiment, in which cell numbers were measured as a function of time for 48 h after seeding (Figure S1).

2.3. Chemical Dosing. A defined volume of the methanolic chemical stock solution was dissolved in 1000 μL of the respective assay medium in a 1.5 mL screwtop GC vial. The vials were closed and vortexed for 15 s. Next, 30 μL of the solution was pipetted into the wells, yielding a defined chemical concentration, a total medium volume of 120 μL, and a methanol concentration of 1% in the well. Suitable test concentrations were determined in preliminary experiments for four chemicals (Table S1): fluorescence signals within the cells were evaluated at three different chemical concentrations in the medium with 10% FBS, at which the highest background signal was observed. Then the lowest suitable concentration was tested at 0.5% medium FBS at which the highest C_{cell} and thus highest toxicity was expected according to the exposure model.[10] Cell viability was visually verified at these concentrations using the bright-field images and cell growth served as indicator for cellular health. Suitable test concentrations for the remaining six chemicals were selected based on the same criteria. The procedure of adjusting suitable test concentrations for the microscopy method, required criteria and related experimental artifacts are discussed in section 3.1. The resulting chemical concentrations in the assay wells are reported in the Supporting Information (Table S2).

2.4. Image Acquisition. A Zeiss PALM CombiSystem (Zeiss, Oberkochen, Germany) that allows simultaneous capturing of bright-field and fluorescence images was employed. The software ZEN blue version 2.3 (Zeiss) was used for measurements in 96-well plate formats. Images were captured with the 10x objective. We used 380 and 470 nm excitation filters, with emission measurements at 435 and 520 nm, respectively. The excitation time varied between the chemicals from 4 to 100 ms, and was optimized for each chemical individually. Wavelengths and excitation times for all chemicals can be found in the Supporting Information (Table S2).

Images were taken from 10 positions per well (Figure 1). The focus level (Z position) was manually adjusted for each well measurement. Note that the fluorescence signal was not measured for a single focus level (such as in confocal microscopy), but for a layer of 7.5 μm

DOI: 10.1021/acs.chemrestox.8b00019
Chem. Res. Toxicol. 2018, 31, 646−657

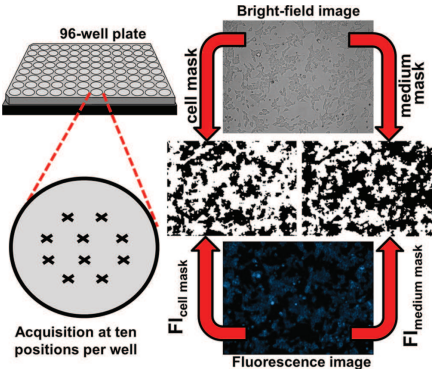

Figure 1. Image acquisition and analysis procedure. Measurements were performed in 96-well plates. Bright-field and fluorescence images were acquired at 10 positions per well. Image analysis as described in the Supporting Information (section S3), was used to create a cell mask from the bright-field images. Fluorescence intensity was quantified in the cell mask ($FI_{cell\ mask}$) and outside the cell mask ($FI_{medium\ mask}$).

(epifluorescence technique), meaning that the fluorescence signal included the cell and the medium fluorescence signals. Preliminary experiments showed that back radiation and Z position deviation was higher at the well edges (Figure S2), therefore measurements were only taken around the well center (Figure 1). The distance between the 10 positions was selected to avoid overlapping images. Preliminary experiments showed that the cells died approximately 10 min after image acquisition, probably due to the high-energy light (Figure S3). The effect was more pronounced after chemical exposure, particularly to the polycyclic aromatic hydrocarbons, presumably due to photo-induced cytotoxicity.[42,43] Therefore, the fluorescence in each well was measured only once for all chemicals and controls without chemical exposure, requiring that sufficient replicate plates with replicate wells were prepared for each experiment.

Each chemical was dosed into three wells of each 96-well plate, yielding nine replicates on three plates for fluorescence imaging. Measurements were taken at different time points during 24 h, which is a common incubation time for the reporter gene based assays applied in this study. The timestamp of each well image acquisition allowed the calculation of the exact time of measurement. The image acquisitions lasted for approximately 20 min. With three measurements per plate, each plate was removed from the 37 °C incubator for a maximum of 1 h during the experiment. Since the cells in the controls looked healthy and cell growth was measured in parallel (Figure S4), we can thus conclude that cell viability was not influenced by the measurement procedure.

2.5. Image Analysis. Fluorescence and bright-field images were analyzed by an image processing workflow created in KNIME (version 3.3.2, Zurich, Switzerland) (Figure S5). The analysis was based on the generation of cell masks from the bright-field images, separating the intracellular space from the medium (Figure 1). The mean fluorescence intensity in the cells in counts per second (cps) within the cell mask of each image ($FI_{cell\ mask}$) was calculated by means of the sum fluorescence in the cell mask ($\sum FI_{cell\ mask}$) and its respective pixel number, representing the area covered by the cells ($pixel_{cell\ mask}$) (eq 1).

$$FI_{cell\ mask} = \frac{\sum FI_{cell\ mask}}{\sum pixel_{cell\ mask}} \quad (1)$$

The mean fluorescence intensity in the extracellular medium mask ($FI_{medium\ mask}$) was calculated analogously.

As mentioned above, the fluorescence in the cells was overlayed by the fluorescence in the medium. Given that medium fluorescence can be obtained from areas not covered by cells, the fluorescence signal in the cells (FI_{cell}) was calculated by subtracting $FI_{medium\ mask}$ from $FI_{cell\ mask}$ (eq 2).

$$FI_{cell} = FI_{cell\ mask} - FI_{medium\ mask} \quad (2)$$

For the calculation of FI_{cell} using eq 2, consideration of the autofluorescence by the system (AF_{system}) was not necessary, since autofluorescence in the cell mask ($AF_{cell\ mask}$) and the medium mask ($AF_{medium\ mask}$) did not significantly differ (Figure S6) and therefore canceled out in eq 2, as illustrated by Figure S7. Therefore, AF_{system} was defined as the mean value of the resulting linear fits for $AF_{cell\ mask}$ and $AF_{medium\ mask}$ at the respective excitation time (Figure S6).

For Rhod-110[Zw] at 0.5% medium FBS concentration, measurement of FI_{cell} in the presence of medium was not possible due to the high medium signals, causing $FI_{medium\ mask}$ to be higher than $FI_{cell\ mask}$. The calculation of FI_{cell} by eq 2 would then lead to the result that FI_{cell} equals zero due to the cell signal getting lost in the medium background. As an alternative method, the medium was completely removed before image acquisition. By subtracting the AF_{system} at the respective exposure time and wavelength, FI_{cell} was calculated (eq 3).

$$FI_{cell} = FI_{cell\ mask} - AF_{system} \quad (3)$$

FI_{medium} was calculated by subtracting the AF_{system} from $FI_{medium\ mask}$ (eq 4), similar to FI_{cell} in eq 3.

$$FI_{medium} = FI_{medium\ mask} - AF_{system} \quad (4)$$

In order to quantitatively compare the chemicals, the relative chemical enrichment factor in the cells compared to the medium (EF_{cell}) was calculated by dividing FI_{cell} with the 24-h mean value of FI_{medium} ($FI_{medium\ mean}$) (eq 5), provided that the standard deviation of $FI_{medium\ mean}$ was <20% within the 24-h assay duration.

$$EF_{cell} = \frac{FI_{cell}}{FI_{medium\ mean}} \quad (5)$$

FI_{cell} as a function of time was fitted with a first-order uptake kinetics equation (eq 6) in GraphPad Prism (version 7, La Jolla, CA, USA), from which the uptake rate constant (k, h^{-1}) and the respective FI_{cell} at equilibrium ($FI_{cell,eq}$) were derived.

$$FI_{cell}(t) = FI_{cell,eq}(1 - e^{-kt}) \quad (6)$$

For chemicals that sorbed to the cell membrane instantaneously to a certain extent, the equation was extended for the FI_{cell} at time 0 ($FI_{cell,0}$) (eq 7).

$$FI_{cell}(t) = FI_{cell,0} + (FI_{cell,eq} - FI_{cell,0})(1 - e^{-kt}) \quad (7)$$

The time needed until 95% equilibrium ($t_{95\%}$, h) was calculated from k by eq 8.

$$t_{95\%}\ (h) = \frac{2.94}{k} \quad (8)$$

The area under the curve of the resulting fits from eqs 6 and 7 ($AUC(FI_{cell})$) were analytically integrated with eq 9.

$$AUC(FI_{cell}) = \int_0^{24} FI_{cell} = FI_{cell,eq}\left((24 - 0) + \frac{1}{k}(e^{-k\times 24} - 1)\right) \quad (9)$$

The AUC that would theoretically result from instantaneous chemical partitioning between medium and cells ($FI_{cell,eq}$ achieved at time 0) was calculated with eq 10.

$$AUC(FI_{cell,eq}\ \text{at time}\ 0) = 24 \times FI_{cell,eq} \quad (10)$$

The fraction of maximum exposure was derived from the ratio of AUC (FI_{cell}) and AUC ($FI_{cell,eq}$ at time 0) (eq 11).

DOI: 10.1021/acs.chemrestox.8b00019
Chem. Res. Toxicol. 2018, 31, 646−657

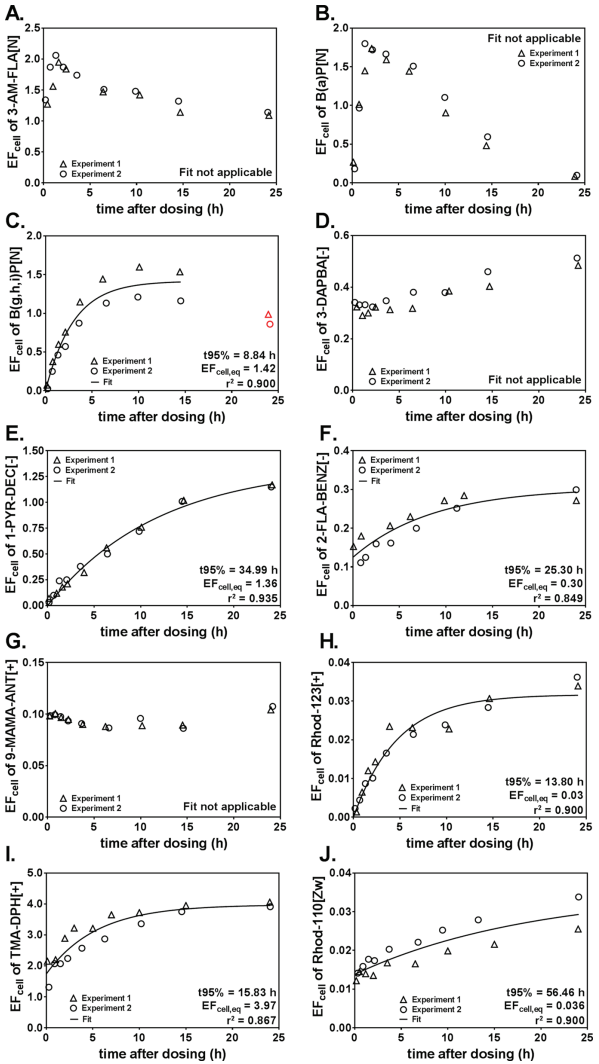

Figure 2. EF_{cell} of the 10 chemicals (A–J) in the AREc32 assay over the assay duration of 24 h in medium supplemented with 0.5% FBS. Two independent experiments were performed (circles and triangles). A first-order kinetics model was fitted to the data (eq 6 or 7) when this was supported by a continuous increase in fluorescence with tendency to approach equilibrium and if the FI_{medium} was constant during the 24 h. For B(g,h,i)P[N], two data points that were marked red were excluded from the fit.

$$\text{fraction maximum exposure} = \frac{\text{AUC}(FI_{cell})}{\text{AUC}(FI_{cell,eq} \text{ at time } 0)} \quad (11)$$

2.6. Experiments. All 10 chemicals were tested at defined chemical concentrations in the AREc32 and GR assays (Table S2). The medium FBS concentration was adjusted to 0.5% for good differentiation between cell and medium fluorescence signals. $FI_{cell\ mask}$ and

DOI: 10.1021/acs.chemrestox.8b00019
Chem. Res. Toxicol. 2018, 31, 646–657

$FI_{medium\ mask}$ were measured within the 24-h assay duration at nine different time points. Two experiments with different cell batches and freshly prepared dosing vials were performed at different days. FI_{cell} were calculated for each time point (eq 2) and the data was fitted with the first-order uptake kinetics equation (eq 6 or 7). In order to compare the cellular exposure between the chemicals, the FI_{cell} values were converted to EF_{cell} according to eq 5.

The influence of the medium FBS concentration (0.5%, 1%, 2%, 5%, and 10%) on cellular uptake kinetics and extent of uptake was evaluated for B(a)P[N], TMA-DPH[+], and 1-PYR-DEC[−] at one concentration in the AREc32 and GR assays. This set of experiments was performed three times with different cell batches and freshly prepared dosing vials at different days. $FI_{cell\ mask}$ and $FI_{medium\ mask}$ were measured 9-fold within the 24-h assay duration. FI_{cell} were calculated for each time point (eq 2) and the data was fitted with the first-order uptake kinetics equation (eq 6 or 7).

3. RESULTS AND DISCUSSION

3.1. Method Development and Evaluation. Figure 2 shows that the kinetic curves of EF_{cell} for the evaluated chemical derived from different experiments were very similar and all curves were therefore fitted together. Standard deviations of EF_{cell} between images of single measurements were <20% in most cases. Since FI_{cell} normalizes for the size of the cell mask (eq 2), differences in confluency (% of well bottom covered with cells) between single images and wells as well as plates of the same experiment, cancel each other out, resulting in high comparability between plates, wells and experiments. This is encouraging considering that the cells were cultured independently for each experiment with possible biological variability in cell growth. Consequently, adaptation of the developed method is possible since data generated in different laboratories should be comparable.

The EF_{cell} describes the extent of chemical enrichment in the cells compared to the medium (eq 5), and is thus a metric comparable to the cell-medium partition constant ($K_{cell/medium}$). In the ratio of FI_{cell} and FI_{medium}, differences in the fluorescence quantum yield between the chemicals cancel out, enabling quantitative comparison between the chemicals. Note that the $EF_{cell,eq}$ relates chemical accumulation in the cells to FI_{medium}, hence both the freely dissolved and FBS sorbed chemicals, and is therefore not directly comparable to the bioconcentration factor, which relates the chemical enrichment in an organism to the C_{free} in the exposure medium. The FI_{cell} on the other hand, represents a suitable parameter for the actual chemical exposure in the cells without relation to the medium exposure, comparable to C_{cell}. However, FI_{cell} is not comparable between different chemicals, since differences in the quantum yield are not canceled out in eq 2. Calculating EF_{cell} and FI_{cell} requires that quenching of the emitted chemical fluorescence between medium and cells can be neglected. There are no literature data reporting the relative importance of quenching in *in vitro* cells and media for the fluorophores tested. Hence, quenching effects cannot be ruled out completely for the experiments.

A critical aspect in the development of the method was to determine suitable chemical concentrations that prevent experimental artifacts from interfering with the measurement of cellular uptake kinetics. Chemical concentrations that caused cytotoxicity were associated with considerable artifacts, such as observed for 2-FLA-BENZ[−] at 10 mg L^{-1} in the AREc32 with 0.5% medium FBS (section S6). This high concentration of 2-FLA-BENZ[−] induced cell-rounding after approximately 12 h of exposure, reducing the cell area and thus the resulting pixel number of the cell mask (Figures S8 and S9). Since the sum of fluorescence signal in the cell mask remained stable during this process, the mean fluorescence normalized to the cell mask area increased. Cell rounding was also observed for the GR-UAS-bla cells at FBS concentrations of 0.5% when extending the experiments to 48 h, probably as a result of the growth arrest induced by starvation of the cells (Figure S4B). The process of cell-rounding can be misinterpreted as increasing cellular uptake, which should be accounted for when applying the method. Therefore, experiments in which the cell mask decreased over time were discarded and chemical concentrations were lowered in order to prevent cytotoxicity. Cell growth is an indicator for cellular health,[44] indicating that chemical exposure was below cytotoxic concentrations, hence, cell membrane integrity is expected to be intact. Experiments were thus classified as valid when cell growth was measured as an increase in cell mask area during chemical incubation.

Chemical concentrations, however, are still required to be sufficiently high in order to induce a high enough fluorescence intensity that can be discriminated from the autofluorescence of the system (Figure S7). Autofluorescence can be caused by light reflection from the well plate plastic and medium, and can vary between single measurements and different experiments due to differences in light conditions and instability of the microscope. Fortunately, variability in the autofluorescence from experiment to experiment cancels out when calculating FI_{cell} by eq 2, since $FI_{cell\ mask}$ and $FI_{medium\ mask}$ should vary by the same factor for each measurement. Still, the signal-to-noise ratio decreased at lower chemical fluorescence signals, which resulted in an increased variability of the data obtained by automated image analysis. It is thus advisable to devote sufficient efforts in determining the suitable test concentrations for each chemical individually, which yield signals that can be clearly distinguished from the autofluorescence.

Higher medium FBS concentrations resulted in higher FI_{medium} and lower FI_{cell}, which is discussed in detail in section 3.3.2. For chemicals that considerably sorb to the medium FBS and exhibit low partitioning to the cells, $FI_{medium\ mask}$ can exceed $FI_{cell\ mask}$, leading to $FI_{cell} \leq 0$ (eq 2) and the false conclusion that these chemicals did not partition into the cells. In the instance where this occurred, the medium was removed right before image acquisition in order to measure FI_{cell} (eq 3). FI_{cell} over 24 h measured in medium and with medium removed before acquisition were similar, as shown for three chemicals in Figure S10. Thus, both methods can be used interchangeably. However, the variability of the data acquired without medium increased compared to the variability of the data acquired with medium, because the removal of the medium is causing acute stress on the cells. Hence medium was only removed if $FI_{medium\ mask}$ was greater than $FI_{cell\ mask}$.

3.2. Medium Exposure during the 24-h Assay Duration. For 9 of the 10 evaluated chemicals, FI_{medium} varied by <20% during the 24-h incubation of the AREc32 cells at 0.5% medium FBS (Figure S11). Only B(a)P[N] was depleted, which can be explained by biotransformation (section S18). In the GR assay with 0.5% medium FBS, the 10 chemicals were not substantially depleted from the medium (<20%, Figure S12). Likewise, at the five evaluated FBS concentrations, FI_{medium} of 1-PYR-DEC[−], TMA-DPH[+] and B(a)P[N] remained constant in both reporter gene assays (Figure S13). Increased FBS concentrations led to considerably higher FI_{medium} for all chemicals, confirming that FBS represents the dominant sorptive sink in the medium.[10,45]

DOI: 10.1021/acs.chemrestox.8b00019
Chem. Res. Toxicol. 2018, 31, 646−657

For the GR assay, substantial cell growth was measured that increased with increasing medium FBS concentration (Figure S4B). However, the unchanged FI_{medium} led to constant FI_{cell} of e.g., B(a)P[N], even though the GR cells doubled within the assay duration after 24 h at 10% FBS (Figure S14). This is a promising result since effect measurement takes place after 24 h with all cells contributing to the measured effects that result from the ligand−receptor binding activity. Hence, constant C_{cell} are established by SMPD within the typical exposure time of 24 h, provided that uptake is fast enough to compensate cellular growth in time.

Sorption to polystyrene, which is the common material for multi-well plates, has been identified as another possible depletive process in aquatic toxicity tests, particularly for neutral hydrophobic chemicals with a log $K_{ow} > 3$.[46] In the GR assay, only B(a)P[N] (log $K_{ow} = 6.13$) was depleted by up to 24% from the medium compared to FI_{medium} at the first measurement (Figure S12B). However, since the more hydrophobic B(g,h,i)-P[N] (log $K_{ow} = 6.63$) was not depleted (Figure S12C), it is likely that these reductions did not result from sorption to the well plate materials, but may be the result of cellular biotransformation (section S18). The chemical fraction sorbed into the polystyrene after a certain time period is expected to increase in the smaller wells of larger well plate formats (e.g., 384- or 1536-well plates) due to the larger well surface area relative to the assay medium. Whether SMPD is able to compensate chemical depletion in these well plates needs to be evaluated in future studies.

The results confirm that the medium FBS represents the dominant sorptive sink for chemicals in the evaluated *in vitro* assays,[10] which was not depleted by cellular uptake and cell growth. For the study chemicals and the used well plate format, cell number and media compositions, SMPD led to constant medium exposure conditions throughout the incubation period, whereby chemical depletion due to evaporation and sorption to well plate materials was apparently compensated by the buffering capacity of the medium FBS. The results indicate that metabolism or other degradation processes may lead to depletion of C_{free}, which means that the buffering capacity of the medium does have limitations if additional degradative processes in addition to partitioning occur. Abiotic degradation by, e.g., hydrolysis and photolysis can decrease C_{free} of labile chemicals. The latter should be less problematic for *in vitro* cell assays since they are usually incubated in the dark. Whether SMPD generally compensates for abiotic degradation of labile chemicals needs to be investigated in future studies. Cellular metabolism is a kinetic loss process, which is part of the biological response to chemical exposure. Since transformation products can also be bioactive, it is thus not necessarily desirable to compensate for all loss by metabolism in a toxicity experiment.

As SMPD led to relatively constant FI_{medium} throughout the test period (<20% variability), eqs 6 and 7 could be used to fit the uptake rate constant, the FI_{cell} and the $EF_{cell,eq}$ in order to quantitatively describe the cellular uptake of the chemicals and the extent of chemical enrichment in the cells.

3.3. Cellular Uptake Kinetics. *3.3.1. Ten Chemicals at 0.5% Medium FBS Concentration.* Cellular uptake varied considerably over time for the 10 evaluated chemicals in both reporter gene assays with 0.5% FBS in the medium (AREc32, Figure 2, and GR, Figure S15).

In the AREc32 cells, the neutral chemicals 3-AM-FLA[N] and B(a)P[N] were taken up relatively fast with EF_{cell} reaching a maximum within the first 2 h (Figure 2A,B). The very hydrophobic neutral B(g,h,i)P[N] (log $K_{ow} = 6.68$) reached $EF_{cell,eq}$ after 8.8 h of exposure (Figure 2C). After reaching a maximum, EF_{cell} continuously decreased over time for the three neutral chemicals. For instance, the EF_{cell} of B(a)P[N] approached the detection limit 24 h after chemical dosing, which hindered the derivation of $t_{95\%}$ by eq 6 for B(a)P[N] and 3-AM-FLA[N]. In the GR assay applying GR-UAS-bla cells, these reductions were not detected for the neutral chemicals (Figure S15A−C). In contrast, EF_{cell} remained relatively constant after equilibrium was achieved. The difference between the cell lines is most likely due to biotransformation and/or a higher amount of efflux pumps in the AREc32 cells compared to the GR-UAS-bla cells, which is discussed in section S18.

Cellular uptake of 2-AM-FLA[N], 3-FLA-BENZ[−], 3-DABPA[−], TMA-DPH[+], and Rhod-110[Zw] was observed to occur to a considerable extent at the first recording, 10−30 min after dosing, however, chemical accumulation continued thereafter (Figures 2 and S15). This initial fast increase in EF_{cell} probably resulted from rapid chemical adsorption to the outer surface of the cell membranes. Afterward, the measured fluorescence indicated the diffusion of the chemicals through the cell membrane with an accumulation occurring in the intracellular space. In contrast, 1-PYR-DEC[−], B(a)P[N], B(g,h,i)P[N], and Rhod-123[+] did not measurably adsorb to the cells after 20 min, as is evidence by EF_{cell} starting at zero at the first measurement point and increasing afterward.

In contrast to the neutral chemicals, chemical uptake of six of the seven charged chemicals was considerably delayed, with no equilibrium attained within the 24-h assay for the three anions 2-FLA-BENZ[−], 3-DAPBA[−], and 1-PYR-DEC[−] as well as the zwitterion Rhod-110[Zw]. 9-MAMA-ANT[+] was taken up by the cells within 30 min, with EF_{cell} remaining relatively constant throughout 24 h. This observation and the low EF_{cell} of 0.1 suggests that 9-MAMA-ANT[+] adsorbed to the cell membranes rapidly, but did not accumulate in the cell to a measurable extent thereafter. The delayed uptake of most of the charged chemicals compared to the neutral chemicals can be explained by findings that the diffusion of the charged species through the hydrophobic center of the membrane is expected to be considerably slower,[47] which led some authors to conclude that only the neutral species of these chemicals can pass the cell membrane by passive diffusion.[21] Moreover, the charged species often exhibits reduced affinity to cell membranes.[48,49]

TMA-DPH[+], a permanently charged cation was taken up by the AREc32 and GR cells to the largest extent of the evaluated chemicals, with $EF_{cell,eq}$ of 3.97 and 4.92 at 0.5% FBS, respectively, indicating that uptake into cells does not solely result from passive diffusion through the cell membranes. Charged organic molecules can be passively taken up via ion transport channels or actively taken up by transport proteins.[24] The co-transport of chemicals that are sorbed to FBS incorporated into the intracellular space by endocytosis may explain the uptake of TMA-DPH[+], which was already used as marker for endocytosis in L929 cells.[50] These transport processes may take more time than passive diffusion, causing chemical concentrations in the cells to continuously increase with time. Passive diffusion of TMA-DPH[+] could still contribute to the accumulation in the cells, since the charged chemical could pass the membrane as an ion pair, together with *p*-toluenesulfonate, which is the counterion in the solid TMA-DPH[+] (Table 1). Partitioning with counterions is deemed relevant for octanol−water partitioning of organic acids and

DOI: 10.1021/acs.chemrestox.8b00019
Chem. Res. Toxicol. 2018, 31, 646−657

Table 2. $FI_{cell,eq}$ and $t_{95\%}$ Derived from the First-Order Uptake Kinetics Fits (Eqs 6 and 7)[a]

	GR assay (GR-UAS-bla)						AREc32 assay (AREc32)			
	B(a)P[N]		TMA-DPH[+]		1-PYR-DEC[−]		TMA-DPH[+]		1-PYR-DEC[−]	
FBS	$FI_{cell,eq}$ (cps)	$t_{95\%}$ (h)	$FI_{cell,eq}$ (cps)	$t_{95\%}$ (h)	$FI_{cell,eq}$ (cps)	$t_{95\%}$ (h)	$FI_{cell,eq}$ (cps)	$t_{95\%}$ (h)	$FI_{cell,eq}$ (cps)	$t_{95\%}$ (h)
0.5%	460 ± 50	3.3 ± 0.4	342 ± 18	14.8 ± 2.4	199 ± 49	29.6 ± 8.4	333 ± 4	16.4 ± 3.5	116 ± 10	36.5 ± 3.7
1%	315 ± 12	3.0 ± 0.1	331 ± 44	12.6 ± 2.2	126 ± 32	51.0 ± 13.8	280 ± 20	15.3 ± 3.0	67 ± 15	28.4 ± 11.1
2%	262 ± 6	2.4 ± 0.3	295 ± 50	10.1 ± 2.2	linear increase		236 ± 46	14.9 ± 3.1	42 ± 7	23.2 ± 6.7
5%	167 ± 9	1.8 ± 0.3	319 ± 28	9.6 ± 1.6	linear increase		148 ± 21	9.7 ± 1.3	47 ± 3	41.2 ± 5.0
10%	102 ± 16	1.4 ± 0.3	310 ± 17	10.1 ± 2.1	linear increase		129 ± 4	7.5 ± 0.8	linear increase	

[a]Graphs and fits from all experiments can be found in sections S13 and S14 of the Supporting Information.

bases[51] but not for partitioning to lipid bilayer membranes.[52] Hence this hypothesis requires further testing.

Chemical uptake into the cells was observed to occur to different extents with $EF_{cell,eq}$ ranging from 0.02 (Rhod-123[+] in AREc32) to 4.92 (TMA-DPH[+] in GR) at 0.5% FBS. Neutral chemicals were generally accumulated in the cells to a larger extent, except for TMA-DPH[+] and 1-PYR-DEC[−]. $EF_{cell,eq}$ of 1-PYR-DEC[−] was 1.36 in AREc32 and 2.08 in GR, which represents a considerably larger enrichment, as compared to the other anions tested, with $EF_{cell,eq}$ between 0.02 and 0.4 being reported. These differences may result from the high hydrophobicity of 1-PYR-DEC[−] caused by its long-chain fatty acid tail.

3.3.2. Cellular Uptake Kinetics at Varying Medium FBS Concentrations. The uptake kinetics of one neutral (B(a)P-[N]), one cationic (TMA-DPH[+]), and one anionic (1-PYR-DEC[−]) chemical were evaluated as a function of the FBS content of the medium ranging from 0.5 to 10% FBS. FI_{cell} was quantified as a proxy for the cellular exposure (C_{cell}). In the AREc32 and GR assays, the $FI_{cell,eq}$ and time until 95% equilibrium differed for each of the chemicals between the five medium FBS concentrations studied (Table 2). B(a)P[N] in the AREc32 assay was excluded from the quantification of cellular uptake kinetics due to rapid decrease in FI_{cell} (section S18). The $FI_{cell,eq}$ was considerably reduced at higher FBS concentrations for all three chemicals in both cell lines (Table 2, Figure 3), such as a reduction in FI_{cell} of B(a)P[N] by a factor of 4.5 (Table 2), which is generally consistent with the expectations from the mass balance *in vitro* exposure model.[10] Decreasing FI_{cell} with increasing FBS concentrations is most likely the result of decreased bioavailability in the medium due to the increased chemical partitioning to medium proteins and lipids, as is evidenced by the higher FI_{medium} at increased medium FBS concentrations (Figure S13). Increasing the medium FBS concentration by a factor of 20 from 0.5% to 10% did not lead to a reduction in FI_{cell} by the same factor. Experimental determination of protein- and lipid content showed that DMEM Glutamax contains 0.86 mL proteins and 0.19 mL lipids per liter basic medium.[10] Thus, the basic medium also represents a sorptive sink for chemicals, not leading to a 20-fold decrease in FI_{cell} when increasing the medium FBS from 0.5% to 10%. Model calculations based on the exposure model[10] predicted that C_{cell} of B(a)P[N] only decreases by a factor of 1.75 compared to the measured decrease in FI_{cell} by a factor of 4.5 (section S16). This discrepancy might be the result of actual lower sorptive capacity of the basic medium than predicted based on the protein and lipid concentrations that were determined experimentally.[10]

FI_{cell} can serve as a metric describing C_{cell}, that should be constant at different FBS concentrations when adjusting

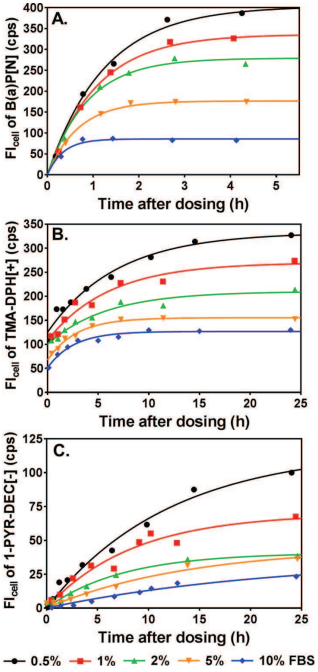

Figure 3. FI_{cell} and first-order uptake kinetics fits of B(a)P[N] in GR-UAS-bla cells (A, eq 6) as well as TMA-DPH[+] (B, eq 7) and 1-PYR-DEC[−] (C, eq 6) in AREc32 cells at 0.5% (black dots), 1% (red squares), 2% (green triangles), 5% (orange triangles), and 10% FBS concentration (blue diamonds) in the medium within the first 4.5 h of the assay (A) and over 24 h (B,C).

constant C_{free} in the medium, as was exemplarily shown for B(a)P[N] (Figure S16A). The effects of different FBS concentrations on FI_{cell} confirm that increased medium FBS concentrations lead to a decrease in C_{cell}, which thus results in reduced test sensitivity of *in vitro* cell assays,[45] which has been shown in theory for a variety of chemicals in model studies.[10,11]

An exception represents the uptake observed for TMA-DPH[+] in the GR assay. TMA-DPH[+] was taken up by the cells to the same extent, resulting in similar FI_{cell}, independent of

DOI: 10.1021/acs.chemrestox.8b00019
Chem. Res. Toxicol. 2018, 31, 646−657

the concentrations of FBS (Table 2, Figure S22A). This phenomenon could be the result of endocytosis, by which TMA-DPH[+] sorbed to FBS is transported into the cells, similar to the HSA-mediated transport *in vivo*.[25,53] In this instance, the chemical can be desorbed within the cell and hence FBS acts as a shuttle. This active transport process may even exceed the C_{cell} that would result from chemical partitioning between medium and cells following the chemical gradient if FBS is metabolized, which would explain why the FI_{cell} of TMA-DPH[+] in GR-UAS-bla cells was not reduced at higher medium FBS concentrations, despite an increase in FI_{medium}, which is representative of a reduced C_{free} (Figure S13C). Increased uptake of chemicals due to FBS-mediated transport was discussed to enhance *in vitro* hepatic clearance of neutral and anionic chemicals in both cultured rat and human hepatocytes when using FBS instead of serum-free medium,[54−56] and increased accuracy of QIVIVE methods that include FBS-mediated transport was recently verified.[57,58] The similar FI_{cell} of TMA-DPH in the GR cells (embryonic kidney cells) at different medium FBS concentrations indicate that FBS-mediated transport can play a role for other *in vitro* cell lines and not just for hepatocytes. Active transport could have also occurred for the other chemicals tested, however, faster desorption into the medium by passive membrane diffusion could have compensated the postulated active transport.

Chemical uptake into the GR-UAS-bla cells was higher than into the AREc32 cells, which, as noted above, could be the result of increased biotransformation of the chemicals by the AREc32 cells. However, co-transport of chemicals by FBS-mediated transport may have contributed more to chemical uptake in the GR-UAS-bla cells because these cells showed signs of starvation at 0.5% FBS after 48 h even in the controls without chemical exposure (Figure S4B), indicating the potential for high metabolic turnover of FBS, whereas the AREc32 cells looked healthy and cell growth was still observed in the controls after 48 h at 0.5% medium FBS (Figure S4A).

The $t_{95\%}$ decreased by a factor of 2 when increasing the medium FBS concentrations by a factor of 20 for B(a)P[N] (Figure 3A, Table 2). The effect of the FBS concentration on $t_{95\%}$ of TMA-DPH[+] was less pronounced, but was impacted by the very fast initial sorption, which led to higher uncertainty for the derivation of the uptake rate constant (Figure 3B, Table 2). The results for B(a)P[N] and TMA-DPH[+] illustrate that higher medium FBS concentrations can lead to faster attainment of equilibrium between the medium and cells. This correlation could result from facilitated transport over the ABL into the cells at higher medium FBS concentrations, comparable to the HSA-facilitated transport from blood into human cells *in vivo*.[25] However, whether more chemicals were transported over the ABL by FBS-facilitated transport and/or increased co-transport by FBS-mediated transport led to the lower $t_{95\%}$ in this study cannot be clarified by the presented method and is beyond the scope of this study. It is likely that active transport by FBS-mediated transport might be more important for chemicals that considerably bind to the medium FBS compared to chemicals that are predominantly freely dissolved in the medium.

For 1-PYR-DEC[−], equilibrium between cells and medium was achieved faster when adjusting the medium FBS from 0.5% to 1% and 2%, whereas 5% and 10% FBS led to slower kinetics (Figure 3C, Table 2). However, time to equilibrium exceeded 24 h for 1-PYR-DEC[−] in both assays and all evaluated FBS concentrations. Earlier studies investigated cellular phospholipidosis (synthesis of phospholipids in the lysosomes)[59] and the formation of lipid droplets as reaction to chemical stress for this chemical.[60] The accumulation of lipids would increase the cellular sorptive capacity for lipophilic chemicals thus leading to a continuous increase in $K_{cell/medium}$, which could explain the delayed increase in FI_{cell}. 1-PYR-DEC[−] is a long-chain organic acid that is expected to have a high sorptive affinity to the fatty acid tail of phospholipids due to structural similarities, and was shown to stimulate the synthesis of lipids in cultured fibroblasts.[61] In our experiments, highly fluorescent black spots were observed in the AREc32 cells after 24 h of 1-PYR-DEC[−] exposure, which could be lipid droplets in which 1-PYR-DEC[−] accumulated to a large extent (Figure S23). This lipid synthesis may have been expressed to a higher extent at higher medium FBS concentrations, leading to an almost linear increase of FI_{cell} of 1-PYR-DEC[−] at 5 and 10% FBS throughout the 24-h assay duration. This change in cell morphology could explain the greatly delayed attainment of equilibrium between medium and cells. However, it is questionable whether this increased enrichment of 1-PYR-DEC[−] would also result in increased expression of measured effects. On the contrary, we suggest that the continuous synthesis of cellular lipids would reduce the C_{free} in the cell, leading to reduced binding to the target site and reduction of toxicity.

3.4. Relevance of Exposure Kinetics in *in Vitro* Exposure Models. Although cellular uptake kinetics were considerably delayed for most chemicals, with time to equilibrium partly exceeding the 24-h test period, cell exposure as a function of the AUC (eq 9) did not differ considerably from the exposure that would result from instantaneous cell-medium equilibrium even at the lowest evaluated FBS content of 0.5% at which chemical uptake was the slowest (Table 3).

Table 3. $t_{95\%}$ and Fraction of Maximum Exposure of Six Chemicals in the GR-UAS-bla Cells in Medium Supplemented with 0.5% FBS

chemical	$t_{95\%}$ (h) (eq 8)	area under the curve (AUC) (eq 9)	fraction of maximum exposure (%) (eq 11)
B(a)P[N]	3.6	53.3	94.9
B(g,h,i)P[N]	7.1	44.7	89.7
1-PYR-DEC[−]	33.7	46.7	58.2
2-FLA-BENZ[−]	43.2	2.4	50.8
Rhod-123[+]	9.0	0.4	87.3
TMA-DPH[+]	13.7	95.4	80.8

Although reaching the cell-medium equilibrium partitioning typically required greater than one-third of the assay duration, exposure was reduced by less than 20% by the delayed kinetics. For 3-AM-FLA[N], 3-DABPA[−], and 9-MAMA-ANT[+], uptake kinetics were too fast to adequately fit uptake rates, indicating that uptake kinetics can be neglected for these chemicals. For 1-PYR-DEC[−] and 2-FLA-BENZ[−], a significant reduction in exposure of 40 to 50% was observed, however, cellular uptake exceeded the 24 h assay duration, possibly as a result of changing cellular morphology throughout the test, as discussed earlier. $FI_{cell,eq}$ was extrapolated from the fit, questioning whether it realistically represents C_{cell} in equilibrium for the these anions.

These results indicate that even though cellular uptake kinetics can be delayed, the cell-medium equilibrium assumption in *in vitro* mass balance models holds for most of the

DOI: 10.1021/acs.chemrestox.8b00019
Chem. Res. Toxicol. 2018, 31, 646−657

evaluated chemicals that cover a large range of hydrophobicity, functional groups and speciation. However, this has to be proven for further chemicals and test setups that apply 384- and 1536-well plates in future experiments. Increasing the medium FBS concentration helps to control exposure concentrations in the medium and facilitates faster equilibrium between the medium and cells, further increasing the accuracy of predicted C_{cell} and C_{free} by *in vitro* mass balance models that work with the equilibrium assumption.

4. CONCLUSIONS

The method is limited to autofluorescent chemicals hampering the time-dependent quantification of cell exposure for a large list of non-fluorescent chemicals, which would be needed to identify physicochemical properties influencing uptake and intracellular distribution of neutral and charged organic chemicals. The experiments did not enable the discrimination of different transport processes in the external medium, in the cell membrane and within the cell. Still, the developed method represents a suitable tool to quantify chemical exposure and cellular dose in a realistic scenario. Representative dose metrics such as FI_{cell} and EF_{cell} that can be quantitatively linked to *in vitro* effects can be derived by automated image analysis.

The study results demonstrate the complexity of cell exposure in *in vitro* assays, since it can be influenced over time by different toxicokinetic processes including uptake, distribution, metabolism and elimination in the cells and the composition of the medium, dependent on the physicochemical properties of the tested chemical(s). In contrast to the neutral chemicals, chemical uptake of six of the seven charged chemicals was considerably delayed, with no equilibrium attained within the 24-h assays for the three anions 2-FLA-BENZ[−], 3-DAPBA[-], and 1-PYR-DEC[−] as well as Rhod-110[Zw] at 0.5% FBS.

Cell exposure is strongly dependent on the applied medium FBS concentration, which should be considered when changing the experimental setup of an assay or when comparing similar assays with different cell lines and different media compositions. The large reservoir of reversibly bound chemicals associated with the relative mass of FBS in the medium resulted in fairly constant medium exposure conditions for all evaluated chemicals, indicating that SMPD may be a suitable dosing method for *in vitro* assays. The suitability of SMPD to control exposure in different well plate formats and various *in vitro* assays needs to be confirmed in future studies. The downside of using high FBS concentrations, is that more chemical or sample needs to be added to obtain critical cellular concentrations for biological response and cytotoxicity. Furthermore, high FBS concentration might not be tolerated by certain cell lines. However, classic passive dosing from a third phase polymer would require even higher total amounts of test chemical because most cell assays would not work without serum-supplemented medium.

Biotransformation by the cells can represent an additional source of uncertainty. The two cell lines applied here show clearly differing biotransformation capacities, as deduced by the difference in uptake curves of B(a)P[N]. Moreover, differences in the amount and rates of efflux pumps can lead to altered extents of chemical uptake between cell lines. However, we argue that biotransformation should be considered as part of the cell response to chemical exposure.

The contribution of active and passive transport processes to the overall chemical uptake can differ between *in vitro* reporter gene assays that utilize different cell lines, dependent on whether they express certain transport proteins. The extent of FBS-mediated transport can furthermore depend on the metabolism of the applied cell line as well as the sorption affinity of the chemical to FBS. Clearly, given the large variety of assay systems, more case studies will be needed to generate further knowledge for a wider range of chemicals and to identify relevant cellular transport and metabolic processes involved. In chemical risk assessment, cellular uptake and metabolism of chemicals of emerging concern is hard to predict for each individual chemical but as this and earlier studies have demonstrated, it is possible to estimate cellular concentrations by equilibrium partition models and the loss of AUC is negligible to moderate over 24 h in comparison to the assumption of instantaneous attainment of steady state. Still, risk assessors should be informed about critical processes such as the metabolic activity of different cell lines, as well as the high sorptive capacity of the FBS for certain chemicals such as anions, decreasing the cell exposure considerably.

■ ASSOCIATED CONTENT

Supporting Information

The Supporting Information is available free of charge on the ACS Publications website at DOI: 10.1021/acs.chemrestox.8b00019.

Chemical concentrations applied in the assays as well as relevant filter settings for each chemical; KNIME code for image analysis; figures and data on experimental artifacts; graphs describing the medium exposure; all relevant data on the 10 chemicals tested in two reporter gene assays at 0.5% FBS and three chemicals at varying FBS concentrations including fits and standard deviations; and images of the merged bright-field and fluorescence images for all chemicals and experiments, including Figures S1−S27 and Tables S1−S3 (PDF)

■ AUTHOR INFORMATION

Corresponding Author

*Phone: +49 341 235-1512. Fax: +49 341 235-1787. E-mail: fabian.fischer@ufz.de.

ORCID

Fabian C. Fischer: 0000-0002-9511-0506

Beate I. Escher: 0000-0002-5304-706X

Funding

We gratefully acknowledge the financial support by the CEFIC Long-Range Research Initiative (LRI), project ECO36.

Notes

The authors declare no competing financial interest.

■ ACKNOWLEDGMENTS

We thank Lisa Glauch and Christin Kühnert for the laboratory support. Kai-Uwe Goss, Todd Gouin, and Martijn Rooseboom are gratefully acknowledged for their critical review of the manuscript. We thank Jessica Hellweg for proofreading and her critical review of the manuscript structure. The Centre for Chemical Microscopy (ProVIS) at the Helmholtz Centre for Environmental Research supported by European Regional Development Funds (EFRE−Europe funds Saxony) is acknowledged for providing their analytical facilities. We thank Tobias Busch for implementation of the microscope software. The authors thank Martin Krauss for performing the LC-HRMS analysis.

DOI: 10.1021/acs.chemrestox.8b00019
Chem. Res. Toxicol. 2018, 31, 646−657

ABBREVIATIONS

C_{cell}, cellular concentration; C_{free}, freely dissolved concentration; C_{nom}, nominal concentration; EF_{cell}, enrichment factor between cells and medium; FI_{cell}, mean fluorescence signal in cells; FI_{medium}, mean fluorescence signal in medium; FBS, fetal bovine serum; HSA, human serum albumin

REFERENCES

(1) Judson, R. S., Houck, K. A., Kavlock, R. J., Knudsen, T. B., Martin, M. T., Mortensen, H. M., Reif, D. M., Rotroff, D. M., Shah, I., Richard, A. M., and Dix, D. J. (2010) *In Vitro* Screening of Environmental Chemicals for Targeted Testing Prioritization: The ToxCast Project. *Environ. Health Perspect. 118*, 485−492.

(2) Neale, P. A., Altenburger, R., Ait-Aissa, S., Brion, F., Busch, W., de Aragao Umbuzeiro, G., Denison, M. S., Du Pasquier, D., Hilscherova, K., Hollert, H., Morales, D. A., Novak, J., Schlichting, R., Seiler, T. B., Serra, H., Shao, Y., Tindall, A. J., Tollefsen, K. E., Williams, T. D., and Escher, B. I. (2017) Development of a bioanalytical test battery for water quality monitoring: Fingerprinting identified micropollutants and their contribution to effects in surface water. *Water Res. 123*, 734−750.

(3) Escher, B. I., and Leusch, F. (2012) *Bioanalytical tools in water quality assessment*, IWA Publishing, London, UK.

(4) Gülden, M., and Seibert, H. (2003) In *vitro*−*in vivo* extrapolation: estimation of human serum concentrations of chemicals equivalent to cytotoxic concentrations in vitro. *Toxicology 189*, 211−222.

(5) Wetmore, B. A. (2015) Quantitative *in vitro*-to-*in vivo* extrapolation in a high-throughput environment. *Toxicology 332*, 94−101.

(6) Escher, B. I., and Hermens, J. L. M. (2004) Internal exposure: Linking bioavailability to effects. *Environ. Sci. Technol. 38*, 455A−462A.

(7) McCarty, L. S., Landrum, P. F., Luoma, S. N., Meador, J. P., Merten, A. A., Shephard, B. K., and van Wezel, A. P. (2011) Advancing Environmental Toxicology through Chemical Dosimetry: External Exposures Versus Tissue Residues. *Integr. Environ. Assess. Manage. 7*, 7−27.

(8) Escher, B. I., Ashauer, R., Dyer, S., Hermens, J. L. M., Lee, J.-H., Leslie, H. A., Mayer, P., Meador, J. P., and Warne, M. S. J. (2011) Crucial role of mechanisms and modes of toxic action for understanding tissue residue toxicity and internal effect concentrations of organic chemicals. *Integr. Environ. Assess. Manage. 7*, 28−49.

(9) Groothuis, F. A., Heringa, M. B., Nicol, B., Hermens, J. L. M., Blaauboer, B. J., and Kramer, N. I. (2015) Dose metric considerations in in vitro assays to improve quantitative in vitro−in vivo dose extrapolations. *Toxicology 332*, 30−40.

(10) Fischer, F. C., Henneberger, L., König, M., Bittermann, K., Linden, L., Goss, K. U., and Escher, B. I. (2017) Modeling Exposure in the Tox21 *in Vitro* Bioassays. *Chem. Res. Toxicol. 30* (5), 1197−1208.

(11) Armitage, J. M., Wania, F., and Arnot, J. A. (2014) Application of Mass Balance Models and the Chemical Activity Concept To Facilitate the Use of *in Vitro* Toxicity Data for Risk Assessment. *Environ. Sci. Technol. 48*, 9770−9779.

(12) Kramer, N. I., Busser, F. J. M., Oosterwijk, M. T. T., Schirmer, K., Escher, B. I., and Hermens, J. L. M. (2010) Development of a partition-controlled dosing system for cell assays. *Chem. Res. Toxicol. 23*, 1806−1814.

(13) Oostingh, G. J., Smith, K. E. C., Tischler, U., Radauer-Preiml, I., and Mayer, P. (2015) Differential immunomodulatory responses to nine polycyclic aromatic hydrocarbons applied by passive dosing. *Toxicol. In Vitro 29*, 345−351.

(14) Lin, J. H., and Lu, A. Y. H. (1997) Role of Pharmacokinetics and Metabolism in Drug Discovery and Development. *Pharmacol. Rev. 49*, 403−449.

(15) Ruiz-Garcia, A., Bermejo, M., Moss, A., and Casabo, V. G. (2008) Pharmacokinetics in Drug Discovery. *J. Pharm. Sci. 97*, 654−690.

(16) Yabe, Y., Galetin, A., and Houston, J. B. (2011) Kinetic Characterization of Rat Hepatic Uptake of 16 Actively Transported Drugs. *Drug Metab. Dispos. 39*, 1808−1814.

(17) Salvage, J. P., Smith, T., Lu, T., Sanghera, A., Standen, G., Tang, Y., and Lewis, A. L. (2016) Synthesis, characterisation, and in vitro cellular uptake kinetics of nanoprecipitated poly(2-methacryloyloxyethyl phosphorylcholine)-b-poly(2-(diisopropylamino)ethyl methacrylate) (MPC-DPA) polymeric nanoparticle micelles for nanomedicine applications. *Appl. Nanosci. 6*, 1073−1094.

(18) Egger, A. E., Rappel, C., Jakupec, M. A., Hartinger, C. G., Heffeter, P., and Keppler, B. K. (2009) Development of an experimental protocol for uptake studies of metal compounds in adherent tumor cells. *J. Anal. At. Spectrom. 24*, 51−61.

(19) Stadnicka-Michalak, J., Tanneberger, K., Schirmer, K., and Ashauer, R. (2014) Measured and Modeled Toxicokinetics in Cultured Fish Cells and Application to *In Vitro - In Vivo* Toxicity Extrapolation. *PLoS One 9*, e92303.

(20) Ali, R., Trump, S., Lehmann, I., and Hanke, T. (2015) Live cell imaging of the intracellular compartmentalization of the contaminate benzo[a]pyrene. *Journal of Biophotonics 8*, 361−371.

(21) Bean, R. C., Shepherd, W. C., and Chan, H. (1968) Permeability of Lipid Bilayer Membranes to Organic Solutes. *J. Gen. Physiol. 52*, 495−508.

(22) Ponizovskiy, M. R. (2011) Driving Mechanisms of Passive and Active Transport Across Cellular Membranes as the Mechanisms of Cell Metabolism and Development as well as the Mechanisms of Cellular Distance Reactions on Hormonal Expression and the Immune Response. *Crit. Rev. Eukaryotic Gene Expression 21*, 267−290.

(23) Dobson, P. D., and Kell, D. B. (2008) Carrier-mediated cellular uptake of pharmaceutical drugs: an exception or the rule? *Nat. Rev. Drug Discovery 7*, 205.

(24) Poulin, P., and Haddad, S. (2015) Albumin and Uptake of Drugs in Cells: Additional Validation Exercises of a Recently Published Equation that Quantifies the Albumin-Facilitated Uptake Mechanism(s) in Physiologically Based Pharmacokinetic and Pharmacodynamic Modeling Research. *J. Pharm. Sci. 104*, 4448−4458.

(25) Poulin, P., Burczynski, F. J., and Haddad, S. (2016) The Role of Extracellular Binding Proteins in the Cellular Uptake of Drugs: Impact on Quantitative *In Vitro*-to-*In Vivo*. Extrapolations of Toxicity and Efficacy in Physiologically Based Pharmacokinetic-Pharmacodynamic Research. *J. Pharm. Sci. 105*, 497−508.

(26) Kwon, J. H., Wuethrich, T., Mayer, P., and Escher, B. I. (2009) Development of a dynamic delivery method for *in vitro* bioassays. *Chemosphere 76*, 83−90.

(27) ter Laak, T. L., ter Bekke, M. A., and Hermens, J. L. M. (2009) Dissolved Organic Matter Enhances Transport of PAHs to Aquatic Organisms. *Environ. Sci. Technol. 43*, 7212−7217.

(28) ter Laak, T. L., Van Eijkeren, J. C. H., Busser, F. J. M., Van Leeuwen, H. P., and Hermens, J. L. M. (2009) Facilitated Transport of Polychlorinated Biphenyls and Polybrominated Diphenyl Ethers by Dissolved Organic Matter. *Environ. Sci. Technol. 43*, 1379−1385.

(29) Ziv, O., Zaritsky, A., Yaffe, Y., Mutukula, N., Edri, R., and Elkabetz, Y. (2015) Quantitative Live Imaging of Human Embryonic Stem Cell Derived Neural Rosettes Reveals Structure-Function Dynamics Coupled to Cortical Development. *PLoS Comput. Biol. 11*, e1004453.

(30) Chen, T., Gomez-Escoda, B., Munoz-Garcia, J., Babic, J., Griscom, L., Wu, P. Y. J., and Coudreuse, D. (2016) A drug-compatible and temperature controlled microfluidic device for live-cell imaging. *Open Biol. 6* (8), 160156.

(31) Suzuki, T., Matsuzaki, T., Hagiwara, H., Aoki, T., and Takata, K. (2007) Recent Advances in Fluorescent Labeling Techniques for Fluorescence Microscopy. *Acta Histochem. Cytochem. 40*, 131−137.

(32) Wink, S., Hiemstra, S., Huppelschoten, S., Danen, E., Niemeijer, M., Hendriks, G., Vrieling, H., Herpers, B., and van de Water, B. (2014) Quantitative High Content Imaging of Cellular Adaptive Stress Response Pathways in Toxicity for Chemical Safety Assessment. *Chem. Res. Toxicol. 27*, 338−355.

(33) Ulrich, N., Endo, S., Brown, T. N., Watanabe, N., Bronner, G., Abraham, M. H., and Goss, K.-U. (2017) UFZ-LSER database v 3.2.1, Helmholtz Centre for Environmental Research-UFZ, Leipzig, Germany, http://www.ufz.de/lserd [accessed on Dec 10, 2017].

DOI: 10.1021/acs.chemrestox.8b00019
Chem. Res. Toxicol. 2018, 31, 646−657

(34) *ACD/LAB* (2015), Advanced Chemistry Development, Inc., Toronto, ON, Canada.
(35) *OPERA* (OPEn (quantitative) structure-activity Relationship Application), version 1.02, National Center for Computational Toxicology, U.S. Environmental Protection Agency, Research Triangle Park, NC, USA.
(36) Wang, X. J., Hayes, J. D., and Wolf, C. R. (2006) Generation of a Stable Antioxidant Response Element−Driven Reporter Gene Cell Line and Its Use to Show Redox-Dependent Activation of Nrf2 by Cancer Chemotherapeutic Agents. *Cancer Res. 66*, 10983−10994.
(37) Wolf, D. M., and Jordan, V. C. (1994) Characterization of tamoxifen stimulated MCF-7 tumor variants grown in athymic mice. *Breast Cancer Res. Treat. 31*, 117−127.
(38) Wolf, D. M., and Jordan, V. C. (1994) The estrogen receptor from a tamoxifen stimulated MCF-7 tumor variant contains a point mutation in the ligand binding domain. *Breast Cancer Res. Treat. 31*, 129−138.
(39) Natsch, A., Emter, R., and Ellis, G. (2009) Filling the Concept with Data: Integrating Data from Different In Vitro and In Silico Assays on Skin Sensitizers to Explore the Battery Approach for Animal-Free Skin Sensitization Testing. *Toxicol. Sci. 107*, 106−121.
(40) Escher, B. I., van Daele, C., Dutt, M., Tang, J. Y., and Altenburger, R. (2013) Most oxidative stress response in water samples comes from unknown chemicals: the need for effect-based water quality trigger values. *Environ. Sci. Technol. 47*, 7002−7011.
(41) Attene-Ramos, M. S., Miller, N., Huang, R., Michael, S., Itkin, M., Kavlock, R. J., Austin, C. P., Shinn, P., Simeonov, A., Tice, R. R., and Xia, M. (2013) The Tox21 robotic platform for the assessment of environmental chemicals - from vision to reality. *Drug Discovery Today 18*, 716−723.
(42) Oris, J. T., and Giesy, J. P. (1987) The Photoinduced Toxicity of Polycyclic Aromatic-Hydrocarbons to Larvae of the Fathead Minnow (Pimephales-Promelas). *Chemosphere 16*, 1395−1404.
(43) Lampi, M. A., Gurska, J., McDonald, K. I. C., Xie, F. L., Huang, X. D., Dixon, D. G., and Greenberg, B. M. (2006) Photoinduced toxicity of polycyclic aromatic hydrocarbons to *Daphnia magna*: Ultraviolet-mediated effects and the toxicity of polycyclic aromatic hydrocarbon photoproducts. *Environ. Toxicol. Chem. 25*, 1079−1087.
(44) Vander Heiden, M. G., Cantley, L. C., and Thompson, C. B. (2009) Understanding the Warburg Effect: The Metabolic Requirements of Cell Proliferation. *Science 324*, 1029−1033.
(45) Gülden, M., Morchel, S., Tahan, S., and Seibert, H. (2002) Impact of protein binding on the availability and cytotoxic potency of organochlorine pesticides and chlorophenols in vitro. *Toxicology 175*, 201−213.
(46) Riedl, J., and Altenburger, R. (2007) Physicochemical substance properties as indicators for unreliable exposure in microplate-based bioassays. *Chemosphere 67*, 2210−2220.
(47) Ussing, H. H. (1949) Transport of ions across cellular membranes. *Physiol. Rev. 29*, 127−155.
(48) Escher, B. I., Schwarzenbach, P., and Westall, J. C. (2000) Evaluation of Liposome−Water Partitioning of Organic Acids and Bases. 1. Development of a Sorption Model. *Environ. Sci. Technol. 34*, 3954−3961.
(49) Bittermann, K., Spycher, S., and Goss, K. U. (2016) Comparison of different models predicting the phospholipid-membrane water partition coefficients of charged compounds. *Chemosphere 144*, 382−391.
(50) Illinger, D., and Kuhry, J. G. (1994) The kinetic aspects of intracellular fluorescence labeling with TMA-DPH support the maturation model for endocytosis in L929 cells. *J. Cell Biol. 125*, 783−794.
(51) Johnson, C. A., and Westall, J. C. (1990) Effect of pH and KCl concentration on the octanol water distribution of methylanilines. *Environ. Sci. Technol. 24*, 1869−1875.
(52) Escher, B. I., and Sigg, L. (2004) Chemical Speciation of Organics and of Metals at Biological Interfaces, in *Physicochemical Kinetics and Transport at Biointerfaces 9*, Van Leeuwen, H. P., and Köster, W., Eds., John Wiley & Sons, Chichester, pp 205−271.
(53) Poulin, P., Bteich, M., and Haddad, S. (2017) Supplemental Analysis of the Prediction of Hepatic Clearance of Binary Mixtures of Bisphenol A and Naproxen Determined in an Isolated Perfused Rat Liver Model to Promote the Understanding of Potential Albumin-Facilitated Hepatic Uptake Mechanism. *J. Pharm. Sci. 106*, 3207−321.
(54) Blanchard, N., Hewitt, N. J., Silber, P., Jones, H., Coassolo, P., and Lavé, T. (2006) Prediction of hepatic clearance using cryopreserved human hepatocytes: a comparison of serum and serum free incubations. *J. Pharm. Pharmacol. 58*, 633−641.
(55) Fukuchi, Y., Toshimoto, K., Mori, T., Kakimoto, K., Tobe, Y., Sawada, T., Asaumi, R., Iwata, T., Hashimoto, Y., Nunoya, K. I., Imawaka, H., Miyauchi, S., and Sugiyam, Y. (2017) Analysis of Nonlinear Pharmacokinetics of a Highly Albumin-Bound Compound: Contribution of Albumin-Mediated Hepatic Uptake Mechanism. *J. Pharm. Sci. 106*, 2704−2714.
(56) Miyauchi, S., Masuda, M., Kim, S. J., Tanaka, Y., Lee, K. R., Iwakado, S., Nemoto, M., Sasaki, S., Shimono, K., Tanaka, Y., and Sugiyama, Y. (2018) The phenomenon of "albumin-mediated" hepatic uptake of organic anion transport polypeptide substrates: Prediction of the *in vivo* uptake clearance from the *in vitro* uptake by isolated hepatocytes using a "facilitated-dissociation" model. *Drug Metab. Dispos. 46*, 259−267.
(57) Poulin, P., and Haddad, S. (2018) Extrapolation of the hepatic clearance of drugs in the absence of albumin *in vitro* to that in the presence of albumin *in vivo*: comparative assessement of two extrapolation models based on the albumin-mediated hepatic uptake theory and limitations and mechanistic insights. *J. Pharm. Sci. 107*, 1791−1797.
(58) Da-silva, F., Boulenc, X., Vermet, H., Compigne, P., Gerbal-Chaloin, S., Daujat-Chavanieu, M., Klieber, S., and Poulin, P. (2018) Improving prediction of metabolic clearance using quantitative extrapolation of results obtained from human hepatic micropatterned cocultures model and by considering the impact of albumin binding. *J. Pharm. Sci. 107*, 1957−1972.
(59) Halliwell, W. H. (1997) Cationic amphiphilic drug-induced phospholipidosis. *Toxicol. Pathol. 25*, 53−60.
(60) Rohwedder, A., Zhang, Q., Rudge, S. A., and Wakelam, M. J. O. (2014) Lipid droplet formation in response to oleic acid in Huh-7 cells is mediated by the fatty acid receptor FFAR4. *J. Cell Sci. 127*, 3104−3115.
(61) Radom, J., Salvayre, R., Maret, A., Negre, A., and Douste blazy, L. (1987) Metabolism of 1-Pyrenedecanoic Acid and Accumulation of Neutral Fluorescent Lipids in Cultured Fibroblasts of Multisystemic Lipid Storage Myopathy. *Biochim. Biophys. Acta, Lipids Lipid Metab. 920*, 131−139.

NOTE ADDED AFTER ASAP PUBLICATION

This article was published ASAP on July 16, 2018, with an error in eq 7. The corrected version was reposted on August 2, 2018.

DOI: 10.1021/acs.chemrestox.8b00019
Chem. Res. Toxicol. 2018, 31, 646−657

Publication 3

Application of experimental polystyrene partition constants and diffusion coefficients to predict the sorption of neutral organic chemicals to multiwell plates in *in vivo* and *in vitro* bioassays

Fabian C. Fischer[1], Olaf A. Cirpka[2], Kai-Uwe Goss[3], Luise Henneberger[1], Beate I. Escher[1,2]*

[1] Helmholtz Centre for Environmental Research - UFZ, Department Cell Toxicology, Permoserstraße 15, 04318 Leipzig, Germany

[2] Eberhard Karls University Tübingen, Environmental Toxicology, Centre for Applied Geoscience, 72074 Tübingen, Germany

[3] Helmholtz Centre for Environmental Research - UFZ, Department Analytical Environmental Chemistry, Permoserstraße 15, 04318 Leipzig, Germany

*Address correspondence to: fabian.fischer@ufz.de

Published in Environmental Science & Technology, DOI: 10.1021/acs.est.8b04246 .

Environmental Science & Technology

Article

Cite This: *Environ. Sci. Technol.* 2018, 52, 13511−13522

pubs.acs.org/est

Application of Experimental Polystyrene Partition Constants and Diffusion Coefficients to Predict the Sorption of Neutral Organic Chemicals to Multiwell Plates in in Vivo and in Vitro Bioassays

Fabian C. Fischer,*[†] Olaf A. Cirpka,[‡] Kai-Uwe Goss,[§] Luise Henneberger,[†] and Beate I. Escher[†,‡]

[†]Helmholtz Centre for Environmental Research - UFZ, Department Cell Toxicology, Permoserstraße 15, 04318 Leipzig, Germany

[‡]Eberhard Karls University Tübingen, Center for Applied Geoscience, 72074 Tübingen, Germany

[§]Helmholtz Centre for Environmental Research - UFZ, Department Analytical Environmental Chemistry, Permoserstraße 15, 04318 Leipzig, Germany

Supporting Information

ABSTRACT: Sorption to the polystyrene (PS) of multiwell plates can affect the exposure to organic chemicals over time in in vitro and in vivo bioassays. Experimentally determined diffusion coefficients in PS (D_{PS}) were in a narrow range of 1.25 to 8.0 · 10^{-16} m^2 s^{-1} and PS-water partition constants ($K_{PS/w}$) ranged from 0.04 to 5.10 log-units for 22 neutral organic chemicals. A kinetic model, which explicitly accounts for diffusion in the plastic, was applied to predict the depletion of neutral organic chemicals from different bioassay media by sorption to various multiwell plate formats. For chemicals with log K_{ow} > 3, the medium concentrations decreased rapidly and considerably in the fish embryo toxicity assay but medium concentrations remained relatively constant in the cell-based bioassays with medium containing 10% fetal bovine serum (FBS), emphasizing the ability of the protein- and lipid-rich medium to compensate for losses by multiwell plate sorption. The PS sorption data may serve not only for exposure assessment in bioassays but also to model the contaminant uptake by and release from plastic packaging material and the chemical transport by PS particles in the environment.

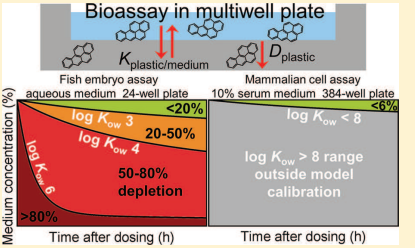

1. INTRODUCTION

Miniaturization and standardization of in vivo and in vitro bioassays in multiwell plate formats (6-, 24-, 96-, 384-, and 1536-well plates) facilitates their implementation in high-throughput screening, toxicity, and risk assessment of organic chemicals and their mixtures. A large number of bioassays have already been applied to multiwell plates, such as the fish embryo toxicity test with *Danio rerio* (FET assay),[1] phytotoxicity tests with algae,[2] acute and chronic reproductive toxicity tests with *Caenorhabditis elegans*,[3] and immobilization tests with *Daphnia magna*.[4] While these whole-organism in vivo bioassays can be carried out in glass jars or glass-coated multiwell plates, in vitro cell assays require plastic multiwell plates because most cell lines need to adhere to the plastic surface for optimal growth.[5]

Use of plastic multiwell plates can lead to depletion of the medium concentrations of the evaluated chemical(s) (C_{medium}) that organisms or cells are exposed to. Chemical sorption to multiwell plate materials might considerably reduce C_{medium}, leading to a reduced assay sensitivity and an underestimation of chemical effects. The reduction in C_{medium} can differ between chemicals dependent on their affinity and kinetics of sorption to the multiwell plate materials, impeding the quantitative comparison of single chemical exposure effects and the evaluation of mixture effects. Polystyrene (PS) is the common material used for multiwell plates, however, their surface can be treated differently depending on the purpose of use, such as the PS in cell culture plates that is usually cross-linked with carboxyl and amine groups (TC-treated) and/or surface-coated with biopolymers such as poly-D-lysine for improved cell attachment.[5]

Sorption of organic chemicals to PS is expected to be time-dependent, with diffusion in the polymer significantly controlling the overall mass-transfer process.[6] In contrast to amorphous, rubbery polymers such as polydimethylsiloxane (PDMS) with relatively high diffusion coefficients (log D_{PDMS} (m^2 s^{-1}) ≈ −9.5 to −11),[7] diffusion is substantially slower in glassy polymers such as PS (log D_{PS} (m^2 s^{-1}) ≈ −13 to −19),[8−10] which are characterized by low segmental mobility

Received: July 31, 2018
Revised: October 5, 2018
Accepted: October 8, 2018
Published: October 9, 2018

DOI: 10.1021/acs.est.8b04246
Environ. Sci. Technol. 2018, 52, 13511−13522

of and a low free volume between the polymer chains.[6,11] Some studies reported higher diffusion coefficients in PS (log D_{PS} (m^2 s^{-1}) ≈ −10 to −12).[12,13] However, as discussed by Chlebowski et al. (2016),[13] it is likely that only pseudoequilibrium between PS and medium was achieved within the measurement duration leading to a large overestimation of D_{PS} and a corresponding underestimation of PS-water partition constants ($K_{PS/w}$). Availability of D_{PS} and $K_{PS/w}$ in the literature remains scarce and the reported data is inconsistent considering the wide application of PS, calling for an improved experimental approach.

For PDMS and low-density polyethylene (LDPE), it was shown that the diffusion of smaller chemicals with low molecular weight is generally faster.[7] It is not clear whether this behavior also applies to diffusion within glassy PS. In PDMS and LDPE, the sorption affinity of the chemicals to the polymers was higher for larger, hydrophobic chemicals.[14] Sorption of ionized chemicals to PS is expected to be negligible due to the lack of ionic interactions. Previous studies demonstrated that even polymers with polar functional groups such as polyacrylate and ethylene-vinyl acetate do not significantly extract organic ions from aqueous solutions.[15,16] Hence, we assume that this is the case for the nonpolar PS as well. However, plate coatings such as poly-D-lysine that are used for certain in vitro cell lines to improve cell attachment might be an additional sorptive sink, in particular for anions, since poly-D-lysine is an anion exchanger with positively charged hydrophilic amino groups at pH 7.4.[17]

The binding to multiwell plates can influence exposure in different bioassays: Gellert and Stommel (1999)[18] compared half maximal effective concentrations (EC_{50}) from assays with *Aliivibrio fischeri* generated in plastic and glass plates. Significantly higher apparent EC_{50} were observed for organic chemicals in plastic plates. The difference between plastic and glass plates was thereby higher for very hydrophobic chemicals. Decreased phenanthrene concentrations of >99% were measured in the FET assay, which was performed in aqueous medium without serum supplements.[19] Riedl & Altenburger (2007)[20] concluded that in the algal growth assay with a mainly inorganic medium, C_{medium} decrease due to multiwell plate sorption should be considered for chemicals with an octanol-water partition constant (K_{ow}) > 1000. The chemical fraction sorbed into the PS after a certain time period is generally expected to increase linearly with the ratio of PS surface-to-well volume, which is 6.6 times larger in 1536- than in 24-well plates.

Our recent mass balance modeling study on exposure in in vitro cell assays indicated that a large proportion of the chemicals is bound to the protein- and lipid-rich medium originating from the fetal bovine serum (FBS) supplemented to the medium as nutrient supply for the cells, thus overall stabilizing exposure while reducing freely dissolved concentrations (C_{free}).[21] This observation led to the assumption that the medium acts as a chemical reservoir potentially compensating for chemical depletion by multiwell plate sorption. With reference to the common passive dosing procedure using technical polymers such as PDMS, we suggested the term serum-mediated passive dosing (SMPD).[22]

Depletion of C_{medium} by sorption to multiwell plates was already measured for phenanthrene in 24-well plates, and higher medium concentrations of FBS counteracted the degree of depletion.[23] C_{medium} remained stable over the assay duration of 24 h for three neutral and seven ionizable chemicals in two reporter gene assays carried out in 96-well plates,[22] validating the applicability of SMPD for these chemicals in 96-well plates.

Studies on the effects of multiwell plate sorption on exposure in bioassays are still scarce. More systematic approaches are needed to quantitatively describe this phenomenon under different test conditions and bioassay setups. Here, we applied partitioning experiments between round PS discs and water to measure $K_{PS/w}$ and D_{PS} of 22 chemicals with physicochemical properties that cover a wide range of hydrophobicity and molecular weights. The derived data were applied in a kinetic model that predicts the depletion of organic chemicals from medium by PS sorption for various in vivo and in vitro bioassays and for different multiwell plate formats. The model explicitly accounts for diffusion within the PS rather than relying on first-order approximations. We validated the model by experimental exposure measurements in a simulated FET assay carried out in colloid-free aqueous medium in 24-well plates as well as by such experiments in the AREc32 in vitro cell assay supplemented with 10% of the protein- and lipid-rich FBS in the medium in 96-well plates. We hypothesized that D_{PS} are higher for chemicals with lower molecular weights (and thus smaller size) and that $K_{PS/w}$ would correlate with molecular weight and hydrophobicity. The degree of PS sorption in bioassays would depend on (i) the chemicals' physicochemical properties, (ii) the sorptive capacity of the medium, and (iii) the ratio of PS surface-to-well volume of the applied multiwell plate. We expected that depletion of C_{medium} by multiwell plate sorption would generally be of higher relevance for bioassays carried out in aqueous media without sorptive colloids compared to in vitro cell assays for which depletion is compensated by the colloid-rich medium.

2. THEORY

2.1. Governing Equations. Neutral organic chemicals that are dissolved in an aqueous assay medium will distribute evenly in the water phase in a relatively short time, based on their diffusion coefficient in water (D_w), which are generally in the range of log D_w (m^2 s^{-1}) ≈ −9 to −10.[24] In an aqueous medium with a defined uniform chemical concentration (C_w, mg L_w^{-1}), the concentration of the chemical in a round PS disc (C_{PS}, mg kg_{PS}^{-1}) meets the one-dimensional diffusion equation:

$$\frac{\partial C_{PS}}{\partial t} - D_{PS}\frac{\partial^2 C_{PS}}{\partial x^2} = 0 \quad (1)$$

subject to the following boundary and initial conditions:

$$C_{PS}\left(\pm\frac{w}{2}, t\right) = K_{PS/w}C_w(t) \text{ for all } t > 0 \quad (2)$$

$$C_{PS}(x, t = 0) = 0 \text{ for all } x \quad (3)$$

x denotes the coordinate orthogonal to the surface ($x = 0$ is the center coordinate of the disc), w is the width of the PS, t is time, and $K_{PS/w}$ is the PS-water partition constant. Please note that diffusion from the shell surface into the PS discs was neglected because it only contributes for 0.6% of the total surface area.

The aqueous boundary layer (ABL) can represent a kinetic limitation for the mass transfer from water into rubbery polymers with high diffusion coefficients such as PDMS (log D_{PDMS} (m^2 s^{-1}) ≈ −10 to −11).[7] As a preliminary sensitivity

DOI: 10.1021/acs.est.8b04246
Environ. Sci. Technol. 2018, 52, 13511−13522

analysis, we estimated the relevance of the ABL for the overall mass transfer (see Supporting Information (SI) Section S1 for corresponding equations). For the PS-water system, in which D_{PS} is expected to be over 6 orders of magnitude smaller than D_w, the mass transfer over the ABL is 100 times faster compared to the diffusion in the PS and was therefore neglected when fitting experiments of mass transfer into the multiwell plates. Then, the mass balance in the water phase can be calculated by

$$\frac{dC_w}{dt} = -\frac{2A_{PS}}{V_w} D_{PS} \varrho_{PS} \left.\frac{\partial C_{PS}}{\partial x}\right|_{x=w/2} \quad (4)$$

in which A_{PS} is the surface area of the PS disc and V_w is the volume of the water phase. The multiplication by the mass density ϱ_{PS} of the PS (1.04 kg L^{-1}) is needed because C_{PS} is expressed as mass of chemical per mass of PS (mg kg^{-1}). $\left.\frac{\partial C_{PS}}{\partial x}\right|_{x=w/2}$ denotes the concentration gradient at the surface.

2.2. Laplace-Domain Solution for a Depleting Concentration in the Medium. The analytical solution to eqs 1 and 4 was derived after Laplace transformation (SI Section S1):

$$\tilde{C}_w = \frac{C_w(0) + \frac{a_{PS}}{K_{PS/w}} \frac{C_{PS}(0)}{s}}{a_{PS} + s} \quad (5)$$

$$\text{with } a_{PS} = 2\tanh\left(\frac{w}{2}\sqrt{\frac{s}{D_{PS}}}\right)\frac{\sqrt{D_{PS}s}}{w} K_{PS/w} \frac{m_{PS}}{V_w} \quad (6)$$

in which $\tilde{C}_w(s)$ is the Laplace transform of $C_w(t)$ and s is the complex Laplace coordinate (1/t).

The model predicting C_{medium} in different multiwell plates is a special case of eq 6 with an initial concentration in the PS of zero ($C_{PS}(x, t = 0) = 0$):

$$\tilde{C}_{medium}(s) = \frac{C_{medium}(0)}{s + \sqrt{D_{PS}s}\frac{A_{PS}}{V_{medium}} K_{PS/medium} \varrho_{PS} \tanh\left(\sqrt{\frac{s}{D_{PS}}} w\right)} \quad (7)$$

Back-transformation into the time-domain was done numerically.[25] In order to run the model, the PS-medium partition constant ($K_{PS/medium}$) and the D_{PS} of the chemical(s), the volume of the medium (V_{medium}), the surface area (A_{PS}), and the thickness of the PS (w) that is in contact with the medium in the well are needed. Table 1 provides the system parameters for standard multiwell plates that can be readily applied in the model. The MATLAB code to run the model is included in the SI Section S2. Note that the model only implements a simplified well geometry, as discussed in the SI Section S3.

2.3. Laplace-Domain Solution for a Constant Concentration in the Medium. If the chemical concentration in the water phase is kept constant by a PDMS reservoir, the average concentration in the PS ($\overline{C_{PS}}$) is calculated by

$$\overline{C_{PS}}(t) = \frac{2}{w}\int_0^{w/2} C_{PS}(x, t)dx \quad (8)$$

The one-dimensional diffusion equation with given initial and boundary conditions (eqs 1−3) and a constant aqueous-phase concentration C_w has the following analytical solution in the Laplace domain:

Table 1. System Parameters of Multiwell Plates Applied in the Predictive Model[a]

multiwell plate format	volume of medium (V_{medium}, m^3)	surface area of PS (A_{PS}, m^2)	thickness of PS (w, m)	V_{medium} to A_{PS} ratio (m)
12-well plate	3.00×10^{-6}	9.33×10^{-4}	1.27×10^{-3}	3.22×10^{-3}
24-well plate	2.00×10^{-6}	7.04×10^{-4}	1.27×10^{-3}	2.84×10^{-3}
96-well plate	2.00×10^{-7}	1.26×10^{-4}	5.00×10^{-4}	1.58×10^{-3}
384-well plate	4.00×10^{-8}	5.90×10^{-5}	6.35×10^{-4}	6.78×10^{-4}
1536-well plate	6.00×10^{-9}	1.40×10^{-5}	9.00×10^{-4}	4.29×10^{-4}

[a]Data on well plate dimensions were derived from the Corning product selection guide (www.corning.com/lifesciences). Note that the dimensions can change between different types of multiwell plates purchased from different suppliers.

$$\overline{\tilde{C}_{PS}}(s) = \frac{K_{PS/w}C_w}{s}\sqrt{\frac{4D_{PS}}{w^2 s}}\tanh\left(\sqrt{\frac{w^2 s}{4D_{PS}}}\right) \quad (9)$$

in which $\overline{\tilde{C}_{PS}}(s)$ is the Laplace transform of $\overline{C_{PS}}(t)$. Again, back-transformation into the time-domain was done numerically.[25]

3. MATERIALS AND METHODS

3.1. Chemicals and Solvents. The tested chemicals are listed in Table S2 with more details on suppliers and physicochemical properties. Methanol (HPLC grade, Merck KGaA, Darmstadt, Germany), *n*-heptane (HPLC grade, Merck), and HPLC water (HPLC grade, Carl Roth GmbH + Co. KG, Karlsruhe, Germany) were used as solvents.

3.2. Preparation, Cleaning, and Loading of PS and PDMS Discs. PDMS with a thickness of 125 μm (±5 μm tolerance) was purchased from Specialty Silicone Products, Inc. (Ballston Spa, NY). The PDMS was stamped with a steel cutting tool yielding uniform round PDMS discs with a diameter of 8 mm. The discs were purified by Soxhlet extraction for at least 6 h using *n*-heptane as cleansing solvent. After purification, the discs were stored dry in closed glass vials. Weighing of 20 discs resulted in an average weight of 14.0 ± 0.3 mg (n = 20).

The PS with a thickness of 25 μm was bought from Goodfellow Cambridge Ltd. (Huntingdon, UK). Similar to the PDMS, round discs with a diameter of 8 mm were stamped with a cutting tool. The PS discs were stored dry until being used in the experiments. Although Goodfellow states a tolerance of 20% for the PS thickness, the resulting weight of the stamped discs varied <5% with an average weight of 1.34 ± 0.07 mg (n = 20).

3.3. PS-Water and PDMS-Water-PS Partitioning Experiments. Depending on the expected partitioning behavior of the chemicals, we performed experiments (a) with loaded water and initially chemical-free PS discs, (b) with loaded PDMS discs for passive dosing, water, and PS discs, and (c) with loaded PDMS discs and PS discs without water in between. SI Table S3 lists an overview of which method was used for which chemicals. Chemicals with a log K_{ow} < 5 were dosed directly by pipetting 50 μL of a methanolic stock solution with defined chemical concentrations (SI Table S4) into a vial (screw caps with Teflon septum, Order No. EC-

DOI: 10.1021/acs.est.8b04246
Environ. Sci. Technol. 2018, 52, 13511−13522

1087, neoLab) containing 1.8 mL of HPLC water. One 8 mm PS disc was transferred into the solution. The volume of the aqueous medium completely filled the storage vial and no air bubbles were observed in the water nor on the PS disc throughout the experiments. Chemicals with a log K_{ow} > 3 were loaded on 8 mm PDMS discs by incubation of cleansed PDMS discs in saturated methanolic stock solutions for at least 7 days (SI Table S5). The loaded PDMS discs were transferred into HPLC water for a 7-day preequilibration. The volume of HPLC water was adjusted to yield the same PDMS-to-water volume ratio used in the experiment vials. 1.8 mL of the incubated HPLC water were pipetted into a 1.5 mL vial (neoLab) with a glass pipet (eVol xR, Trajan Scientific, Australia) and one 8 mm PS disc was transferred into the solution. One loaded PDMS disc was pressed into the cap of the storage vial and the vial was closed, leaving no headspace in the vial. By that means, the PDMS disc was in permanent contact with the water phase while direct contact between the PDMS and PS disc was prevented by the bottleneck of the vial. All prepared PS-water and PDMS-water-PS vials were incubated on a roller shaker at 100 rpm and a constant temperature of 21 ± 1.4 °C. In this way, the PS disc inside the storage vial constantly rotated in the water phase ensuring homogeneous mixing throughout the whole experiment. At different points in time, some of the vials were opened and 1 mL of the water phase was pipetted into a vial for extraction with 300 μL *n*-heptane. The PS and PDMS discs were transferred into storage vials and extracted with 200 and 1000 μL *n*-heptane, respectively. All discs and water samples were extracted for at least 72 h.

3.4. PDMS−PS Partitioning Experiments. Highly hydrophobic chemicals are difficult to test in water (SI Table S3), therefore direct PDMS-PS partitioning experiments were performed. PS and PDMS discs were cut with 15 mm diameters and thicknesses of 25 and 125 μm (average weights of 2.77 ± 0.11 and 42.3 ± 0.3, n = 20), respectively. The PDMS discs were loaded with the test chemicals using a saturated methanolic stock solution (SI Table S5). One loaded PDMS disc and one unloaded PS disc were stacked in an airtight steel block and pressed tightly with a steel bolt of 15 mm diameter. After different time points during 94 days, PS and PDMS discs were sampled and extracted with 1 and 3 mL *n*-heptane, respectively. Chemical concentrations in the extracts were analyzed by GC-MS.

3.5. Quantifying C_{medium} in the FET and the AREc32 Cell Assay. The C_{medium} of eight chemicals were measured using the protocol media of the FET assay in 24-well plates (Product No.: 92024, TPP Techno Plastic Products AG, Trasadingen, Switzerland) over the entire test duration of 96 h. No fish embryos were used to focus on the role of partitioning to PS. Thirty mL ISO-water[1] were prepared in a 50 mL flask and spiked with 300 μL of a saturated methanolic stock solution (SI Table S5) containing the mixture of the chemicals. The flask was vortexed and 2 mL of the solution were pipetted into each well of the 24-well plate. The plates were incubated at a constant temperature of 21 °C not complying with the OECD guideline of 26 °C,[1] because we preferred to align the experiment temperature to the PS-partitioning experiments for consistency (Section 3.3). After 0.5, 2, 6, 24, 48, 72, and 96 h, the medium was completely removed with a glass pipet and transferred into a 4 mL storage vial (neoLab) for extraction with 1 mL *n*-heptane. The empty wells were extracted with 2 mL *n*-heptane for 15 min.

C_{medium} of the same eight chemicals was measured in the AREc32 antioxidant response assay (AREc32 assay) in 96-well plates (Product No.: CLS3603, Corning Life Sciences, Tewksbury, MA) with Dulbecco's Modified Eagle Medium (DMEM) supplemented with 10% FBS following standard protocols.[26] 7 mL of the medium was prepared in 10 mL vials (neoLab) and spiked with 70 μL of a methanolic stock solution of the chemicals (SI Table S5). The vials were vortexed and 200 μL of the solution were pipetted into the wells of the 96-well plate and the plate was incubated at 37 °C and 5% CO_2. After 0.5, 2, 6, and 24 h, the medium was completely removed with a glass pipet and transferred into a 2 mL storage vial (neoLab) for extraction with 300 μL *n*-heptane. The empty vials were extracted with 200 μL *n*-heptane for 15 min. All medium and well extracts were analyzed by GC−MS or HPLC.

3.6. Chemical Analysis. The chemical concentrations in the *n*-heptane extracts were determined either directly by gas chromatography-tandem mass spectrometry (GC-MS/MS; 7000 Triple Quadrupole-GC-MS/MS, Agilent) with a HP-5MS column (30 m × 250 μm × 0.25 μm, 5% phenyl methyl siloxane, Agilent), or by high-performance liquid chromatography (HPLC; Agilent 1100 system equipped with a diode array detector set to 240 nm and a Kinetex C18 reversed phase silica column, 100 × 3.0 mm, 2.6 μm particle size from Phenomenex) after drying the *n*-heptane extracts under nitrogen followed by redissolving in 200 μL methanol. Drying of *n*-heptane standards and redissolving in methanol demonstrated that the procedure did not lead to significant losses of the evaluated chemicals (<3% losses). Chemical concentrations were quantified by external standard calibration. Calibration standards were prepared at a concentration range of 1−2000 μg L^{-1} in *n*-heptane for GC-MS analysis and at a concentration range of 50−10 000 μg L^{-1} in methanol for HPLC analysis. Instrument performance throughout the measurements were checked by repeated measurements of standards and PCB 126 was used as internal standard for the GC−MS measurements because we observed a low but measurable PCB background in the blanks.

3.7. Fit of Kinetic Uptake in the Partitioning Experiments. The applied fits were programmed in MATLAB (R2017); the codes are included in SI Section S2. For the PDMS-water-PS system, we estimated the logarithms of D_{PS} and $K_{PS/w}$ from the measured time series of $\overline{C_{PS}}(t)/C_w$ using DREAM(ZS), a Markov-Chain Monte Carlo code that estimates distributions of the log-parameters conditioned on the measurements.[27,28] A uniform prior distribution with a wide range was considered for each log-parameter. As objective function, we took the sum of squared differences between all measurements and simulated values scaled by the variance of the measurements. The computed medians and uncertainty ranges are based on a conditional sample size of 4000. Given the similarity of the two independent experiments in the PS-water and PDMS-water-PS experiment, all data of one chemical were jointly fitted.

3.8. Prediction of Experimental Bioassay Scenarios. The analytical model (eq 7) was used to predict the depletion of C_{medium} by multiwell plate sorption in different bioassays. The MATLAB code is included in SI Section S2. The analytical model reflects the realistic scenario of mass transfer in the PS to a maximum degree, particularly when assessing the mass transfer within a short time frame and/or from an aqueous phase into a thin polymer. It is applicable to any one-

DOI: 10.1021/acs.est.8b04246
Environ. Sci. Technol. 2018, 52, 13511−13522

dimensional partitioning scenario from an aqueous phase into a defined volume of PS with defined surface area and thickness.

3.9. Excel Prediction Sheet for Simplified Prediction. In addition to the analytical model, a simplified numeric model in Microsoft Excel is attached to the manuscript to facilitate the routine use of the model for diverse bioassay setups and chemicals. Please note that the temporal and spatial resolution of the Excel model was reduced (450 time points and 11 PS slices) for easier usage and improved performance, which leads to a less accurate model output particularly for the early stage of mass transfer between PS and water, at which the chemical gradient and the mass transfer velocity is the highest. The Excel prediction sheet may be used for optimizing the chemical dosing in in vitro and in vivo bioassays with typical durations between 24 and 120 h. The user needs to enter the log K_{ow} of the chemical, the dimensions of the applied multiwell plate, and the protein and lipid contents and total volume of the medium. By including the chemical sorption to medium constituents, the Excel sheet integrates the kinetics of multiwell plate sorption with the existing mass balance model and reported experimental data.[21] The model can be extended for the chemical partitioning to cellular lipids and proteins by adding their respective volumes to the total volume of proteins and lipids in the system. The model sheet reports the relative concentrations in the medium and in the PS, which is separated into 11 slices for better spatial resolution. The relative medium concentration was set to 100 mmol L^{-1}, but can be replaced by the nominal medium concentration applied in the experiment.

4. RESULTS AND DISCUSSION

4.1. Partition Constants to and Diffusion Coefficients in PS. Figure 1 and SI Figure S4 show the experimental data points and the resulting fits for both the PS-water and PDMS-water-PS experiments. The good agreement between the data and model fits confirmed that the model realistically reflects the sorption of the chemicals from an aqueous medium into PS. The total mass of the chemical in the test systems remained stable even in long-term experiments of up to 750 h. Equilibrium was attained for all chemicals in 75 to 450 h. The robustness and repeatability of the experiments emphasizes that this experimental setup can be adapted in future studies to measure additional chemicals and other commonly used glassy polymers, such as polytetrafluoroethylene or graphene.

Measured concentrations in the water and in the PS were fitted with eqs 5 and 6 if the water concentration was depleted by PS sorption (PS-water experiment) or with eq 9 if kept constant by the PDMS reservoir (PDMS-water-PS experiment), as shown for phenanthrene and PCB 180 in Figure 1 and for all other chemicals in SI Figure S4. Coefficients of variation (CV, %) of log $K_{PS/w}$ and log $D_{PS/w}$ (Table 2) were <5% in most cases, however, slightly higher in the PDMS-water-PS experiments with the PDMS reservoir than in the PS-water experiments (5−10%).

The measured log $K_{PS/w}$ of the evaluated chemicals correlate with their corresponding log K_{ow} (r^2 = 0.82) (Figure 2) and hexane-water partition constant (log $K_{hexane/w}$) (r^2 = 0.88) (SI Figure S6). The $K_{PS/w}$ derived from the PS-water and PDMS-water-PS experiments were consistent for the chemicals evaluated by both methods (SI Table S3). The kinetic curves of the PDMS-PS experiments were not fitted with the kinetic model because the total amounts of chemicals in PDMS and PS decreased over the long incubation period of 94 days.

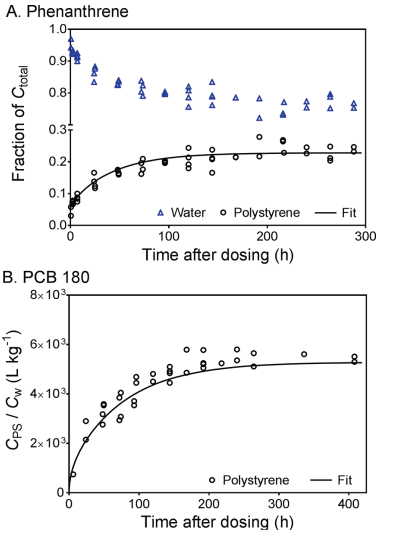

Figure 1. Measured data and model fits. A: phenanthrene in the PS-water experiment (eq 5); B: PCB 180 in the PDMS-water-PS experiment (eq 9).

Therefore, log $K_{PDMS/PS}$ were extrapolated from the measured concentration ratios $C_{PDMS/PS}$ between PDMS and PS ($K_{PDMS/PS}$, SI Figure S5) and translated into $K_{PS/w}$ by eq 10.

$$K_{PS/w} = \frac{K_{PDMS/w}}{K_{PDMS/PS}} \tag{10}$$

Although the log $K_{PS/w}$ determined by the PDMS-PS experiment agreed with the log $K_{PS/w}$ from the PS-water partition experiments (Figure 2), they were not included in the linear regression of log K_{ow} and log $K_{PS/w}$ because of the decreasing total amounts in the test system and were only plotted in Figure 2 to demonstrate the robustness and consistency of the three experimental methods.

PS is composed of a hydrocarbon center, to which phenyl groups are attached, making it very hydrophobic, thus, chemicals with higher hydrophobicity exhibit higher sorptive affinities to PS via van der Waals forces with possible electron donor and acceptor interactions between the chemicals and the phenyl group. The slopes of the linear regressions between log $K_{PS/w}$ and log K_{ow} were 0.56 (Figure 2) and 0.41 between log $K_{PS/w}$ and log $K_{hexane/w}$ (SI Figure S6). The slope <1 means that more hydrophobic chemicals do not proportionally partition between octanol or hexane and PS. This is in contrast to the rubbery polymers PDMS and LDPE, for which the regressions of the log polymer-water partition constants with log K_{ow} have slopes close to one while their absolute values are approximately one log-unit lower (log $K_{PDMS/w}$).[14,29] This difference might be the result of the inflexible matrix of the PS that is characterized by little void space, in which larger, more hydrophobic chemicals lack space thus do not accumulate to the same extent as in PDMS and LDPE, which are

DOI: 10.1021/acs.est.8b04246
Environ. Sci. Technol. 2018, 52, 13511−13522

Table 2. Physicochemical Properties of the Chemicals (see SI Table S2 for Details and Literature References)[a]

chemical	log K_{ow} (L L^{-1})	log $K_{hexane/w}$ (L L^{-1})	mol wt (g mol^{-1})	log $K_{PS/w}$ (L kg^{-1})	CV (%)	log D_{PS} (m^2 s^{-1})	CV (%)
2,4-dinitrotoluene	1.98	1.24	182.14	1.27	±1%	−15.79	±3%
carbamazepine	2.45	−1.10	236.27	0.04	±5%	−15.90	±5%
atrazine	2.61	0.44	215.68	1.42	±4%	−15.82	±4%
diuron	2.68	−0.05	233.09	0.93	±4%	−15.95	±3%
boscalid	2.96	3.10	343.21	1.94	±2%	−15.68	±4%
terbutylazine	3.40	1.71	229.71	1.82	±3%	−15.96	±4%
diazinon	3.81	N.A.	304.35	3.24	±5%	−15.90	±6%
progesterone	3.87	1.59	314.46	2.60	±2%	−15.38	±4%
acenaphthene	3.92	3.96	154.20	2.26	±4%	−15.41	±18%
chlorpyrifos methyl	4.31	4.40	322.53	2.53	±2%	−15.81	±3%
anthracene	4.45	4.43	178.23	2.76	±3%	−15.89	±3%
phenanthrene	4.46	4.49	178.23	2.55	±2%	−15.45	±2%
penconazole	4.67	N.A.	284.18	2.49	±2%	−15.69	±4%
pyrene	4.88	4.67	202.25	3.17	±1%	−15.45	±3%
fluoranthene	5.16	4.90	202.25	3.08	±2%	−15.43	±3%
benzo(a)anthracene	5.76	5.51	228.29	3.16	±3%	−15.26	±8%
PCB 52	6.09	6.22	291.99	2.83	±3%	−15.47	±9%
benzo(a)pyrene	6.13	5.53	252.31	3.04	±3%	−15.13	±10%
PCB 153	6.90	7.22	360.86	3.81	±5%	−15.59	±17%
PCB 118	7.12	6.87	326.40	4.00	±4%	−15.88	±10%
PCB 180	7.72	7.71	395.31	3.95	±3%	−15.43	±10%
PCB 194	8.68	8.29	395.90	5.10	±3%	−15.68	±10%

[a]Measured PS-water partition constants (log $K_{PS/w}$) and diffusion coefficients (D_{PS}) that resulted from fitting the experimental data illustrated in Figure 1 and SI Figure S4 (coefficients of variations (CV), standard deviation divided by the best-fit value (%)). The $K_{PS/w}$ can be transformed into L L^{-1} by multiplication with the mass density ϱ_{PS} of the PS (1.04 kg L^{-1}).

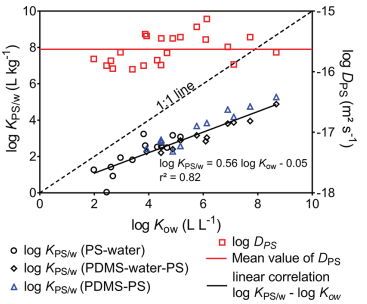

Figure 2. Measured log $K_{PS/w}$ determined by the PS-water (black circles) and the PDMS-water-PS (black diamonds) partition experiments, as well as corresponding log D_{PS} (red squares) of the chemicals, plotted against their log K_{ow}. The black solid line is the linear regression of log $K_{PS/w}$ and log K_{ow}. The apparent log $K_{PS/w}$ determined by the PDMS-PS setup are plotted as blue triangles (data from SI Figure S5), which are only displayed for method comparison and were not included in the linear regression. The red line is the average of the measured log D_{PS} suggested as general surrogate for log D_{PS} of neutral organic chemicals.

characterized by a large free volume between the molecules.[6] We calculated apparent surface water partition constants $K_{surf/w(apparent, 48h)}$ from the absorbed concentration in the PS after 48 h in units of m^3/m^2 to perform a comparison between the current and a literature study that determined 48-h partitioning of polycyclic hydrocarbons (PAHs) to PS (SI Figure S7).[30] There is a good agreement for four overlapping chemicals and only the very hydrophobic chemicals benzo(a)-pyrene and chrysene deviate by a factor of >10 between the two studies.

Diffusion into the PS was by orders of magnitude slower compared to the rubbery polymers PDMS (log D_{PDMS} (m^2 s^{-1}) ≈ −9.5 to −11) and LDPE (log D_{LDPE} (m^2 s^{-1}) ≈ −12 to −13.5),[7] with measured D_{PS} (m^2 s^{-1}) in the range of −15 (Table 2, Figure 2). The low D_{PS} considerably delay the uptake of chemicals from the aqueous phase into the PS compared to rubbery polymer-water systems, favoring PDMS and LDPE for passive sampling and dosing of neutral organic chemicals. The measured D_{PS} did not considerably differ between the chemicals, with log D_{PS} (m^2 s^{-1}) ranging from −15.1 to −15.9. Diffusion coefficients in the rubbery polymers PDMS and LDPE were reported to correlate with the molecular weight of PAHs and polychlorinated biphenyls (PCBs), with larger chemicals diffusing slower through polymers.[7] Studies on the diffusion in glassy polymers state that due to the limited void space in the polymer matrix, diffusion of organic chemicals through the polymer is more complex compared to diffusion in rubbery polymers.[6,31] Here, we did not observe a correlation between molecular weight and D_{PS}, which contradicts the general observation of an exponential decrease in D with molecular weight for rubbery and glassy polymers.[32] For PS, this correlation was reported based on D_{PS} of eight organic chemicals of which six have a molecular weight between 92 and 200 g mol^{-1}.[33] It is possible that for the 22 chemicals tested with molecular weights between 180 and 400 g mol^{-1}, this correlation does not hold. Further experiments with more chemicals covering a wider range of molecular weights need to be performed to evaluate the correlation between molecular weight and D_{PS}.

4.2. Comparison of Experimental Losses in Multiwell Plates and Kinetic Model Predictions. The $K_{PS/w}$ and D_{PS} measured in the PS-water and PDMS-water-PS experiments

DOI: 10.1021/acs.est.8b04246
Environ. Sci. Technol. 2018, 52, 13511−13522

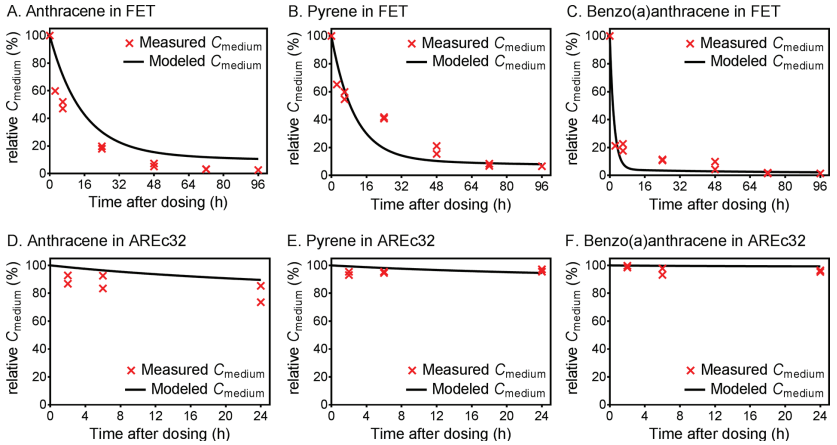

Figure 3. Modeled (black lines) and measured (red crosses) relative C_{medium} of three chemicals in the FET assay (A., B., C.) and the AREc32 assay applying 10% FBS (D., E., F.) over the assay duration of 96 and 24 h, respectively.

were applied to estimate the depletion of C_{medium} of the evaluated chemicals by sorption to multiwell plates in the FET and the AREc32 assays (eq 7). These predictions were compared with experimental data to validate the predictive model. Both assays were run without fish embryos and cells to concentrate on the medium depletion by sorption to plastic rather than losses due to uptake by the fish embryos and cells. The magnitude of measured D_{PS} ($2.33 \cdot 10^{-16}$ m^2 s^{-1}, Table 2) emphasize the need of thin PS sheets to attain equilibrium during the experimental determination of D_{PS} and $K_{PS/w}$. After having obtained robust experimental data of D_{PS} and $K_{PS/w}$, we could predict that for a typical multiwell plate with 1 mm thick PS walls, the equilibrium between medium and well plate would be attained after approximately 55 years. For the FET assay, bioconcentration is an additional depletion process for more hydrophobic chemicals, while in typical cell assay setups, the sorption capacity of the cells is much smaller than that of the medium.[21] Figure 3 and SI Figures S8 and S9 compare the predicted C_{medium} of the chemicals in the FET assay (24-well plate and 96 h exposure) and the AREc32 assay (96-well plate and 24 h exposure) with C_{medium} measured after liquid-liquid extraction of the medium as described in Section 3.5. Predicted C_{medium} generally agreed with the measured C_{medium} in both assays. The model often predicted a slightly different curvature of C_{medium} (t) than measured, which may be caused by processes not considered in the model that explain the drop of concentration from the first to the second measurement. Still, the results confirm that the model adequately reflects the physical structure of and thermodynamic conditions in the medium-well system. This is satisfying considering that $K_{PS/w}$ and D_{PS} were measured with generic, untreated PS, whereas the PS of the multiwell plates were treated depending on their purpose of use. The 24-well plates from TPP used for the FET assay were mechanically treated to increase the surface of the PS, whereas the Corning 96-well plates used for the AREc32 assay were charged negatively by corona discharge to increase cell attachment. Such treatments can influence the sorptive capacity of the PS for neutral organic chemicals and can represent an uncertainty when adapting the predictive model and data from this study. Still, predictions in C_{medium} were sufficiently accurate for the multiwell plates evaluated here.

For the 3-ring PAHs anthracene and phenanthrene, the measured C_{medium} were systematically lower than predicted (Figure 3 and SI Figure S8), which could be the result of losses to the air, because the multiwell plates were only covered with a standard lid but not air-tightly sealed, demonstrating that the prediction model is not applicable for chemicals with high air-medium partition constants (SI Table S6). The difference between measured and modeled C_{medium} was also observed for these chemicals in the AREc32 assay despite its lower $K_{air/medium}$ for the cell assay supplemented with FBS (Figure 3 and SI Figure S9). Mass balance calculations confirmed that air-medium partitioning can deplete C_{medium} of these chemicals to a considerable degree, for example, by up to 30% in the AREc32 assay, whereas nonvolatile chemicals such as benzo-(a)anthracene were depleted by <1% within the 24 h (SI Section S10).

4.3. Predictions of Multiwell Plate Sorption in the in Vivo Fish Embryo Toxicity Test. Due to the relatively small range of measured D_{PS} we used an average log D_{PS} of −15.6, that is, a D_{PS} of $2.33 \cdot 10^{-16}$ m^2 s^{-1} for the kinetic predictive model. $K_{PS/w}$ can be derived from log K_{ow} or log $K_{hexane/w}$ by quantitative structure-activity relationships (QSARs, eqs 11 and 12) to predict the sorption of diverse neutral organic chemicals to multiwell plates in bioassays (Figure 3 and SI Figure S6).

$$\log K_{PS/w} = 0.56 \times \log K_{ow} - 0.05 \quad \text{RMSE: } 0.45 \qquad (11)$$

$$\log K_{PS/w} = 0.41 \times \log K_{hexane/w} + 0.90 \quad \text{RMSE: } 0.39 \qquad (12)$$

Because the average measured log D_{PS} (m^2 s^{-1}) of −15.6 and the correlation between log K_{ow} and log $K_{PS/w}$ (Figure 2) can be used as approximations, the predictive model solely requires

DOI: 10.1021/acs.est.8b04246
Environ. Sci. Technol. 2018, 52, 13511−13522

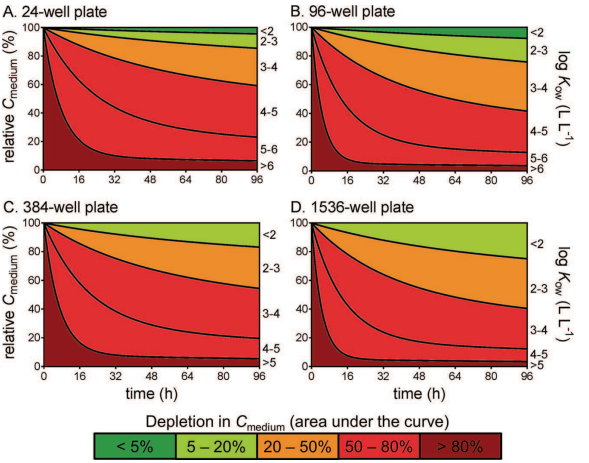

Figure 4. Modeled relative C_{medium} over time in the FET assay applied to A. 24-, B. 96-, C. 384-, and D. 1536-well plates binned into different log K_{ow} ranges. The colors indicate the percentage of reduction in the area under the curve representative for time-dependent exposure.

the log K_{ow} of the chemical, the ratio of PS surface-to-well volume and the thickness of the PS of the applied multiwell plate (Table 1). Note that the model was calibrated by experimental $K_{PS/w}$ and D_{PS} of chemicals with molecular weights between 180 and 400 g mol^{-1}. The application of the suggested average D_{PS} could lead to a high prediction error for chemicals with lower or higher molecular weight. Furthermore, a nonlinear relationship between log K_{ow} and log $K_{PS/w}$ can occur for very large and/or hydrophobic chemicals, as was already shown for superhydrophobic chemicals in PDMS.[34,35]

The kinetic prediction model (eq 7) was applied to the multiwell plates and media used in the FET assay. Depletion of C_{medium} was predicted for chemicals with a log K_{ow} ranging from 0 to 8 (eq 11). $K_{PS/w}$ was used as a proxy for $K_{PS/medium}$ because the FET medium is composed of ISO water containing low concentrations of salts but no sorptive colloids. The area under the curve (AUC) of C_{medium} was used as criterion for the decrease in time-dependent medium exposure (eq 13) and was derived by integration of the curve using the trapezoidal rule.

$$\mathrm{AUC}(C_{medium}) = \int_{t_0}^{t_{end}} C_{medium}(t)\,dt \tag{13}$$

The percentage depletion of C_{medium} (depletion) by multiwell plate sorption was calculated by subtracting the AUC (C_{medium}) from the maximum AUC that would result from a constant C_{medium} throughout the assay duration ($C_{medium,const}$) (eq 14).

$$\mathrm{depletion} = C_{medium,const}\cdot(t_{end} - t_0) - \int_{t_0}^{t_{end}} C_{medium}(t)\,dt \tag{14}$$

Sorption to the multiwell plate is expected to deplete C_{medium} by up to 99.9% throughout the test duration of 96 h in the FET assay (Figure 4). With increasing number of wells, C_{medium} is predicted to be depleted to a higher extent, such as a reduction of 8% in a 24-well plate compared to a reduction of 40% in a 1536-well plate when testing a log K_{ow} 3 chemical. The increased sorption in higher tier multiwell plates results from the ratio of medium volume-to-PS surface area that decreases from $2.84 \cdot 10^{-3}$ m to $4.29 \cdot 10^{-4}$ m when switching from 24-well to 1536-well plates (Table 1). This difference should be considered when applying bioassays to higher tier multiwell plates for increased throughput of experiments.

Depletion of C_{medium} in the FET assay is expected to be minor for chemicals with log K_{ow} < 2 in all evaluated multiwell plates (Figure 4). With increasing log K_{ow}, C_{medium} depletion would increase. Neutral chemicals with log K_{ow} of 6 would be considerably reduced in all evaluated multiwell plates to a maximum of 90%, emphasizing that multiwell plate sorption is a major issue when testing very hydrophobic chemicals in assays applying aqueous media, whereas multiwell plate sorption is generally a minor issue for hydrophilic chemicals. Our results agree with earlier studies on multiwell plate sorption from aqueous media[13,18,36,37] and support the conclusion that multiwell plate sorption significantly affects exposure and needs to be considered for chemicals with a log K_{ow} > 3 in these test systems.[20] It is thus advisible to either use glass multiwell plates or apply polymer-based passive dosing when testing hydrophobic chemicals in colloid-free media in bioassays such as the FET but also *Daphnia magna* and other invertebrates and cell-based assays applying serum-free medium, such as tests with fish cell lines[37,38] or algae and bacteria.

4.4. Predictions of Multiwell Plate Sorption in in Vitro Cell Bioassays. The degree of depletion by multiwell plate sorption was much different for the cell-based assays with mammalian cell lines that are supplemented with FBS. C_{medium} in the AREc32 remained relatively stable over the test period of 24 h in 96-well plates (Figure 5). The difference between the FET and cell-based assays mainly results from the sorptive capacity of protein and lipids that are present in the 10%

DOI: 10.1021/acs.est.8b04246
Environ. Sci. Technol. 2018, 52, 13511−13522

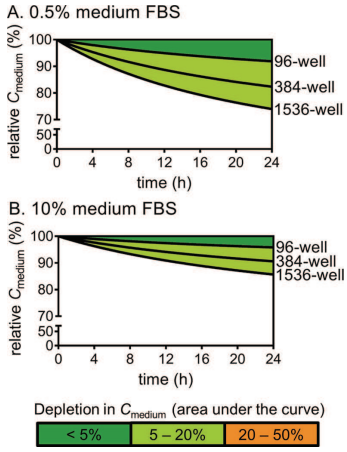

Figure 5. Modeled relative C_{medium} over time in two in vitro cell assay that apply A. 0.5% and B. 10% FBS in 96-, 384-, and 1536-well plates. The colors indicate the percentage of reduction in the area under the curve representative for time-dependent exposure. The results are valid for all chemicals with log K_{ow} between 2 and 8 and molecular weights between 180 and 400 g mol^{-1} that fall within the range of log K_{ow} based on which the QSAR was calibrated (Figure 2).

medium FBS of the AREc32 assay,[21] confirming the applicability of SMPD in this test system. Because the chemicals are reversibly bound to the medium constituents, the PS-medium partition constant ($K_{PS/medium}$) is lower compared to the colloid-free assay medium of the FET assay (corresponding $K_{PS/medium}$ compiled in SI Tables S7–S9). Thus, the driving force between the medium and the PS is lower in in vitro cell assays, decreasing the amount of chemicals diffusing into the PS during a certain time. The constant C_{medium} indicate constant C_{free}, because the desorption kinetics of chemicals from medium proteins are expected to be in the range of minutes,[39,40] which is considerably faster compared to the mass transfer of chemicals into the PS, at least after the initial period in which steep concentration gradients in the PS close to the water-PS interface cause rapid mass transfer.

Figure 5 illustrates the model results for chemicals with log K_{ow} between 2 and 8 in two in vitro cell-based bioassays that apply 0.5% and 10% FBS in the medium, respectively. The PS-medium partition constants ($K_{PS/medium(\%FBS)}$), which depend on the content of FBS in the medium, and their derivation are reported in SI Section S11. C_{medium} was reduced by a maximum of 15.8% when only 0.5% FBS was used and 8.5% in the presence of 10% FBS, respectively, emphasizing again that multiwell plate sorption is generally less affecting exposure in in vitro cell assays that apply protein- and lipid-rich media compared to bioassays with aqueous media.

Similar to the FET assay, C_{medium} was more reduced in higher tier multiwell plates, such as 2.5% in a 96-well plate compared to 8.8% in a 1536-well plate for a log K_{ow} 3 chemical at 10% FBS. Interestingly, depletion of C_{medium} is expected to be highest for chemicals with log K_{ow} 3–4, because the slope of the correlation between log K_{ow} and log $K_{PS/w}$ is 0.56 which is comparable to the correlation between log K_{ow} and protein–water partition constants (log $K_{BSA/w}$),[41] whereas membrane lipid–water partition constants ($K_{lip/w}$) of neutral chemicals correlate with log K_{ow} almost 1:1.[42] With increasing log K_{ow}, the sorptive capacity of the medium lipids increases non-proportionally to the sorptive affinity of these lipophilic chemicals to PS, leading to a reduced sorption to the PS. In other words, the PS-medium partition constant in in vitro cell assays increases with log K_{ow} until a log K_{ow} 3–4 while decreasing for chemicals with log K_{ow} > 5 (Figure 6). Note that the prediction in Figure 5 is valid for all chemicals with a log K_{ow} between 2 and 8 because that is the range of log K_{ow} the prediction model was calibrated with. A possible source of uncertainty for the model output represent the degradation of chemicals either by abiotic processes such as hydrolysis or photolysis, or by biotransformation by the cells.

When decreasing the medium FBS concentration from 10% to 0.5%, C_{medium} depletion increased, such as from 6.7% at 10% FBS to 15.8% at 0.5% FBS. Higher medium FBS concentrations increase the amount of sorptive proteins and lipids in the medium and thus its ability to compensate for depletion by multiwell plate sorption, agreeing with earlier studies that were conducted at different medium FBS concentrations.[21,23] Still, 0.5% is sufficient to compensate for multiwell plate sorption so that C_{medium} is reduced by <20%, which can be considered as acceptable. However, in the model calculations we solely considered mass transfer from the assay medium into the PS,

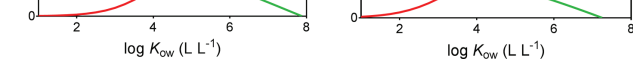

Figure 6. Log $K_{PS/w}$, log $K_{medium/w}$, and log $K_{PS/medium}$ that were derived by eq 11 and SI eqs S53 and S54, plotted against the corresponding log K_{ow} that was used for the prediction of the partition constants.

DOI: 10.1021/acs.est.8b04246
Environ. Sci. Technol. 2018, 52, 13511–13522

whereas combined depletion by multiwell plate sorption, volatilization, cellular uptake and growth as well as degradation could ultimately lead to a considerable depletion in C_{medium}.

In the experiments and predictions, no cells and fish embryos were used to exclusively measure and model the mass transfer from the medium into the PS. Under realistic exposure scenarios, chemical partitioning into the cells and the embryos represents an additional process that needs to be considered. For in vitro cell assays, we have previously shown that chemical uptake leads to a maximum reduction in C_{medium} of 16% in 1536-well plates applying 0.5% medium FBS.[21] The combined reduction in C_{medium} could ultimately lead to a high uncertainty when applying 0.5% FBS in higher tier multiwell plates. Therefore, it is advisible to use higher medium FBS concentrations for increased suitability of the medium components to stabilize exposure throughout the assay duration, provided that the applied cells tolerate the increased medium FBS. The model results generally confirm that SMPD largely counteracts the depletion of test chemicals by multiwell plate sorption in in vitro cell assays with mammalian cell lines that apply between 0.5% and 10% FBS, such as the cell-based bioassays incorporated in the ToxCast screening program. The ability of other types of nutrient such as the wild type proteins used for tissue-based cell-free assays (e.g., NovaScreen assays) to compensate for multiwell plate sorption needs to be assessed in the future but it is likely that any type of protein- and/or lipid-containing matrix will stabilize the medium concentration and reduce the influence of plastic sorption. The number of evaluated chemicals and assays need to be extended to further describe the applicability domain of SMPD to compensate sorption to multiwell plate materials and identify scenarios that lie outside, such as depletion of volatile chemicals.

4.5. Implications for Bioassay Applications in Risk Assessment and Environmental Monitoring. The generated dataset of $K_{PS/w}$ and D_{PS}, the associated QSARs and prediction models can readily be applied to evaluate the multiwell plate sorption of neutral organic chemicals in different multiwell plates. The attached Excel model in the SI can be adapted without much effort and required data to enhance the quality of chemical dosing by considering the proportion of chemicals depleted from the medium over the bioassay duration. By that means, users can quickly evaluate whether multiwell plate sorption represents a source of uncertainty in their assays and potentially optimize test conditions prior to running experiments. Please be aware of that the model was calibrated with a relatively low number of chemicals and that the predictions were based exclusively on the K_{ow}, therefore, will only hold for neutral chemicals with $K_{medium/w}$ proportional to K_{ow} or $K_{hexane/w}$. Predictions on multiwell plate sorption of polar chemicals and chemicals with high molecular weights are uncertain. Future studies should aim to complement the dataset to extend the applicability domain of the prediction model and to identify physicochemical properties determining diffusion.

The measured and modeled C_{medium} in the FET, chosen as representative example for an assay using colloid-free medium emphasize that sorptive losses to multiwell plates represent a huge source of uncertainty when testing hydrophobic chemicals with log K_{ow} > 3 in pure water systems, even when using large-volume wells. In contrast, we confirmed that the FBS in in vitro cell assay media can compensate for multiwell plate sorption. This finding indicates that existing exposure models that neglect sorption to multiwell plates still sufficiently predict exposure in in vitro cell assays.[21,43,44] While the C_{medium} can be adjusted and kept constant throughout the experiment by SMPD, it must be noted that the addition of colloids reduces the C_{free} and C_{cell} and therefore the apparent sensitivity of the assay. Employing in vitro bioassays with SMPD therefore requires measuring or modeling C_{free} for in vitro−in vivo extrapolations (IVIVE) and risk assessment.

For environmental monitoring, where effects of unresolved complex environmental mixtures are benchmarked against the effects of single chemicals, it is important to keep the composition of the mixture reaching the cells intact, which can be accomplished by SMPD. For environmental monitoring applications it is important that only results from assays run with the same assay setup and medium composition are compared and effect-based trigger values[45−47] are derived specifically for each bioassay in a standardized setup with defined medium composition and ratio of medium volume-to-PS surface area.

4.6. Implications for Research on Plastic in the Environment. This study provides mechanistic and quantitative data on the partitioning of neutral organic chemicals to PS, which is a common plastic material that is also present in large quantities as macro- and microparticles in the environment.[48] The kinetics of diffusion in PS are highly relevant for the packaging industry, such as for the application of PS in food packaging or waste management, because it is used to prevent contamination of the products or can release pollutants into the environment.[49] PS was also discussed to be a source of contamination of chemicals in food.[50] The ability of plastic particles (macro and micro) to sorb, transport, and release pollutants from and into environmental compartments has been and is continuously discussed in the recent and current literature.[51−53] Most studies lack experimental methods to generate quantitative data on chemical sorption to plastics of different size and shape. The partition constants $K_{PS/w}$ and diffusion coefficients D_{PS} determined here can be applied to appropriate mass-transfer models for systems involving PS and organic chemicals.

■ ASSOCIATED CONTENT

Supporting Information

The Supporting Information is available free of charge on the ACS Publications website at DOI: 10.1021/acs.est.8b04246.

Equations, fits and models that were used for predictions and corresponding MATLAB codes; a discussion on the well geometry; information on the extraction efficacy of PS by *n*-heptane; information on the study chemicals; experimental data and corresponding fits; data and information applied in the prediction model (PDF)

Simplified prediction model (XLSX)

■ AUTHOR INFORMATION

Corresponding Author

*Phone: +49 341 235−1512; fax: +49 341 235−1787; e-mail: fabian.fischer@ufz.de.

ORCID

Fabian C. Fischer: 0000-0002-9511-0506
Olaf A. Cirpka: 0000-0003-3509-4118
Kai-Uwe Goss: 0000-0002-9707-5505
Luise Henneberger: 0000-0002-3181-0044

DOI: 10.1021/acs.est.8b04246
Environ. Sci. Technol. 2018, 52, 13511−13522

Beate I. Escher: 0000-0002-5304-706X

Notes

The authors declare no competing financial interest.

■ ACKNOWLEDGMENTS

We thank Marion Heinrich, Cedric Abele, Jörg Watzke, Maria König, Lisa Glauch, and Marie Mühlenbrink for the laboratory support. We thank Jessica Hellweg for assistance with MATLAB coding, proofreading and her critical review of the manuscript structure. Jon Arnot, Annika Jahnke, Nynke Kramer, and Sven Seidensticker are thanked for reviewing the manuscript and providing useful discussions on the topic. We gratefully acknowledge the financial support of the CEFIC Long-Range Research Initiative (LRI), project ECO36.

■ REFERENCES

(1) OECD. Test No. 236: *Fish Embryo Acute Toxicity (FET) Test*, 2013.

(2) Eisenträger, A.; Dott, W.; Klein, J.; Hahn, S. Comparative studies on algal toxicity testing using fluorometric microplate and Erlenmeyer flask growth-inhibition assays. *Ecotoxicol. Environ. Saf.* **2003**, *54* (3), 346−354.

(3) ISO 10872: *Water quality—Determination of the toxic effect of sediment and soil samples on growth, fertility and reproduction of Caenorhabditis elegans (Nematoda)*, 2010.

(4) Grintzalis, K.; Dai, W.; Panagiotidis, K.; Belavgeni, A.; Viant, M. R. Miniaturising acute toxicity and feeding rate measurements in *Daphnia magna*. *Ecotoxicol. Environ. Saf.* **2017**, *139*, 352−357.

(5) Ryan, J. A. Evolution of Cell Culture Surfaces. *BioFiles* **2008**, *3* (8), 21.

(6) George, S. C.; Thomas, S. Transport phenomena through polymeric systems. *Prog. Polym. Sci.* **2001**, *26*, 985−1017.

(7) Rusina, T. P.; Smedes, F.; Klanova, J. Diffusion Coefficients of Polychlorinated Biphenyls and Polycyclic Aromatic Hydrocarbons in Polydimethylsiloxane and Low-Density Polylethylene Polymers. *J. Appl. Polym. Sci.* **2010**, *116*, 1803−1810.

(8) Gavara, R.; Hernandez, R. J.; Giacin, J. Methods to determine partition coefficient of organic compounds in water/polystyrene systems. *J. Food Sci.* **1996**, *61*, 947−952.

(9) Begley, T.; Castle, L.; Feigenbaum, A.; Franz, R.; Hinrichs, K.; Lickly, T.; Mercea, P.; Milana, M.; O'Brien, A.; Rebre, S.; Rijk, R.; Piringer, O. Evaluation of migration models that might be used in support of regulations for food-contact plastics. *Food Addit. Contam.* **2005**, *22*, 73−90.

(10) Bernardo, G. Diffusivity of alkanes in polystyrene. *J. Polym. Res.* **2012**, *19*, 9836.

(11) Claudy, P.; Letoffe, J. M.; Camberlain, Y.; Pascault, J. P. Glass-Transition of Polystyrene Versus Molecular-Weight. *Polym. Bull.* **1983**, *9*, 208−215.

(12) Pascall, M. A.; Zabik, M. E.; Zabik, M. J.; Hernandez, R. J. Uptake of polychlorinated biphenyls (PCBs) from an aqueous medium by polyethylene, polyvinyl chloride, and polystyrene films. *J. Agric. Food Chem.* **2005**, *53*, 164−169.

(13) Chlebowski, A. C.; Tanguay, R. L.; Simonich, S. L. M. Quantitation and prediction of sorptive losses during toxicity testing of polycyclic aromatic hydrocarbon (PAH) and nitrated PAH (NPAH) using polystyrene 96-well plates. *Neurotoxicol. Teratol.* **2016**, *57*, 30−38.

(14) Mayer, P.; Vaes, W. H. J.; Hermens, J. L. M. Absorption of Hydrophobic Compounds into the Poly(dimethylsiloxane) Coating of Solid-Phase Microextraction Fibers: High Partition Coefficients and Fluorescence Microscopy Images. *Anal. Chem.* **2000**, *72*, 459−464.

(15) Broeders, J. J. W.; Blaauboer, B. J.; Hermens, J. L. M. Development of a negligible depletion-solid phase microextraction method to determine the free concentration of chlorpromazine in aqueous samples containing albumin. *Journal of Chromatography A* **2011**, *1218*, 8529−8535.

(16) Oemisch, L.; Goss, K.-U.; Endo, S. Ion exchange membranes as novel passive sampling material for organic ions: Application for the determination of freely dissolved concentrations. *Journal of Chromatography A* **2014**, *1370*, 17−24.

(17) Sitterley, G. BioFiles: Attachement and Matrix Factors. *Sigma LifeScience* **2008**, *3* (8).

(18) Gellert, G.; Stommel, A. Influence of microplate material on the sensitivity of growth inhibition tests with bacteria assessing toxic organic substances in water and waste water. *Environ. Toxicol.* **1999**, *14*, 424−428.

(19) Schreiber, R.; Altenburger, R.; Paschke, A.; Küster, E. How to deal with lipophilic and volatile organic substances in microtiter plate assays. *Environ. Toxicol. Chem.* **2008**, *27*, 1676−1682.

(20) Riedl, J.; Altenburger, R. Physicochemical substance properties as indicators for unreliable exposure in microplate-based bioassays. *Chemosphere* **2007**, *67*, 2210−2220.

(21) Fischer, F. C.; Henneberger, L.; König, M.; Bittermann, K.; Linden, L.; Goss, K.-U.; Escher, B. I. Modeling Exposure in the Tox21 in Vitro Bioassays. *Chem. Res. Toxicol.* **2017**, *30*, 1197−1208.

(22) Fischer, F. C.; Abele, C.; Droge, S. T. J.; Henneberger, L.; König, M.; Schlichting, R.; Scholz, S.; Escher, B. I. Cellular uptake kinetics of neutral and charged chemicals in in vitro assays measured by fluorescence microscopy. *Chem. Res. Toxicol.* **2018**, *31* (8), 646−657.

(23) Kramer, N. I.; Krismartina, M.; Rico-Rico, A.; Blaauboer, B. J.; Hermens, J. L. M. Quantifying Processes Determining the Free Concentration of Phenanthrene in Basal Cytotoxicity Assays. *Chem. Res. Toxicol.* **2012**, *25*, 436−445.

(24) Schwarzenbach, R. P.; Gschwend, P. M.; Imboden, D. M. *Environmental Organic Chemistry*, 3rd ed.; Wiley: NJ, 2016, ISBN: 978-1-118-76723-8.

(25) de Hoog, F. R.; Knight, J. H.; Stokes, A. N. An improved method for numerical inversion of Laplace transforms. *SIAM J. Sci. Stat. Comput.* **1982**, *3*, 357−366.

(26) Wang, F.; Nguyen, M.; Qin, F. X.-F.; Tong, Q. SIRT2 deacetylates FOXO3a in response to oxidative stress and caloric restriction. *Aging Cell* **2007**, *6*, 505−514.

(27) Laloy, E.; Vrugt, J. A. High-dimensional posterior exploration of hydrologic models using multiple-try DREAM((ZS)) and high-performance computing. *Water Resour. Res.* **2012**, *48* (1), W01526.

(28) Vrugt, J. A. Markov chain Monte Carlo simulation using the DREAM software package: Theory, concepts, and MATLAB implementation. *Environmental Modelling & Software* **2016**, *75*, 273−316.

(29) Zhu, T.; Jafvert, C. T.; Fu, D.; Hu, Y. A novel method for measuring polymer−water partition coefficients. *Chemosphere* **2015**, *138*, 973−979.

(30) Kramer, N. I. *Measuring, Modeling, And Increasing the Free Concentration of Test Chemicals in Cell Assays*; Institute for Risk Assessment Sciences, Unversity of Utrecht: Netherlands, 2010, ISBN: 978-90-393-5250-2.

(31) Vrentas, J. S.; Vrentas, C. M. Sorption in Glassy-Polymers. *Macromolecules* **1991**, *24*, 2404−2412.

(32) Fang, X.; Vitrac, O. Predicting Diffusion Coefficients of Chemicals in and through Packaging Materials. *Crit. Rev. Food Sci. Nutr.* **2017**, *22* (2), 275−312.

(33) Dole, P.; Feigenbaum, A. E.; De La Cruz, C.; Pastorelli, S.; Paseiro, P.; Hankemeier, T.; Voulzatis, Y.; Aucejo, S.; Saillard, P.; Papaspyrides, C. Typical diffusion behaviour in packaging polymers - application to functional barriers. *Food Addit. Contam.* **2006**, *23* (2), 202−11.

(34) Hsieh, M.-K.; Fu, C.-T.; Wu, S.-c. Simultaneous Estimation of Glass−Water Distribution and PDMS−Water Partition Coefficients of Hydrophobic Organic Compounds Using Simple Batch Method. *Environ. Sci. Technol.* **2011**, *45*, 7785−7791.

(35) Grant, S.; Schacht, V. J.; Escher, B. I.; Hawker, D. W.; Gaus, C. Experimental Solubility Approach to Determine PDMS−Water Partition Constants and PDMS Activity Coefficients. *Environ. Sci. Technol.* **2016**, *50*, 3047−3054.

DOI: 10.1021/acs.est.8b04246
Environ. Sci. Technol. 2018, 52, 13511−13522

(36) Wolska, L.; Rawa-Adkonis, M.; Namiesnik, J. Determining PAHs and PCBs in aqueous samples: finding and evaluating sources of error. *Anal. Bioanal. Chem.* **2005**, *382*, 1389−1397.
(37) Stadnicka-Michalak, J.; Tanneberger, K.; Schirmer, K.; Ashauer, R. Measured and Modeled Toxicokinetics in Cultured Fish Cells and Application to In Vitro - In Vivo Toxicity Extrapolation. *PLoS One* **2014**, *9* (3), e92303.
(38) Schirmer, K. Proposal to improve vertebrate cell cultures to establish them as substitutes for the regulatory testing of chemicals and effluents using fish. *Toxicology* **2006**, *224*, 163−183.
(39) Kramer, N. I.; van Eijkeren, J. C. H.; Hermens, J. L. M. Influence of albumin on sorption kinetics in solid-phase microextraction: consequences for chemical analyses and uptake processes. *Anal. Chem.* **2007**, *79*, 6941−6948.
(40) Krause, S.; Ulrich, N.; Goss, K. U. Desorption kinetics of organic chemicals from albumin. *Arch. Toxicol.* **2018**, *92*, 1065−1074.
(41) Endo, S.; Goss, K. U. Serum Albumin Binding of Structurally Diverse Neutral Organic Compounds: Data and Models. *Chem. Res. Toxicol.* **2011**, *45*, 2293−2301.
(42) Endo, S.; Escher, B. I.; Goss, K. U. Capacities of Membrane Lipids to Accumulate Neutral Organic Chemicals. *Environ. Sci. Technol.* **2011**, *45*, 5912−5921.
(43) Armitage, J. M.; Wania, F.; Arnot, J. A. Application of Mass Balance Models and the Chemical Activity Concept To Facilitate the Use of in Vitro Toxicity Data for Risk Assessment. *Environ. Sci. Technol.* **2014**, *48*, 9770−9779.
(44) Paini, A.; Sala Benito, J. V.; Bessems, J.; Worth, A. P. From in vitro to in vivo: Integration of the virtual cell based assay with physiologically based kinetic modelling. *Toxicol. In Vitro* **2017**, *45*, 241−248.
(45) Brand, W.; de Jongh, C. M.; van der Linden, S. C.; Mennes, W.; Puijker, L. M.; van Leeuwen, C. J.; van Wezel, A. P.; Schriks, M.; Heringa, M. B. Trigger values for investigation of hormonal activity in drinking water and its sources using CALUX bioassays. *Environ. Int.* **2013**, *55*, 109−118.
(46) Escher, B. I.; Neale, P. A.; Leusch, F. D. L. Effect-based trigger values for in vitro bioassays: Reading across from existing water quality guideline values. *Water Res.* **2015**, *81*, 137−148.
(47) Escher, B. I.; Aït-Aïssa, S.; Behnisch, P. A.; Brack, W.; Brion, F.; Brouwer, A.; Buchinger, S.; Crawford, S. E.; Du Pasquier, D.; Hamers, T.; Hettwer, K.; Hilscherová, K.; Hollert, H.; Kase, R.; Kienle, C.; Tindall, A. J.; Tuerk, J.; van der Oost, R.; Vermeirssen, E.; Neale, P. A. Effect-based trigger values for in vitro and in vivo bioassays performed on surface water extracts supporting the environmental quality standards (EQS) of the European Water Framework Directive. *Sci. Total Environ.* **2018**, *628−629*, 748−765.
(48) Song, Y. K.; Hong, S. H.; Jang, M.; Han, G. M.; Shim, W. J. Occurrence and Distribution of Microplastics in the Sea Surface Microlayer in Jinhae Bay, South Korea. *Arch. Environ. Contam. Toxicol.* **2015**, *69*, 279−287.
(49) Marsh, K.; Bugusu, B. Food Packaging—Roles, Materials, and Environmental Issues. *J. Food Sci.* **2007**, *72*, R39−R55.
(50) Arvanitoyannis, I. S.; Bosnea, L. Migration of Substances from Food Packaging Materials to Foods. *Crit. Rev. Food Sci. Nutr.* **2004**, *44*, 63−76.
(51) Bakir, A.; Rowland, S. J.; Thompson, R. C. Transport of persistent organic pollutants by microplastics in estuarine conditions. *Estuarine, Coastal Shelf Sci.* **2014**, *140*, 14−21.
(52) Ziccardi, L. M.; Edgington, A.; Hentz, K.; Kulacki, K. J.; Driscoll, S. K. Microplastics as vectors for bioaccumulation of hydrophobic organic chemicals in the marine environment: A state-of-the-science review. *Environ. Toxicol. Chem.* **2016**, *35* (7), 1667−1676.
(53) Seidensticker, S.; Zarfl, C.; Cirpka, O. A.; Fellenberg, G.; Grathwohl, P. Shift in Mass Transfer of Wastewater Contaminants from Microplastics in the Presence of Dissolved Substances. *Environ. Sci. Technol.* **2017**, *51*, 12254−12263.

DOI: 10.1021/acs.est.8b04246
Environ. Sci. Technol. 2018, 52, 13511−13522